Synthesis of imidazo[1,2-a] pyridine and pyrazolo[1,5-a] pyridine Derivatives as Potential Kinase Inhibitors (*Pv*PI4K and *Pf*PKG) of *Plasmodium falciparum* Parasite

MASTER OF SCIENCE

IN

CHEMISTRY

R.S. SEGODI

2024

Synthesis of imidazo[1,2-a] pyridine and pyrazolo[1,5-a] pyridine Derivatives as Potential Kinase Inhibitors (*Pv*PI4K and *Pf*PKG) of *Plasmodium falciparum* Parasite

BY

RS SEGODI

DISSERTATION

Submitted in fulfilment of the requirements for the degree of

MASTER OF SCIENCE

in

CHEMISTRY

in the

FACULTY OF SCIENCE AND AGRICULTURE

(School of Physical and Mineral Science)

At the

UNIVERSITY OF LIMPOPO

Supervisor: PROF W NXUMALO

2024

DECLARATION

I declare that the project titled "**Synthesis of imidazo[1,2-a] pyridine and pyrazolo[1,5-a] pyridine Derivatives as Potential Kinase Inhibitors (*Pv*PI4K and *Pf*PKG) of *Plasmodium falciparum* Parasite**" is my original work and has not been submitted elsewhere for examination, award of a degree or publication. Where other people's work has been used, this has been acknowledged and referenced in accordance with the University of Limpopo requirements.

Signature: 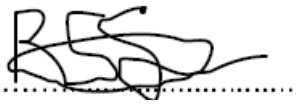 Date: 20/09/2024

SEGODI R.S

DEDICATION

This work is dedicated to my remarkable family for their unwavering support throughout this journey. To my mother, Florence Chiloane, for always believing in me and guiding me; my partner, Patience Mohlala, for her emotional support and always believing in me, my sister, Kholofelo Segodi, for her unceasing love and care.

ACKNOWLEDGMENTS

My academic journey has been blessed and influenced positively by many individuals who have played unforgettable roles towards my academic adventure. With utmost humbleness, I wish to convey my immense gratitude, respect, and admiration to my supervisor, Prof. Winston Nxumalo, for believing in me and for his exemplary work as my supervisor and mentor during my entire MSc period. I will ever remain grateful to you for the opportunity to pursue my MSc studies in your laboratory under your guidance and mentorship. The financial and moral support, inspiration, and more so for the laboratory space, resources, and professional guidance during my entire research period is deeply appreciated. My profound gratitude goes to Dr. Marole Maluleka for the vital role she played in my early career as an Organic Synthetic Chemist. I must say that the synthetic foundation you laid in me really assisted a lot during my MSc studies. To Dr Leboho Tlabo, thank you for believing in me and for your exemplary work and support during my entire MSc period. I would like to acknowledge Dr Emmanuel Agbo for his crucial advice, trust, mentor and support during difficult times. To extend my gratitude, I would like to acknowledge the Holistic Drug Discovery and Development Centre (H3D) for graciously sharing not only their research facilities but also their expertise throughout this project. I would also like to extend my gratitude to both the Parasitology and Drug Metabolism and Pharmacokinetics (DPMK) teams who performed the asexual blood stage antiplasmodial and solubility assays, respectively. Additionally, it is with a grateful heart that I acknowledge the academic group who were quite helpful all through this journey: specifically, Ursula Ralepelle, Lerato Raphoko, Kerryn Maluleke, Lebogang Mabatemela, Terrine Mokoena, Khomotso Mokganya, Jackson Nkoana, Kgaugelo Selowa, Reginald Mothapo, Kabelo Mojapelo, Kgethego Bokgobelo, Alfred Maja and Rosinah Sedibana for their assistance and emotional support; Dr Njabulo Gumede for introducing and training me on the Schrodinger software for molecular docking. Excitedly, I would like to extend my gratitude to NIH and H3D who granted me the opportunity to receive analytical instrument training at the H3D center in 2023. In addition, I heartfully thank my H3D mentors, Dr. Makwena Mmonwa and Dr. Preshen Govender who played a vital role in the progression of my synthesis and research skills. Finally, I would like to hugely thank my funders: NRF-SARchI, NIH and H3D. Their financial support was immeasurable.

CONFERENCES

Conference Presentations: Poster and Flash presentation

- **Segodi, R.S.**; Nxumalo, W. *Synthesis of imidazo[1,2-a] pyridine and pyrazolo[1,5-a] pyridine Derivatives as Potential Kinase Inhibitors (PvPI4K and PfPKG) of Plasmodium falciparum Parasite.* 03rd - 7th January 2023, SACI44th Conference National Convention. Venue: Stelenbosch, Western cape, South Africa.
- **Segodi, R.S.**; Nxumalo, W. *Synthesis of imidazo[1,2-a] pyridine and pyrazolo[1,5-a] pyridine Derivatives as Potential Kinase Inhibitors (PvPI4K and PfPKG) of Plasmodium falciparum Parasite*. 03rd - 7th December 2023, 16th Frank Warren National Convention. Venue: Stelenbosch, Western cape, South Africa.
- **Segodi, R.S.**; Nxumalo, W. *Synthesis of imidazo[1,2-a] pyridine and pyrazolo[1,5-a] pyridine Derivatives as Potential Kinase Inhibitors (PvPI4K and PfPKG) of Plasmodium falciparum Parasite.* 17th - 20th September 2024, 14th Faculty of Science and Agriculture (FSA). Venue: Polokwane (The Ranch Resort), Limpopo, South Africa.

LIST OF ABBREVIATIONS AND ACRONYMS

ACN: Acetonitrile
ACT: Artemisinin-combination therapy
ADP: Adenosine diphosphate
APCI: Atmospheric pressure chemical ionization
AR: Analytical-grade reagent
ATP: Adenosine triphosphate
AQ: Amodiaquine
BMGF: Bill and Melinda Gates Foundation
CC: Column chromatography
13C-NMR: 13Carbon nuclear magnetic resonance
$CDCl_3$: Chloroform
CDC: Centre for Disease Control and Prevention
CDPK: Calcium-dependent protein kinase
cGMP: Cyclic guanosine monophosphate
CHO: Chinese hamster ovarian cell line
CK1: Casein kinase 1
COVID-19: Coronavirus disease 2019
CQ: Chloroquine
$CuBr_2$: Copper(ii) bromide
CYP450: Cytochrome P450
DCM: Dichloromethane
DMF: *N*, *N*-Dimethylformamide
DMSO: Dimethyl sulfoxide
DMSO-d_6: Deuterated Dimethyl sulfoxide
DMPK: Drug metabolism and pharmacokinetics
DTT: Dithiothreitol
EC50: Half-maximal effective concentration
EGTA: Ethylene glycol-bis (β-aminoethyl ether)-*N*,*N*,*N*′,*N*′-tetraacetic acid
ESI: Electrospray ionization
EtOH: Ethanol
EtOAc: Ethyl acetate
FDA: Food and Drug Administration of USA
GSK: GlaxoSmithKline
H_2O: Water
HBD: Hydrogen bond donor
HBr: Hydrobromic acid
H3D: The Holistic Drug Discovery, and Development Centre at UCT
hERG: Human ether-*a-go-go*-related gene.
1H-NMR: Proton nuclear magnetic resonance
HPLC-MS: High-performance liquid chromatography- mass spectrometry
HTS: High-throughput screening
IC_{50}: 50% Inhibitory concentration
ITNs: Insecticide-treated nets
J: NMR coupling constant
K_2CO_3: Potassium carbonate
LC-MS: Liquid chromatography-mass spectrometry
LDH: Lactate dehydrogenase
MD: Molecular docking
MeOH: Methanol
MeOD: Deuterated methanol
MHz: Megahertz
MMV: Medicines for Malaria Venture
MP: Melting point
MS: Mass spectrometry
MTT: 3-(4,5-Dimethylthiazol-2-yl)-2,5-diphenyltetrazolium bromide
MW: Molecular weight
M.W: Microwave
MQ: Mefloquine
MVI: Malaria Vaccine Initiative
m*/*z: Mass to charge ratio.
µM: Micromolar
$NaNO_2$: Sodium Nitrite
NCA: Non-compartmental analysis
ND: Not determined
NIS: *N*-Iodosuccinimide
nM: Nanomolar
NMR: Nuclear magnetic resonance
PBS: Phosphate buffered saline.
Pb: *Plasmodium berghei*
PCy_3: tricyclohexylphosphine
PD: Pharmacodynamics
$PdCl_2(PPh_3)_2$: Palladium (*II*)bis(triphenylphosphine) dichloride
Pd $(PPh_3)_4$: Palladium(0) tetrakis(triphenylphosphine)
PDB: Protein Data Bank
Pf*: *Plasmodium falciparum

***Pf*CRT**: *Plasmodium falciparum* Chloroquine resistance transporter
***Pf*NF54**: Drug-sensitive strain of *Plasmodium falciparum*
***Pf*K1**: Multidrug-resistant strain of *Plasmodium falciparum*
PI: Phosphatidylinositol
PI3K: Phosphoinositide 3-kinase
PI4K: Phosphatidylinositol 4-kinase
PI4P: phosphatidylinositol 4-phosphate
PIP: Piperaquine
PK: Pharmacokinetics
PKG: c-GMP dependent protein kinase G
ppm: Parts per million
PQ: Primaquine
Pv: *Plasmodium vivax*
Q: Quinacrine
QN: Quinine
RBCs: Red blood cells
R*f*: Retardation factor
RI: Resistance index
SAR: Structure-activity relationship
SCID: Severe combined immunodeficiency gamma
SFK: SoftFocus Kinase library
SI: Selectivity index
SREBP: Sterol regulatory elementbinding protein
SUB1: Subtilisin-like serine protease1
t1/2: Half-life
TK: Tyrosine kinases
TLC: Thin layer chromatography
tR: Retention time
UCT: University of Cape Town
UV: Ultraviolet
WHO: World Health Organization

ABSTRACT

5-Amino-3-iodopyrazolo[1,5-a]pyridine was prepared via the iodination of commercially available 5-aminopyrazolo[1,5-a]pyridine in the presence of *N*-iodosuccinimide (NIS) in methanol. Palladium catalyzed Suzuki-Miyaura cross-coupling reaction on the 5-amino-3-iodopyrazolo[1,5-a]pyridine with arylboronic acids in dioxane-water afforded the 3-aryl substituted pyrazolo[1,5-a]pyridin-5-amine derivative, which were in turn, subjected to Sandmeyer reaction in the presence of concentrated hydrobromic acid, copper (ii) bromide and $NaNO_2$ to afforded the desired 5-bromo-3-(4-(methylsulfonyl)phenyl)pyrazolo[1,5-a]pyridine in 70% yield. Subsequent Suzuki-Miyaura cross-coupling on the 5-bromo-3-(4-(methylsulfonyl)phenyl)pyrazolo[1,5-a]pyridine with various arylboronic acids afforded two compounds of the 3,5-substituted pyrazolo[1,5-a]pyridine derivatives in 47% and 53% yield.

Condensation of 5-chloropyridin-2-amine and 2-chloroacetaldehyde in ethanol afforded 6-chloro imidazo[1,2-a]pyridine, which was in turn, treated with NIS in DMF to afford 6-chloro-3-iodo imidazo[1,2-a]pyridine in 71% yield. Sequential, palladium catalyzed Suzuki-Miyaura cross-coupling reaction on the latter with numerous boronic acids afforded 20 compounds of the desired 3,6-substituted imidazo[1,2-a]pyridine derivatives in 47-80% yield. The prepared compounds were characterized using a combination of NMR (^{1}H and ^{13}C) and mass spectrometric techniques. The compounds' antimalarial properties were investigated against *Plasmodium falciparum* and inhibitory studies were conducted against the *Pv*PI4k and *Pf*PKG kinases and some bioactive derivatives were further subjected to molecular docking studies. The enzymatic data displayed moderate anti-plasmodium activity for compound **40b** with IC_{50} values of *Pf*NF54/ *Pf*K1 (IC_{50} = 0.3709 µM/ 0.6447 µM) and *in vitro Pf*PKG/ *Pv*PI4K inhibitory activities (IC_{50} = 2.210/ 0.032 µM).

Keywords: pyrazolo[1,5-a]pyridine, imidazo[1,2-a]pyridine ,Suzuki-Miyaura, kinases, *Plasmodium falciparum*, *Pv*PI4k and *Pf*PKG,

Table of Contents

List of Figures

List of Tables

List of Schemes

CHAPTER 1: INTRODUCTION AND LITERATURE REVIEW.

1. MALARIA.

1.1.1. Background Information and Epidemiology

Malaria is a disease that impacts negatively the global health status and contributes more to the mortality rate in the tropical and subtropical regions, these regions include sub-Saharan Africa, South-East Asia, Eastern Mediterranean, and Western Pacific [1]. The disease arises from the protozoan parasite of the genus *Plasmodium* [2], which consists of various species responsible for causing malaria [3]. The species are *falciparum, vivax, ovale, malariae and knowlesi* [4]. Of the five species, the most prevalent cause of malaria is *falciparum* known to be dominant in sub-Saharan Africa [5], followed by *Plasmodium vivax, which* is dominant in South America [6]. The *P. ovale, malariae* and *knowlesi* were reported to be less virulent compared to *P. falciparum* and *P. vivax* [7]. *P. falciparum* is known to be fatal to both young children and pregnant women [8]. *P*. *vivax* was responsible for about 36% of malaria-related infections of malaria cases globally [9].

According to the World Health Organization (WHO) 2022 report, malaria deaths increased by 10 % in 2020 compared to 2019 with an estimate of 625 000 death cases and a slight decline in 2021 to 619 000 estimated death cases [10]. The 10% increase emanated from the disruption of malaria services, between 2019 and 2021 during the Covid-19 pandemic. One of the affected regions, specifically the African region, reported a decline in malaria deaths from 841 000 in 2000 to 541 000 in 2018, before rising to 599 000 in 2020 with a reduced mortality rate [10], [11]. Despite the decline in global malaria death cases, reports of emerging pandemics such as Covid-19, for example, pose a significant threat to the decrease in death cases due to the disease [10], [12]. Additionally, countries such as Nigeria still deal with a huge malaria burden due to suitable climatic conditions for mosquito breeding, complemented by fewer resources and a struggling economy which results in fewer investments in malaria prevention strategies [13]. Effective control of malaria globally has been remarkably hindered by the high cost, toxicity, and

unsuccessful effect of the known antimalaria drugs due to the development of resistance [14], [15]. This invites the development of new antimalarial drug candidates.

1.1.2 The life cycle of Malaria

The disease is transmitted by a vector called the female *Anopheles* mosquito when taking a blood meal by discharging the *Plasmodium* sporozoites from the salivary glands into the punctured host dermis skin (**Figure 1.1**) [16], [17]. The sporozoites get carried to the liver through the bloodstream. While in the liver, they infect the hepatocytes (liver cells), thus initiating the primary exoerythrocytic cycle (liver cycle) [18]. *P. vivax and P. ovale* species may undergo a dormant period before asexual reproduction during the liver cell invasion, these species are responsible for later relapse [19], [20]. The infected hepatocytes (oval sporozoites) begin dividing into a significant number of merozoites.

The merozoites invade the red blood cells (RBC), resulting in the initiation of the erythrocyte cycle (blood cycle). Once the RBCs have been invaded, the merozoites begin to grow and feed on the haemoglobin resulting in the ring form, then trophozoites and lastly schizonts [21]. The schizonts that contain merozoites rupture and release the merozoites into the bloodstream, although some get destroyed by the immune system, they immediately invade RBCs in which a new erythrocytic cycle begins. After numerous erythrocytic cycles, some of the merozoites develop into male or female gametocytes.

The gametocytes get ingested into the vector's gut when it takes a blood meal. Within the guts they mature into gametes, followed by forming a zygote, which progressively develops into an ookinete [22]. The ookinete then grows into an oocyst in the midgut of the vector. Within days or weeks of maturation the oocyst ruptures, then multiple sporozoites are released and dispersed throughout the mosquito, including the salivary glands. Therefore, the cycle continues again when the mosquito takes a blood meal [23].

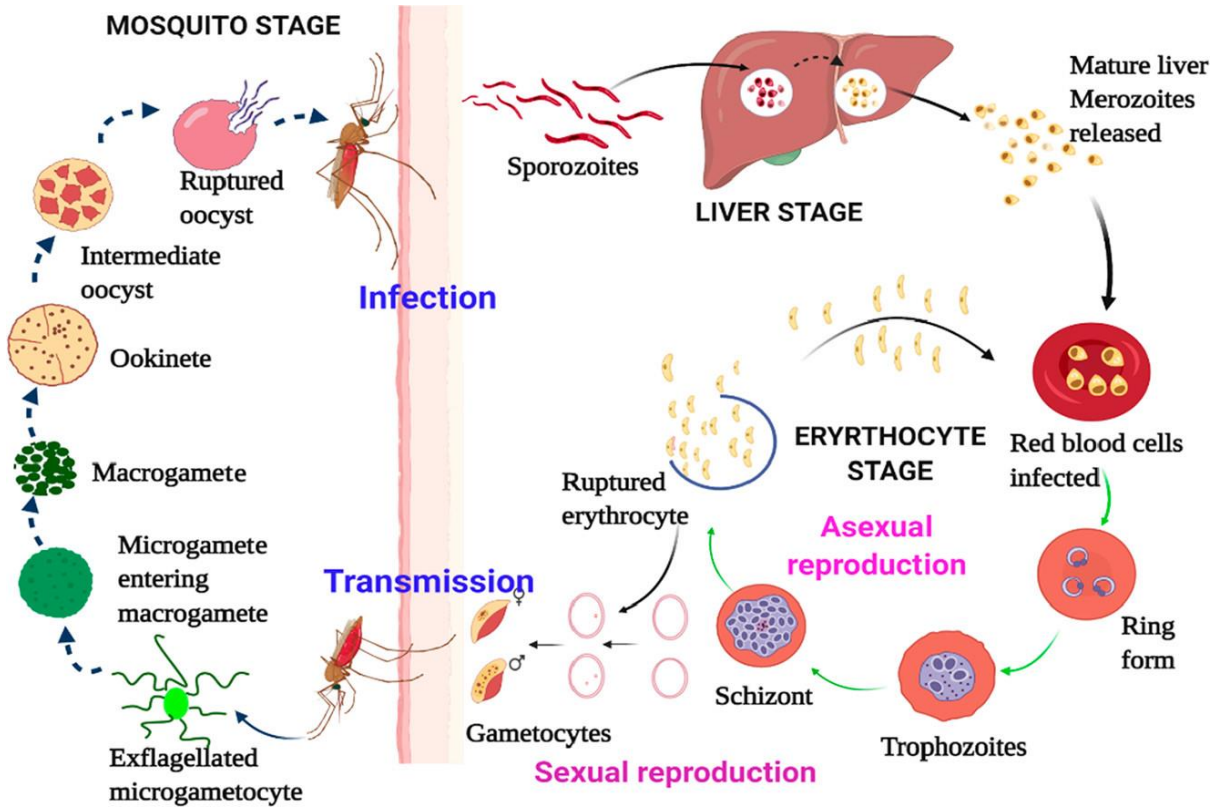

Figure 1.1: Life cycle of Plasmodium parasite in the mosquito vector and human host [24].

1.1.3. Prevention and control of malaria

The continuous spread of malaria may be manageable by various control strategies including the vector management approach, which involves the use of mosquito nets over the bed, wearing of clothes that cover most of the body, insecticides such as larvicides, and removal of potential breeding sites for mosquitoes [25]. However, the vector management approaches are not effective and eventually, the spread of malaria continues, thus, necessitating treatment [26].

Furthermore, eradication of malaria has progressed towards production of vaccine effective against malaria. For instance, pharmaceutical companies such as GlaxoSmithKline (GSK) and non-profit organizations namely the PATH's Malaria Vaccine Initiative (MVI) with support from Bill and Melinda Gates Foundation (BMGF), have been participating in the development of RTS, S/AS01 [27]. Like other various known vaccines,

RTS, S/AS01 works by targeting the circumsporozoite protein of *Plasmodium falciparum*. The vaccine has been primarily used for infants and young children with the aim to provide 3 – 4 years of immunity against the parasite [28]. As a result of the ongoing phase-3 human clinical trials, the WHO recommends the wide spread of the vaccine to children below the age of 5, regardless of moderate effectiveness [27].

1.1.4. Malaria treatment

The first known effective drug for malaria treatment, quinine (QN) **1**, was isolated from the bark of the *Cinchona*, an indigenous tree in South and Central America [29]. The isolated compound is an alkaloid that was found to be effective against blood schizonticide of human malaria, however, poor gametocide activity against *P. vivax* and *P. malariae* [30]. In 1910, the first quinine resistant *P*. *falciparum* case was reported, alerting for new development of new antimalarial drugs [31]. This resulted in the development of synthetic drugs such as chloroquine (CQ) **2**, mefloquine (MQ) **3**, piperaquine (PIP) **4**, amodiaquine (AQ) **5**, primaquine (PQ) **6**, and quinacrine (Q) **7** (**Figure 1.2**), which were found to be effective against the fatal parasite species, *P. falciparum* by inhibiting the hemozoin formation [32], [33].

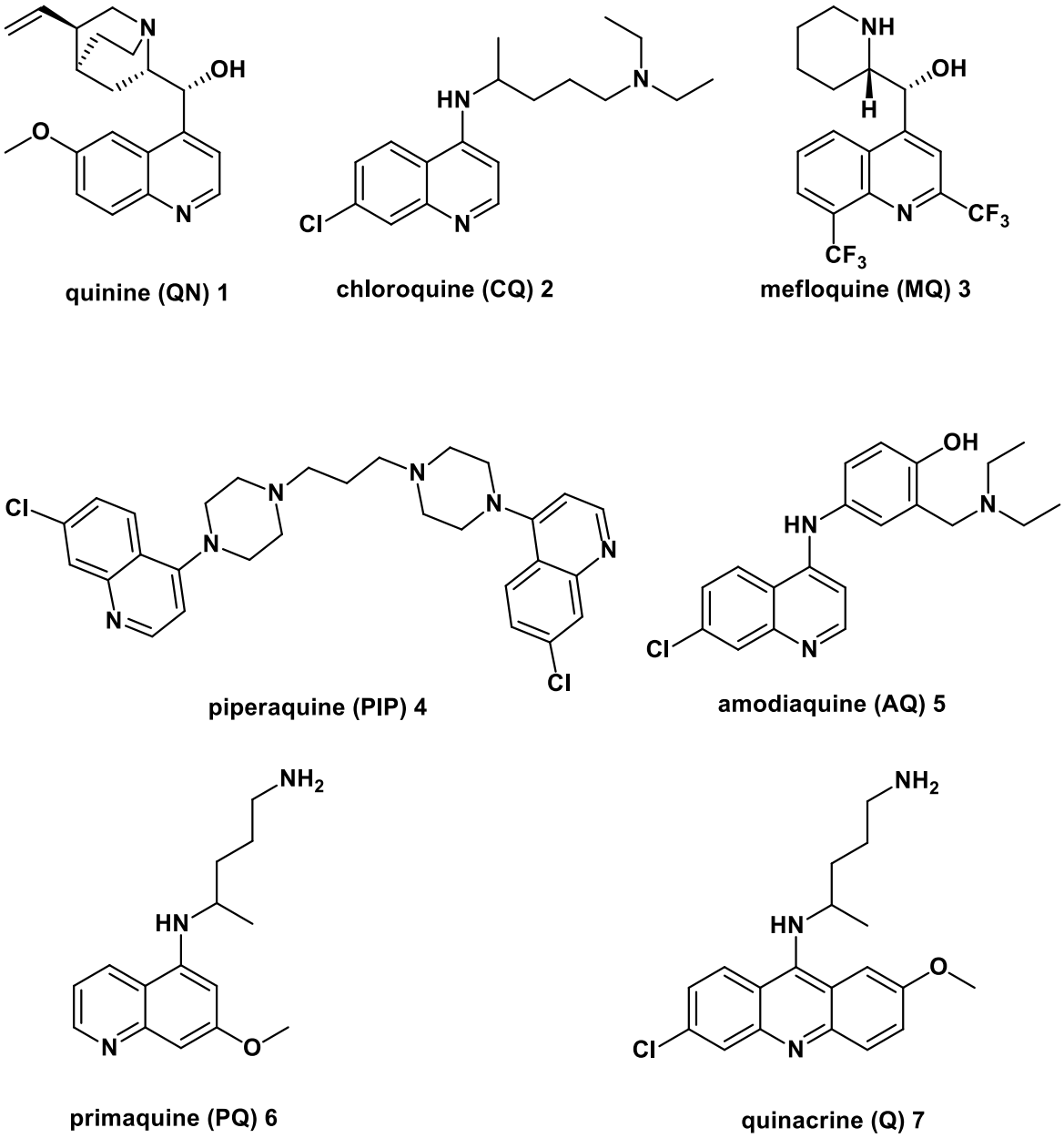

Figure 1.2: Chemical structure of the drugs that were found to be effective against malaria.

However, the parasite developed resistance against these drugs and the *Plasmodium falciparum* chloroquine resistance transporter (*Pf*CRT), a transporter located on the digestive vacuole membrane has the ability to reduce chloroquine accumulation [34] and this has become a burden in Southeast Asia [35]. Furthermore, it was reported that chloroquine, which is the most affordable and widely accessible antimalarial drug, has a

higher failure rate of about 70% - 80% [36]. Drugs such as mefloquine are effective against Chloroquine resistance, however, they exhibit neuro-psychiatric side effects and have a long half-life of 14 – 21 days, which contributes to the development of parasite resistance [25].

Antimalarial chemotherapy has shifted towards the use of Artemisinin Combination Therapies (ACTs), which involves artemisinin derivatives in combination with other drugs and has been reported to be effective against *P. falciparum* [37], [38]. Due to low solubility and bioavailability, soluble artemisinin derivatives were obtained synthetically. The artemisinin **8** derivatives include artesunate **9**, which is used in combination with pyronaridine **13**, amodiaquine **5**, or mefloquine **3**, and dihydroartemisinin **10**, which is used in combination with piperaquine, and artemether **11** is used in combination with lumefantrine **14**, lastly, the arteether **12** which is used as an alternative treatment for complicated cases (**Figure 1.3**) [39].

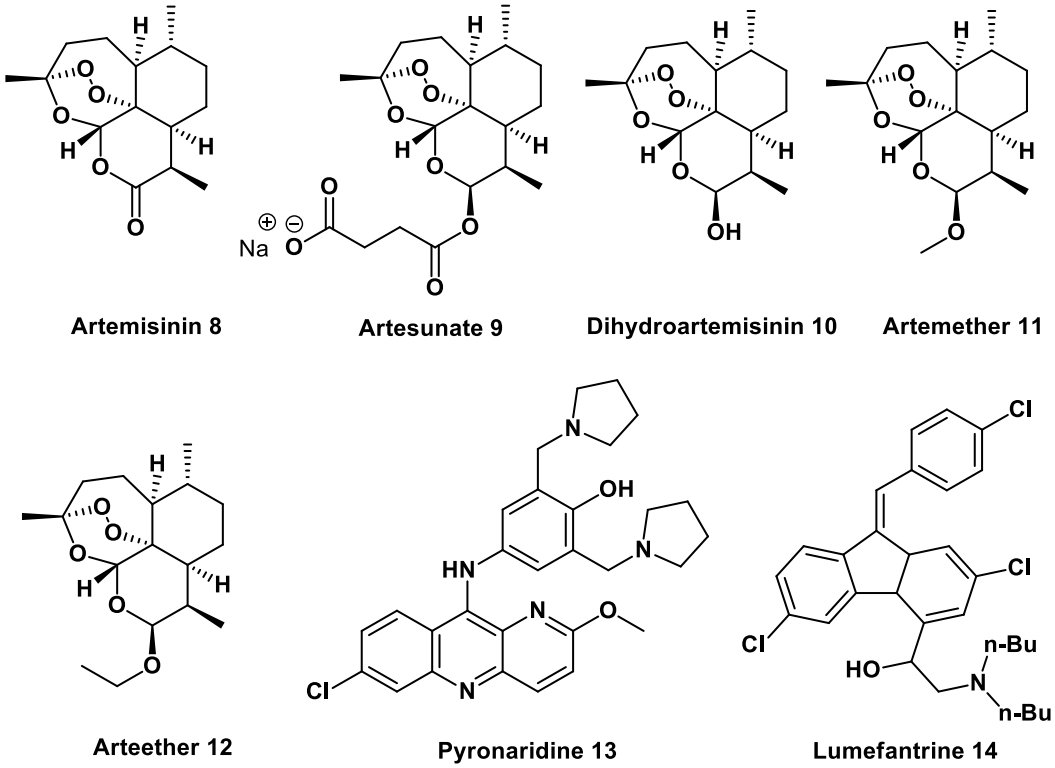

Figure 1.3: Chemical structures of artemisinin(8), arteether (12), artesunate (9), dihydroartemisinin (10), artemether (11) and selected partners.

However, the emergence of resistance towards the ACTs was reported recently in five countries of the Greater Mekong sub-region in Southeast Asia [40], [41]. The resistance is based on a mechanism of entry into quiescence that occurs at the ring stage of the parasite [42].

Therefore, there is a need for the development of more effective drugs with a new mode of action against the *protozoan* parasite, affordable especially for developing regions, safe and effective, and lastly, orally active for ease of administration.

1.2. Biological targets in antimalarial drug discovery

1.2.1. *Plasmodium* Kinase as drug targets.

Protein kinases are pivotal for transduction pathways that control and regulate the cellular processes of growth, reproduction, and development in eukaryotic cells [43]. The importance of the kinases in organisms involves the transfer of a gamma phosphate from ATP to protein, lipids, carbohydrates and/or other molecules via catalysis. The phosphorylation process serves as a key to many functions of proteins and regulates signal transduction to control cellular responses to a particular stimulation [44]. Similarly, lipid kinases serve a significant function in all aspects of cellular functions such as growth, membrane trafficking, and development in both pathogens and humans [45], [46].

Clinically validated human kinase inhibitors from the exploitation of the homologous nature of human kinases targeted for cancer therapy and parasite kinases offer a route for the development of antiparasitic drugs [47]. The *Plasmodium* kinome consists of 86 – 99 protein kinases and a small set of lipid kinases [48]. Due to the absence of tyrosine kinases (TK) and some mammalian orthologues, for example in the CDPK families, it serves as an advantage in achieving selectivity over the host [49].

Currently, drug discovery programs target kinases, *Plasmodium* protein and lipid kinases namely cyclic guanosine monophosphate (cGMP)-dependent protein kinase (*Pf*PKG) and

lipid kinase (*Pf*PI4K) offer a route for the discovery and development of new mode of action against malaria [50], [51].

1.2.2. Cyclic guanosine monophosphate (cGMP)-dependent protein kinase (PKG)

*Pf*PKG is the *Plasmodium* cyclic GMP-dependent serine/threonine protein kinase that is responsible for the phosphorylation of proteins significant for various processes of the *Plasmodium* life cycle [52]. The *Pf*PKG serves various purposes in the life cycle of the *Plasmodium* parasite in both human host and mosquito vector. It is responsible for liver stage invasion by sporozoites and the promotion of merozoite invasion and egression in the blood stage in the host [53], [54], [55]. *Pf*PKG in the vector is involved in the release of male and female gametes (gametogenesis) and ookinete motility [56]. *Pf*PKG is involved in the phosphorylation of lipid precursors for phosphoinositide synthesis, which is responsible for the mobilization of intracellular calcium [57], [52]. The formation of a zygote via fertilization of a female gamete, which develops into a motile ookinete requires a significant quantity of intracellular calcium. This signifies PKG is an important kinase and has a similar performance as that of calcium-dependent protein kinases (CDPKs) [58], [59].

The main starting point is the sporozoite invading the liver (liver stage) in the human host, then undergoing successive developmental stages resulting in hepatic merozoites invading red blood cells (blood stages) [60], [61]. Targeting the sporozoite developmental stages would provide a route to deal with the disease. For example, PKG was reported to be involved in hepatocyte infection by sporozoites of the rodent malaria species *P. berghei* (*Pb*PKG). The *P. berhgei* regulates sporozoite motility by controlling protein release from micronemes [62]. In the blood stages, inhibiting the *Pf*PKG prevents schizont rupture and merozoite egression. *Pf*PKG was shown to be significant in the maturation of merozoites by regulating the discharge of the protease *Pf*SUB1 from the exonemes, an important protease that controls modifications of parasitophorous vacuole and intracellular merozoite surface [63], [64]. An insignificant amount of protease hinders

RBCs invasion by the merozoites consequently denying the parasite access to vital substrates. Inhibition of this enzyme would result in premature development and unsuccessful RBCs rupture and release [53], [65].

*Pf*PKG has been shown to be a suitable target for novel drug discovery programs. PKG has been validated *in vivo* across multiple pathogens including toxoplasmosis, coccidiosis, and *Plasmodium*. Baker *et al*, provided *in vivo* proof in a humanized mouse model of *P*. *falciparum* infection, showing parasites clearance from the blood by oral dosing of **ML10** (**Figure 1.4**), the lead compound from imidazopyridine scaffold of potent PKG inhibitors [66].

Additionally, tri-substituted thiazoles have been shown to be fast acting in vitro for PKG inhibition [67], [68], [69]. More recently, **MMV030084** trisubstituted imidazole was reported to show potent antiplasmodium activity across the parasite life cycle, these scaffolds have subsequently become the subject of several medicinal chemistry programs [70].

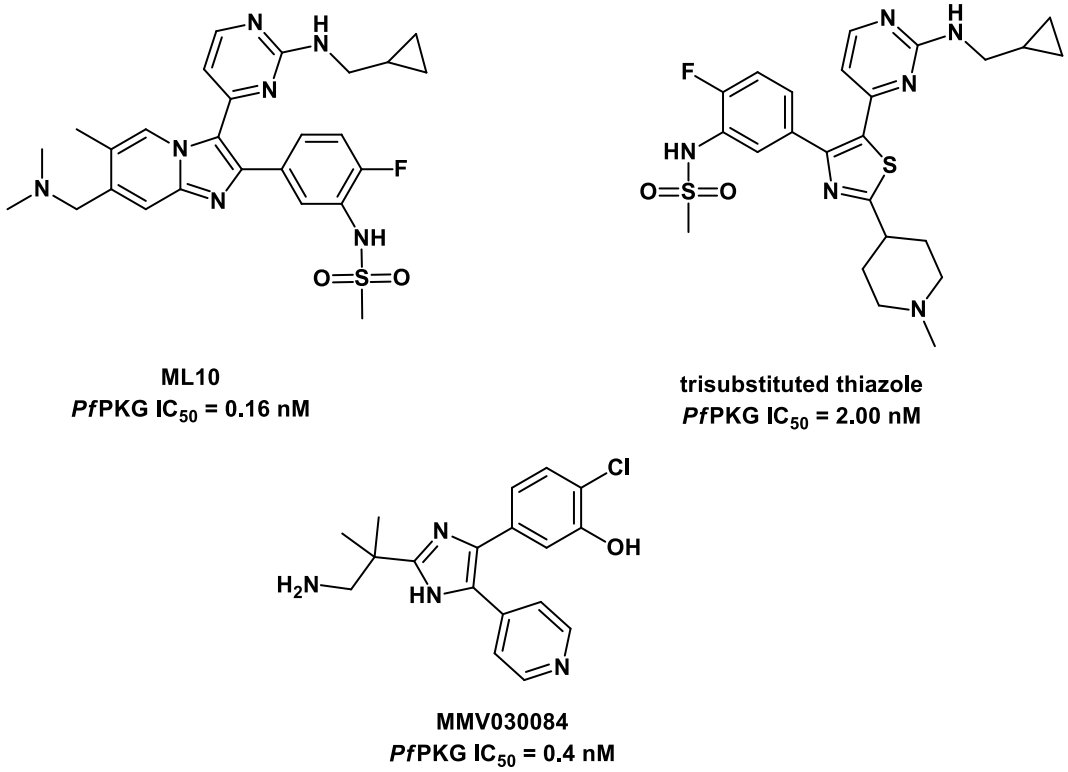

Figure 1.4:Examples of Plasmodium kinase inhibitors (PKG).

1.2.3. *Plasmodium* Phosphatidylinositol 4-kinase

Plasmodium PI4K is an important lipid kinase involved in the phosphorylation of specific substrates, such as lipids, to regulate cellular functions including growth, cell division, and membrane trafficking [71]. The PI4K phosphorylates phosphatidylinositol (PI) to produce phosphatidylinositol 4-phosphate (PI4P) derivatives, which are important lipid precursors for transduction signalling, membrane trafficking and vital for cytokinesis during the development of merozoites with suitable morphology [72], [73]. Targeting the *Plasmodium falciparum* PI4K (*Pf*PI4K) with suitable inhibitors causes complications during cytokinesis, resulting in the deformation of merozoites for continuous RBCs invasion. PI4K has been reported as an important malaria target and clinically approved [74]. Moreover, *Pf*PI4K exhibits an important function during the formation of gametocytes and oocyst development, which serves as a target window for vector-host and host-vector transmission blocking [75].

Plasmodium falciparum PI4K (*Pf*PI4K) and *Plasmodium vivax* PI4K (*Pv*PI4K) share a 97% sequence homology in the catalytic region, despite both having 58.3% sequence homology [72]. Drug development efforts have been constructed to exploit and target PIKs for drug discovery, mainly focusing on PI4K enzymes [71]. Currently, *the Plasmodium* kinase known inhibitor, **MMV390048** (**Figure 1.5**) is in phase II clinical trials as a PI4K target for malaria treatment and is effective against the stages of the parasite life cycle [72], [76]. Other preclinical compounds of similar mode of action such as **BQR695**, **KDU691**, and **UCT943** which was the optimization of **MMV390048** due to poor aqueous solubility [77], [78], [79].

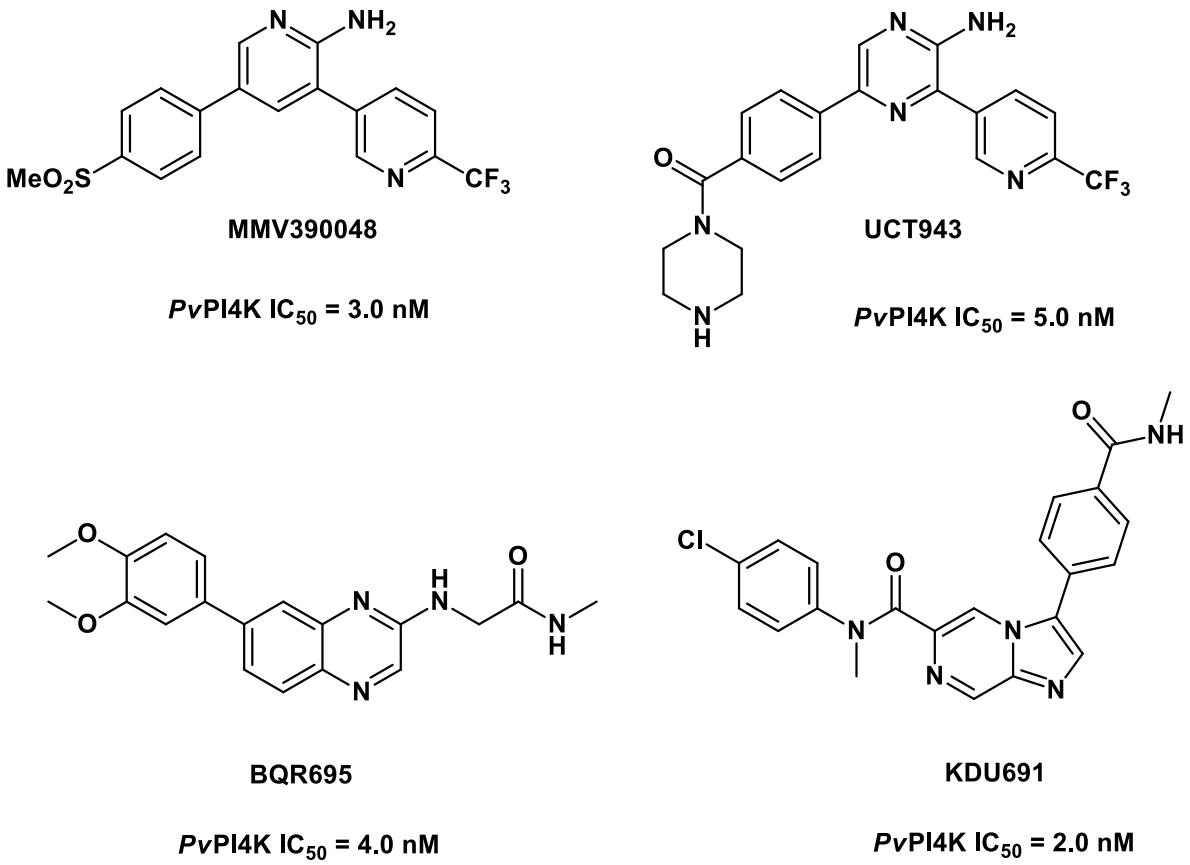

Figure 1.5**:** Structures of clinical and pre-clinical Plasmodium PI4K inhibitors.

1.6 Six: Five-Fused N-containing heteroaromatic ring system with two N-Atoms of biological importance.

Nitrogen containing fused heterocycles and/ or arenes are frequently found in natural and synthetic organic compounds with wide range of biological and pharmaceutical properties, such as anti-mycobacterial [80], anti-microbial [81], anti-viral [82] and antimalarial [83]. Among these heterocycles, pyrazole derivatives, a nitrogen containing five membered ring, have received more attention in drug discovery due to their positive contribution to the efficacy of commercially available drugs [84]. Rimonabant **15**, a nitrogen containing five membered ring, for example, is a cannabinoid ligand used for

treating obesity. Celecoxib **16**, on the other hand, a non-steroidal drug serves an as anti-inflammatory agent by inhibiting the COX-2 enzyme [85].

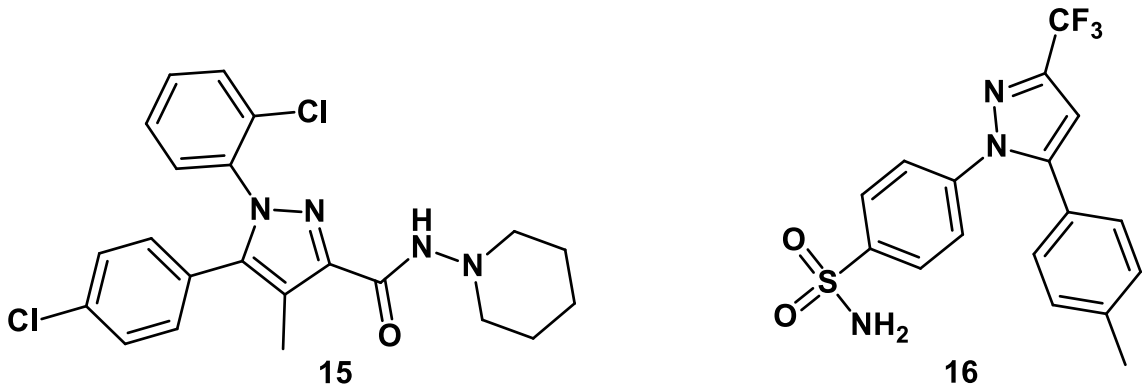

Figure 1.6: Examples of pyrazole derivatives with biological and pharmaceutical properties.

Six membered benzo-fused nitrogen containing heterocycles such as indazoles that has two possible tautomeric forms (1*H*- and 2*H*), in which the 1*H*-indazole is the most stable tautomer serve as important scaffolds in drug molecules due to their numerous pharmacological activities [86]. Sewant *et al.* synthesized and evaluated the biological activities of a series of amide indazole derivatives, among which 6-bromo-1-cyclopentyl-*N*-phenyl-1*H*-indazole-4-carboxamide **17** (**Figure 1.7**), was found to possess antioxidant and anticancer activities [87], [88]. Nassar and co-workers synthesized pyrazolo[3,4-*d*]pyrimidine derivative **18** (**Figure 1.7**), with significant cytotoxic activities against MCF-7 (IC_{50} of 45-97 nM) and HCT-116 (IC_{50} of 6-99 nM) cell lines [89].

The pyrazolo[1,5-*a*]pyridines, firstly stated by Suzue and co-workers, is an indole bioisosteres with antiviral, antibacterial, and antifungal properties [90]. 3-isobutyryl-2-isopropylpyrazolo[1,5-*a*]pyridine **19** (ibudilast), for example, is a known anti-inflammatory drug used for asthma and post-stroke vertigo treatment [91]. 5-(3-(Cyclopropylsulfonyl)phenyl)-3-(4-(methylsulfonyl)-phenyl)pyrazolo[1,5-a]pyridine **20** derived from pyrazolo[1,5-*a*]pyridine scaffold was found to be active against NF54 strain with an IC_{50} value of 2 nM [92]. Alteration of position 3 in **20** gave **21** with enhanced oral pharmacokinetics, physicochemical properties as well as *in vivo* efficacy in both *P. falciparum* SCID and *P.berghei* mouse models [92].

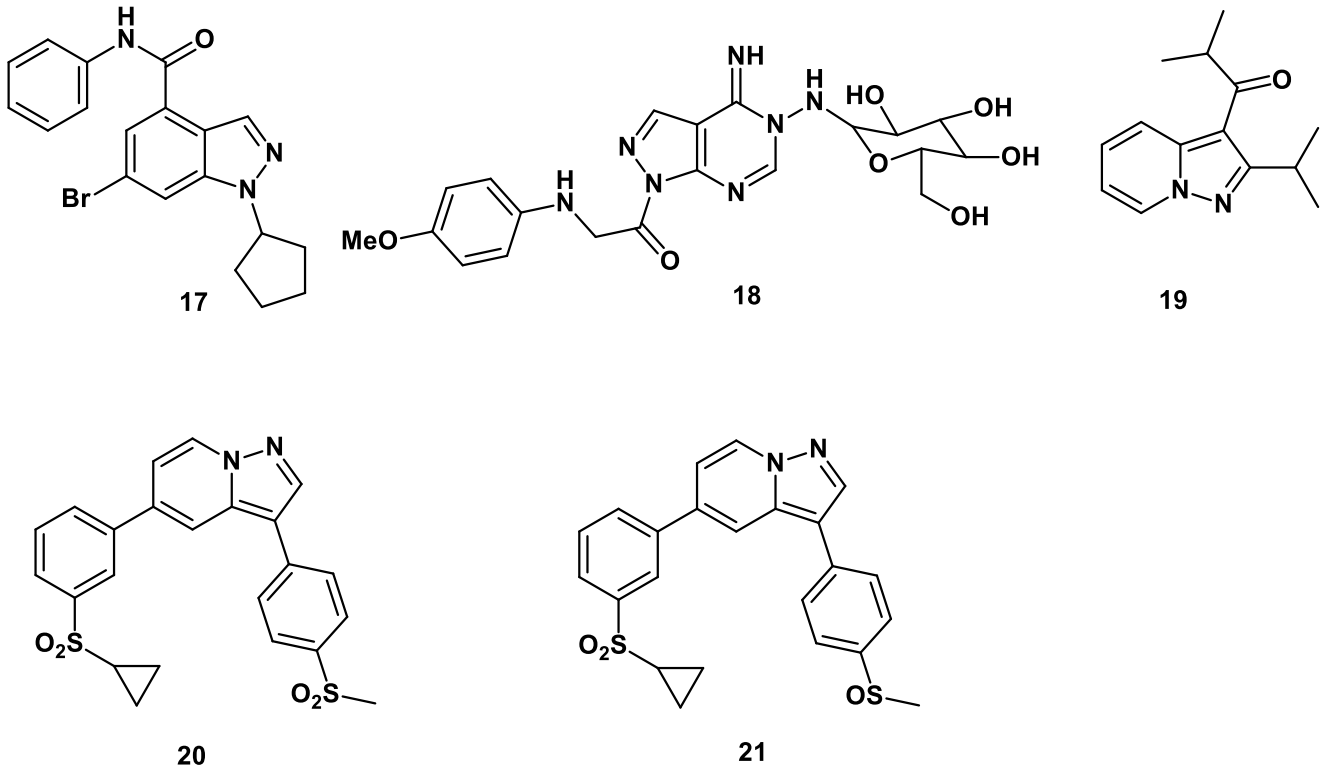

Figure 1.7: Examples of derivatives pyrazolo pyridine/pyrimidine of biological importance.

Imidazoles, which are distinguished from pyrazoles by the arrangement of the nitrogen atoms in the heterocyclic ring are also important heterocycles in the field of medicinal chemistry due to their anti-inflammatory, antibacterial, antifungal, and antiprotozoal activities [93]. Tinidazole **22** and ornidazole **23** containing the imidazole framework, for example, are commercially available drugs with antiprotozoal and antibacterial properties, respectively [94]. In another study conducted by Baker *et al*, ML10 **24**, the lead compound from imidazopyridine scaffold was found to exhibit antimalarial activity with *Pf*PKG = 0.16 nM [66]. In addition, H3D has identified the sulfone imidazopyridine compound **26** as a potent dual *Pv*PI4K and *Pf*PKG inhibitor which showed high *in vitro* and modest reduction in hERG inhibition IC_{50} (0.0048 nM). The compounds **25** and **26** showed good activity with IC_{50} values in the 50−150 nM range for the imidazopyridines (IC_{50} K1/NF54 (nM): **25**, 38/46; **26**, 113/150) [92].

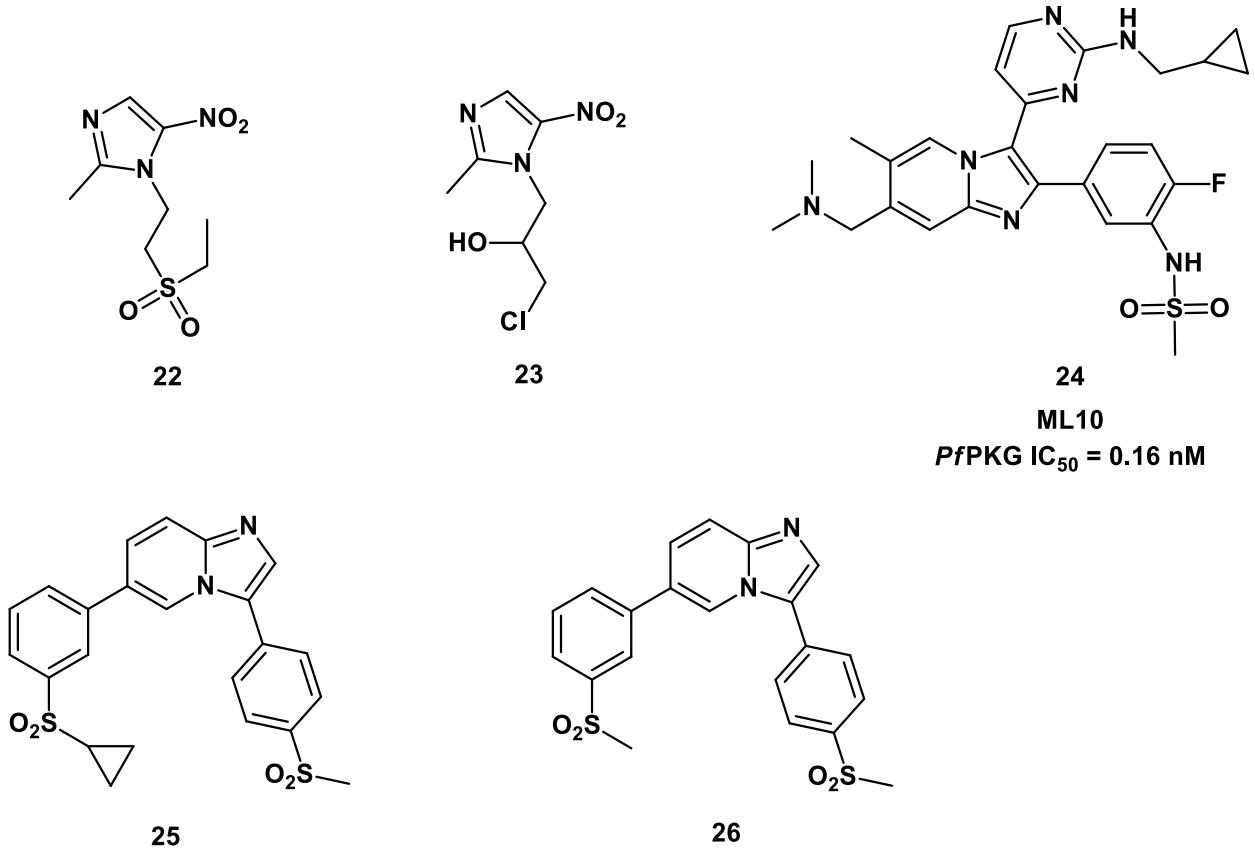

Figure 1.8: Examples of imidazolo and imidazo pyridine derivatives of biological importance.

1.7 Aim

The aim of the study is to synthesise new imidazo[1,2-a] pyridazine and pyrazolo[1,5-a] pyridine derivatives that will be tested for their antimalarial activity through the dual inhibition of *Pv*PI4K and *Pf*PKG.

1.8 Objectives

The objectives of the study will be to:

i) synthesize a new library of imidazo[1,2-a] pyridine and pyrazolo[1,5-a] pyridine derivatives, with substituents at 3rd & 6th positions and 3rd and 5th position, respectively.

ii) evaluate the activity of synthesized compounds against *Plasmodium falciparum.*

iii) investigate the inhibition of *Pv*PI4K and *Pf*PKG kinases by the synthesized compounds complemented by molecular docking studies.

References

[1] Marsh, K, “Malaria disaster in Africa,” *Lancet,* vol. 352, pp. 924 - 925, 1998.

[2] Sato, S, “Plasmodium—a brief introduction to the parasites causing human malaria and their basic biology,” *J. Physiol. Anthropol.,* pp. 1 - 13, 2021.

[3] J. Talapko, I. Škrlec, T. Alebi´c, M. Juki´c and A. V˘cev, “Malaria: The Past and the Present,” *Microorganisms,* vol. 7, no. 179, pp. 1 -17, 2019.

[4] Walker, N.; Nadjm, B.; Whitty, C., “Malaria.,” *Med.,* vol. 42, p. 52 – 58, 2017.

[5] A. K. Botwe, S. Owusu-Agyei, M. Asghar, U. Hammar, F. B. Oppong, S. Gyaase, D. Dosso, G. Jakpa, E. Boamah, M. F. Twumasi, F. Osier, A. Farnert and K. P. Asante, “Profiles of Plasmodium falciparum infections detected by microscopy through the first year of life in Kintampo a high transmission area of Ghana.,” *PLOS ONE. ,* pp. 1 - 20, 2020.

[6] World Health Organization 2015:, “Control and elimination of plasmodium vivax malaria: a technical brief.”.

[7] Al-Awadhi, M; Ahmad, S; Iqbal, J., “Current Status and the Epidemiology of Malaria in the Middle East Region and Beyond.,” *Microorganisms,* vol. 9, pp. 1 - 20., 2021.

[8] Paquet, T.; Gordon, R.; Waterson, D.; Witty, M. J.; Chibale, K., “Antimalarial aminothiazoles and aminopyridines from phenotypic whole-cell screening of a SoftFocus library.,” *Future Med. Chem.,* vol. 4, no. 18, pp. 2265 - 2277., 2012.

[9] World malaria report 2020:, “20 years of global progress and challenges.,” Geneva: World Health Organization..

[10] World malaria report 2022. Geneva:, World Health Organization, 2022.

[11] Monroe, A.; Williams, N.A.; Ogoma, S.; Karema, C.; Okumu, F., “Reflections on the 2021 World Malaria Report and the future of malaria control.,” *Malar. J.,* vol. 21, pp. 1 - 6., 2022.

[12] WHO., “The potential impact of health service disruptions on the burden of malaria: a modelling analysis for countries in sub-Saharan Africa. Geneva: World Health Organization,” 2020.

[13] Yeka, A.; Gasasira, A.; Mpimbaza, A.; Achan, J.; Nankabirwa, J.; Nsobya, S.; Staedke, S. G.; Donnelly, M. J.; Mangen, F. W.; Talisuna, A.; Dorsey, G.; Kamya, M. R.; Rosenthal, P. J., “Malaria in Uganda: Challenges to control on the long road to elimination. I. Epidemiology and current control efforts.,” *Acta Trop.,* vol. 121, pp. 184 - 195., 2012.

[14] Talisuna, A.; Grewal, P.; Rwakimari, J. B.; Mukasa, S.; Jagoe, G.; Banerji, J., “Cost is killing patients: Subsidizing effective antimalarials.,” *Lancet.,* vol. 374, pp. 1224 - 1226., 2009.

[15] Nevin, R. L., “Idiosyncratic quinoline central nervous system toxicity: Historical insights into the chronic neurological sequelae of mefloquine.,” *Int. J. Parasit.,* vol. 4, pp. 118 - 125., 2014.

[16] Tuteja, R., “Malaria – An overview.,” *FEBS J.,* vol. 274, pp. 4670 - 4679., 2007.

[17] Kumar, A.; Hosmani, R.; Jadhav, S., de Sousa, T., Mohanty, A., Naik, M., Shettigar, A., Kale, S., Valecha, N., Chery, L., Rathod, P. K., “Anopheles subpictus carry human malaria parasites in an urban area of western India and may facilitate perennial malaria transmission.,” *Malar. J.,* vol. 15, pp. 124 - 132, 2016.

[18] Vaughan, A.; M.; Mikolajczak, S. A.; Wilson, E. M.; Grompe, M.; Kaushansky, A.; Camargo, N.; Bial, J.; Ploss, A.; Kappe, S. H. I., “Complete Plasmodium falciparum liverstage development in liver-chimeric mice.,” *J. Clin. Invest.,* vol. 122, pp. 3618 - 3628., 2012.

[19] Cowman, A.; Healer, J.; Marapana, D. and Marsh, K., “Malaria.,” *Biol. dis. Cell.,* vol. 167, no. 3, pp. 610 - 624., 2016.

[20] Hawkins, V.; Joshi, H.; Rungsihirunrat, K.; Na-Bangchang, K.; Sibley, C., “Antifolates can have a role in the treatment of Plasmodium vivax.,” *Trends Parasitol.,* vol. 23, no. 5, pp. 213 - 222., 2007.

[21] Chawla, J.; Oberstaller, K.; Adams, J.H., “Targeting Gametocytes of the Malaria Parasite Plasmodium falciparum in a Functional Genomics Era: Next Steps.,” *Pathog.,* vol. 10, p. 1 – 22., 2021.

[22] Vlachou, D.; Zimmermann, T.; Cantera, R.; Janse, C.; Waters, A.; Kafatos, F., “Real-time, in vivo analysis of malaria ookinete locomotion and mosquito midgut invasion.,” *Cellular. Microbio.,* vol. 6, pp. 671 - 685., 2004.

[23] Garcia, L.S., “Malaria.,” *Clin. Lab. Med.,* vol. 30, pp. 93 - 129, 2010.

[24] Patra, S.; Singh, M.; Wasnik, K.; Pareek, D.; Gupta, P. S,; Mukherjee, S.; Paik, P., “Polymeric Nanoparticle Based Diagnosis and Nanomedicine for Treatment and Development of Vaccines dor Cerebral Malaria: A Review on Recent Advancement,” *ACS Appl. Bio Mater.,* vol. 4, no. 10, pp. 7342 - 7365, 2021.

[25] Petersen, I.; Eastman, R.; Lanzer, M., “Drug-resistant malaria: Molecular mechanisms and implications for public health.,” *FEBS Lett.,* vol. 585, no. 11, pp. 1551 - 1562., 2011.

[26] Plebanski, M.; Flanagan, K., “The Economics of Malaria Vaccine Development.,” *Trends Parasitol.,* vol. 33, no. 3, p. 154 – 156., 2017.

[27] RTS, S Partnership, Clinical Trials Partnership., “Efficacy and safety of RTS,S/AS01 malaria vaccine with or without a booster dose in infants and children in Africa: Final results of a phase 3, individually randomised, controlled trial.,” *Lancet.,* vol. 386, no. 9988, pp. 31 - 45, 2015.

[28] WHO, “Historic RTS,S/AS01 recommendation can reinvigorate the fight against malaria.,” https://www.who.int/news/item/06-10-2021-who, 2021.

[29] Achan, J.; Talisuna, A. O.; Erhart, A.; Yeka, A.; Tibenderana, J. K.; Baliraine, F. N.; Rosenthal, P. J; D’Alessandro, U., “Quinine, an old anti-malarial drug in a modern world: Role in the treatment of malaria.,” *Malar J.,* vol. 144, p. 1 – 12., 2011.

[30] Flannery, E. L.; Chatterjee, A. K,; Winzeler, E. A., “Antimalarial drug discovery - approaches and progress towards new medicines.,” *Nat. Rev. Microbiol.,* vol. 11, pp. 849 - 862., 2013.

[31] Wongsrichanalai, C.; Pickard, A.; Wernsdorfer, W; Meshnick, S., “Epidemiology of drug-resistant malaria.,” *Lancet Infect. Dis.,* vol. 2, no. 4, pp. 209 - 218., 2002.

[32] Schwikkard, S.; van Heerden, F., “Antimalarial activity of plant metabolites.,” *Nat. Prod. Rep.,* vol. 19, no. 6, pp. 675 - 692., 2002.

[33] Solomon, V.; Lee, H., “Chloroquine and its analogs: A new promise of an old drug for effective and safe cancer therapies.,” *Eur. J. Pharmacol.,* vol. 625, no. 1 - 3, pp. 220 - 233., 2009.

[34] Chinappi, M.; Via, A.; Marcatili, P.; Tramontano, A., “On the Mechanism of Chloroquine Resistance in Plasmodium falciparum.,” *PLoS ONE.,* vol. 5, no. 11, pp. 1 - 12, 2010.

[35] Gernaat H. B. P.; Dechering, W. H. J. C.; Voorhoeve, H. W. A., “Clinical epidemiology of paediatric disease at Nchelenge, north-east Zambia.,” *Ann. Trop. Paediatr.,* vol. 18, p. 129 – 138., 1998.

[36] Tse, E. G.; Korsik, M.; Todd, M. H., “The past, present and future of anti malarial medicines.,” *Malar. J.,* pp. 1 - 21, 2019.

[37] Li, Q.; Xie, L. H.; Johnson, T. O.; Si, Y.; Haeberle, A. S.; Weina, P. J., “Toxicity and evaluation of artesunate and artelinate in Plasmodium berghei-infected and uninfected rats.,” *Trans. R. Soc. Trop. Med. Hyg.,* vol. 101, pp. 104 - 112., 2007.

[38] O"Neill, P. M.; Barton, V. E.; Ward, S. A., “The molecular mechanism of action of artemisinin – The debate continues.,” *Molecules.,* vol. 15, pp. 1705 - 1721., 2010.

[39] World Health Organization:, “Guidelines for the Treatment of Malaria.,” pp. 1 - 88, 2015.

[40] Egwu, C. O.; P´erio, P.; Augereau, J.-M.; Tsamesidis, I.; Benoit-VicalFran, C.; Reybier, K., “Resistance to artemisinin in falciparum malaria parasites: A redox-mediated phenomenon.,” *Free Radic. Biol. Med.,* vol. 179, pp. 317 - 327., 2022.

[41] Anamika, K.; Srinivasan, N.; Krupa, A., “A Genomic Perspective of Protein Kinases in Plasmodium falciparum.,” *PROTEINS: Struct. Funct. Bioinform.,* pp. 180-189., 2005.

[42] Ouji, M.; Augereau, J.-M.; Paloque, L.; Benoit-Vical, F., “Plasmodium falciparum resistance to artemisinin-based combination therapies: A sword of Damocles in the path toward malaria elimination.,” *Parasite.,* pp. 1 - 12, 2018.

[43] Coppi, A.; Tewari, R.; Bishop, J.; Bennett, B.; Lawrence, R., “Heparan sulfate proteoglycans provide a signal to Plasmodium sporozoites to stop migrating and productively invade cells.,” *Cell Host Microbe.,* vol. 2, no. 5, pp. 316 - 327., 2008.

[44] Bennik, S.; Kiesow, M. J.; Pradel, G., “The development of malaria parasites in the mosquito midgut.,” *Cell. Microbiol.,* vol. 18, no. 7, pp. 905 - 918., 2016.

[45] Burke, J., “Structural basis for regulation of phosphoinositide kinases and their involvement in human disease.,” *Mol. Cell.,* vol. 71, no. 5, pp. 653 - 673., 2018.

[46] Mejdrová, I.; Chalupská, D.; Plačková, P.; Müller, C.; Šála, M.; Klíma, M.; Baumlová, A.; Hřebabecký, H.; Procházková, E.; Dejmek, M.; Strunin, D.; Weber, J.; Lee, G.; Matoušová, M.; Mertlíková-Kaiserová, H.; Ziebuhr, J.; Birkus, G.; Boura, E.; Nencka,

“Rational design of novel highly potent and selective Phosphatidylinositol 4-kinase IIIβ (PI4KB) inhibitors as broad-spectrum antiviral agents and tools for chemical biology.,” *J. Med. Chem.,* vol. 60, no. 1, pp. 100 - 118, 2017.

[47] Njoroge, M.; Njuguna, N.; Mutai, P.; Ongarora, D.; Smith, P.; Chibale, K., “Recent approaches to chemical discovery and development against malaria and the neglected tropical diseases human African trypanosomiasis and schistosomiasis.,” *Chem. Rev.,* vol. 114, no. 22, pp. 11138 - 11163, 2014.

[48] Cabrera, D.; Horatscheck, A.; Wilson, C.; Basarab, G.; Eyermann, C.; Chibale, K., “Plasmodial Kinase Inhibitors: License to Cure?.,” *J. Med. Chem.,* vol. 61, no. 18, pp. 8061 - 8077., 2018.

[49] Arendse, L.; Wyllie, S.; Chibale, K. and Gilbert, I., “Plasmodium kinases as potential drug targets for malaria: Challenges and opportunities.,” *ACS Infect. Dis.,* vol. 7, no. 3, pp. 518 - 534., 2021.

[50] Lucet, I.; Tobin, A.; Drewry, D. and Wilks, A. , “Plasmodium kinases as targets for newgeneration antimalarials.,” *Future Med. Chem. ,* vol. 4, no. 18 , pp. 2295 - 2310., 2012.

[51] Srinivasan, N.; Krupa, A., “ A genomic perspective of protein kinases in Plasmodium falciparum.,” *Proteins.,* vol. 189, no. 6 , pp. 180 - 189., 2005.

[52] Bennink, S.; Pradel, G., “ Vesicle dynamics during the egress of malaria gametocytes from the red blood cell.,” *Mol. Biochem. Parasitol. ,* vol. 243, pp. 1-7, 2021.

[53] Collins, C.; Hackett, F.; Strath, M.; Penzo, M.; Withers-Martinez, C.; Baker, D.; Blackman, M., “ Malaria parasite cGMP-dependent protein kinase regulates blood stage merozoite secretory organelle discharge and egress.,” *PLoS Pathog. ,* vol. 9 , no. 5, pp. 1 - 13, 2013.

[54] Hopp, C.; Bowyer, P.; Baker, D., " The role of cGMP signalling in regulating life cycle progression of Plasmodium.," *Microbes Infect. ,* vol. 14, no. 10, pp. 831 - 837., 2012.

[55] Baker, D., "Cyclic nucleotide signalling in malaria parasites.," *Cell Microbiol. ,* vol. 13, no. 3, pp. 331 - 339., 2011.

[56] Lakshmanan, V.; Fishbaughera, M.; Morrisona, B.; Baldwina, M.; Macarulaya, M.; Vaughana, A.; Mikolajczaka, S.; Kappea, S., " Cyclic GMP balance is critical for malaria parasite transmission from the mosquito to the mammalian host.," *mBio. ,* vol. 6 , no. 2, pp. 1 - 10, 2015.

[57] Mcrobert, L.; Taylor, C.; Deng, W.; Fivelman, Q.; Cummings, R.; Polley, S.; Billker, O.; Baker, D., "Gametogenesis in malaria parasites is mediated by the cGMP-Dependent protein kinase.," *PLoS Bio.,* vol. 6, no. 6, pp. 1 - 10., 2008.

[58] Ishino, T.; Orito, Y.; Chinzei, Y.; Yuda, M. , "A calcium-dependent protein kinase regulates Plasmodium ookinete access to the midgut epithelial cell.," *Mol. Microbio. ,* vol. 59, pp. 1175 - 1184., 2006.

[59] Moon, R.; Taylor, C.; Bex, C.; Schepers, R.; Goulding, D.; Janse, C.; Waters, A.; Baker, D.; Billker, O., "A Cyclic GMP signalling module that regulates gliding motility in a malaria parasite.," *PLoS Pathog. ,* vol. 5, no. 9 , pp. 1 -14., 2009.

[60] Amino, R.; Thiberge, S.; Blazquez, S.; Baldacci, P.; Renaud, O.; Shorte, S.; Ménard, R., "Imaging malaria sporozoites in the dermis of the mammalian host.," *Nat. Protoc.,* vol. 2 , no. 7, pp. 1705 - 1712., 2007.

[61] Thiberge, S.; Blazquez, S.; Baldacci, P.; Renaud, O.; Shorte, S.; Ménard, R.; Amino, R., "In vivo imaging of malaria parasites in the murine liver.," *Nat. Protoc. ,* vol. 2 , no. 7, pp. 1811 - 1818., 2007.

[62] Falae, A.; Combe, A.; Amaladoss, A.; Carvalho, T.; Menard, R.; Bhanot, P., "Role of Plasmodium berghei cGMP-dependent protein kinase in late liver stage development.," *J. Biol. Chem.,* vol. 285 , no. 5, pp. 3282 - 3288, 2010.

[63] Absalon, S.; Blomqvist, K.; Rudlaff, R.; Delano, T.; Pollastri, M.; Dvorin, J., “ Calcium2+ dependent protein kinase 5 is required for egress-specific organelles in Plasmodium falciparum.,” *mBio. ,* vol. 9 , no. 1, pp. 1 - 16., 2018.

[64] Yeoh, S.; O'Donnell, R.; Koussis, K.; Dluzewski, A.; Ansell, K.; Osborne, S.; Hackett, F.; Withers-Martinez, C.; Mitchell, G.; Bannister, L.; Bryans, J.; Kettleborough, C.; Blackman, M., “Subcellular discharge of a serine protease mediates release of invasive malaria parasites from host erythrocytes.,” *Cell.,* pp. 1072 - 1083, 2007.

[65] Govindasamy, K.; Jebiwott, S.; Jaijyan, D.; Davidow, A.; Ojo, K.; Van Voorhis, W.; Brochet, M.; Billker, O.; Bhanot, P. , “Invasion of hepatocytes by Plasmodium sporozoites requires cGMP-dependent protein kinase and calcium dependent protein kinase 4.,” *Mol. MIcrobiol.,* vol. 102, no. 2, pp. 349 - 363, 2016.

[66] Baker, D.; Stewart, L.; Large, J.; Bowyer, P.; Ansell, K.; Jiménez-Díaz, M.; El Bakkouri, M.; Birchall, K.; Dechering, K.; Bouloc, N.; Coombs, P.; Whalley, D.; Harding, D.; Smiljanic-Hurley, E.; Wheldon, M.; Walker, E.; Dessens, J.; Lafuente, M.; Sanz, L;, “A potent series targeting the malarial cGMP-dependent protein kinase clears infection and blocks transmission.,” *Nat. Commun. ,* vol. 8, no. 1, pp. 1 - 9., 2017.

[67] Vanaerschot, M.; Murithi, J.; Pasaje, C.; Ghidelli-Disse, S.; Dwomoh, L.; Bird, M.; Spottiswoode, N.; Mittal, N.; Arendse, L.; Owen, E.; Wicht, K.; Siciliano, G.; Bosche, M.; Yeo, T.; Kumar, T.; Mok, S.; Carpenter, E.; Giddins, M.; Sanz, O.;, “Inhibition of resistance-refractory P. falciparum kinase PKG delivers prophylactic, blood stage, and transmission-blocking antiplasmodial activity.,” *Chembiol. ,* pp. 1 - 11, 2020.

[68] Gurnett, A.; Liberator, P.; Dulski, P.; Salowe, S.; Donald, R.; Anderson, J.; Wiltsie, J.; Diaz, C.; Harris, G.; Chang, B.; Darkin-Rattray, S.; Nare, B.; Crumley, T.; Blum, P.; Misura, A.; Tamas, T.; Sardana, M.; Yuan, J.; Biftu, T.; Schmatz, D., “Purification and molecular characterization of cGMP-dependent protein kinase from Apicomplexan parasites.,” *J. Biol. Chem. ,* vol. 277 , no. 18, p. 15913 – 15922., 2002.

[69] Donald, R.; Zhong, T.; Wiersma, H.; Nare, B.; Yao, D.; Lee, A.; Allocco, J.; Liberator, P., " Anticoccidial kinase inhibitors: Identification of protein kinase targets secondary to cGMP-dependent protein kinase.," *Mol. Biochem. Parasitol. ,* vol. 149, p. 86 – 98, 2006.

[70] Tsagris, D.; Birchall, K.; Bouloc, N.; Large, J.; Merritt, A.; Smiljanic-Hurley, E.; Wheldon, M.; Ansell, K.; Kettleborough, C.; Whalley, D.; Stewart, L.; Bowyer, P.; Baker, D.; Osborne, S., "Trisubstituted thiazoles as potent and selective inhibitors of Plasmodium falciparum protein kinase G (PfPKG).," *Bioorg. Med. Chem. Lett. ,* vol. 28, no. 19, pp. 3168 - 3173., 2019.

[71] Hassett, M.; Roepe, P. , "PIK-ing new malaria chemotherapy.," *Trends Parasitol. ,* vol. 34, no. 11, pp. 925 - 927., 2018.

[72] McNamara, C. W.; Lee, M. C. S.; Lim, C. S.; Lim, S. H.; Roland, J.; Nagle, A.; Simon, O.; Yeung, B. K. S.; Chatterjee, A. K.; McCormack, S. L.; Manary, M. J.; Zeeman, A.-M.; Dechering, K. J.; Kumar, T. R. S.; Henrich, P. P.; Gagaring, K.; Ibanez, M.;, "Targeting Plasmodium PI(4)K to eliminate malaria.," *Nature. ,* vol. 504, pp. 248-253, 2013.

[73] Balla, T. , "Phosphoinositides: Tiny lipids with giant impact on cell regulation.," *Physiol. Rev. ,* vol. 93 , no. 3, pp. 1019 - 1137., 2013.

[74] Dembele, L.; Ang, X.; Chavchich, M.; Bonamy, G.; Selva, J.; Yi-Xiu Lim, M.; Bodenreider, C.; Yeung, B.; Nosten, F.; Russell, B.; Edstein, M.; Straimer, J.; Fidock, D.; Diagana, T.; Bifani, P., "The Plasmodium PI(4)K inhibitor KDU691 selectively inhibits dihydroartemisinin-pretreated Plasmodium falciparum ring-stage parasites.," *Sci. Rep. ,* vol. 7 , no. 1, pp. 1 - 9, 2017.

[75] Zeeman, A.; Lakshminarayana, S.; van der Werff, N.; Klooster, E.; Voorberg-van der Wel, A.; Kondreddi, R.; Bodenreider, C.; Simon, O.; Sauerwein, R.; Yeung, B.; Diagana, T.; Kocken, C., "PI4 Kinase is a prophylactic but not radical curative target

in Plasmodium vivax-type malaria parasites.," *Antimicrob. Agents Chemother.* , vol. 60, no. 5, pp. 2858 - 2863., 2016.

[76] Sinxadi, P.; Donini, C.; Johnstone, H.; Langdon, G.; Wiesner, L.; Allen, E.; Duparc, S.; Chalon, S.; McCarthy, J. S.; Lorch, U.; Chibale, K.; Mohrle, J.; Barnes, K. I., "Safety, tolerability, pharmacokinetics and antimalarial activity of the novel Plasmodium phosphatidylinositol 4-kinase inhibitor MMV390048 in healthy volunteers.," *Antimicrob. Agents Chemother. ,* vol. 64, pp. e01896-19., 2020.

[77] Okombo, J.; Chibale, K., "Recent updates in the discovery and development of novel antimalarial drug candidates.," *Med. Chem. Comm.,* vol. 9, no. 3, pp. 437 - 453., 2018.

[78] Kato, N.; Comer, E.; Sakata-Kato, T.; Sharma, A.; Sharma, M.; Maetani, M.; Bastien, J.; Brancucci, N.; Bittker, J.; Corey, V.; Clarke, D.; Derbyshire, E.; Dornan, G.; Duffy, S.; Eckley, S.; Itoe, M.; Koolen, K.; Lewis, T.; Lui, P.; Lukens, A.; Lund, E.;, "Diversity-oriented synthesis yields novel multistage antimalarial inhibitors.," *Nature,* vol. 538 , no. 7625, pp. 344 - 349, 2016.

[79] Kandepedu, N.; Cabrera, D.; Eedubilli, S.; Taylor, D.; Brunschwig, C.; Gibhard, L. Njoroge, M.; Lawrence, N.; Paquet, T.; Eyermann, C.; Spangenberg, T.; Basarab, G.; Street, L.; Chibale, K., "Identification, characterization, and optimization of 2,8-disubstituted-1,5-naphthyridines as novel Plasmodium falciparum phosphatidylinositol4-kinase inhibitors with in vivo efficacy in a humanized mouse model of malaria.," *J. Med. Chem. ,* vol. 61 , no. 13, pp. 5692 - 5703, 2018.

[80] Quiroga J.; Diaz Y.; Bueno J.; Insuasty B.; Abonia R.; Ortiz A.; Nogueras, M.; Cobo, J., "Microwave induced three-component synthesis and antimycobacterial activity of benzopyrazolo[3,4-b] quinolindiones.," *Eur. J. Med. Chem.,* vol. 74, pp. 216 - 224, 2014.

[81] Selvi S.T., Nadaraj V., Mohan S., Sasi R., Hema M., , “Solvent free microwave synthesis and evaluation of antimicrobial activity of pyrimido[4,5-b]- and pyrazolo[3,4-b]quinolines.,” *Bioorg. Med. Chem. ,* vol. 14, pp. 3896-3903., 2006.

[82] Rádl S., Zikán V., , “Synthesis of 1,2, and 9-methyl derivatives of 4,9-dihydro-6-methoxy-3-methyl-4-oxo-1H(2H)-pyrazolo[3,4-b] quinoline and 4,9-dihydro-6-hydroxy-3-methyl-4-oxo-1H(2H)- pyrazolo[3,4-b] quinoline and their antiviral activity. Collect Czech,” *Chem. Commun,* vol. 52, pp. 788 - 792, 1987.

[83] Stein R.G., Biel J.H., Singh T.,, “Antimalarials. 4-substituted 1H-pyrazolo[3,4-b]quinolines.,” *J. Med. Chem.,* vol. 13, pp. 153-155. , 1970.

[84] Vijesh, A.M.; Isloor, A.M.; Shetty, P.; Sundershan, S.; Fun, H.K., “New pyrazole derivatives containing 1,2,4-triazoles and benzoxazoles as potent antimicrobial and analgesic agents,,” *Eur. J. Med. Chem.,* vol. 62, pp. 410-415, 2013.

[85] Mert, S.; Kasımo˘ gulları, R.; Iça, T.; Çolak, F.; Altun, A.; Ok, S. , “Synthesis, structure–activity relationships, and in vitro antibacterial and antifungal activity evaluations of novel pyrazole carboxylic and dicarboxylic acid derivatives.,” *Eur. J. Med. Chem.,* vol. 78, pp. 86 - 96, 2014.

[86] S. Zhang, C. Liang and W. Zhang, “ Recent advances in indazole-containing derivatives: Synthesis and biological perspectives.,” *Molecules.,* vol. 23, p. 2783., 2018.

[87] Sawant, A.S.; Kamble, S.S.; Pisal, P.M.; Meshram, R.J.; Sawant, S.S.; Kamble, V.A.; Kamble, V.T.; Gacche, R.N., “Synthesis and evaluation of a novel series of 6-bromo-1-cyclopentyl-1H-indazole-4-carboxylic acid-substituted amide derivatives as anticancer, antiangiogenic, and antioxidant agents.,” *Med. Chem. Res. ,* vol. 29, p. 17–32., 2020.

[88] Zhang, M.; Fang, X.;Wang, C.; Hua, Y.; Huang, C.;Wang, M.; Zhu, L.;Wang, Z.; Gao, Y.; Zhang, T.; Liu, H.; Zhang, Y.; Lu, S.; Lu, T.; Chen, Y.; Li, H.,, “Design and synthesis of 1H-indazole-3-carboxamide derivatives as potent and selective PAK1

inhibitors with anti-tumour migration and invasion activities.," *Eur. J. Med. Chem.,* vol. 203, p. 112517, 2020.

[89] Nassar, I.F.; Abdel Aal, M.T.; El-Sayed, W.A.; Shahin, A.E.M.; Elsakka, E.G.E.; Mokhtar, M.M.; Hegazy, M.; Hagras, M.; Mandour, A.A.; Ismail, N.S.M., "Discovery of pyrazolo[3,4-d]pyrimidine and pyrazolo[4,3-e][1,2,4]triazolo[1,5-c]pyrimidine derivatives as novel CDK2 inhibitors: Synthesis, biological and molecular modeling investigations.," *RSC Adv. ,* vol. 12, p. 14865–14882., 2022.

[90] Allen, S. H.; Johns, B. A.; Gudmundsson, K. S.; Freeman, G. A.; Boyd, F. L.; Sexton, C. H.; Selleseth, D. W.; Creech, K. L.; Moniri, K. R. , "Synthesis of C-6 substituted pyrazolo[1,5-a] pyridine with potent activity against herpesviruses," *Bioorg. Med. Chem.,* vol. 14, pp. 944 - 954, 2006.

[91] Rolan, P.; Hutchinson, M. R.; Johnson, K. W. , "Ibudilast: a review of its pharmacology, efficacy and safety in respiratory and neurological disease,," *Expert Opin Pharmacother., ,* vol. 10, pp. 2897-2904., 2009, .

[92] Le Manach, C.; Paquet, T.; Brunschwig, C.; Njoroge, M.; Han, Z.; Cabrera, D. G.; Bashyam, S.; Dhinakaran, R.; Taylor, D.; Reader, J.; Botha, M.; Churchyard, A.; Lauterbach, S.; Coetzer, T. L.; Birkholtz, L. M.; Meister, S.; Winzeler, E. A.; Waterson, D.;, "A Novel Pyrazolopyridine with in Vivo Activity in Plasmodium berghei- and Plasmodium falciparum-Infected Mouse Models from Structure−Activity Relationship Studies around the Core of Recently Identified Antimalarial Imidazopyridazines.," *J. Med. Chem. ,* vol. 58, pp. 8713 - 8722, 2015.

[93] Reyes-Arellano A, Gómez-García O, Torres-Jaramillo J. , "Synthesis of azolines and imidazoles and their use in drug design.," *Med. Chem.,* vol. 6, p. 561 – 570, 2016.

[94] Verma, BK,; Kapoor, S,; Kumar, U,; Pandey, S,; Arya, P. , "Synthesis of new imidazole derivatives as effective antimicrobial agents.," *Indian J Pharm Biol Res. ,* vol. 5, no. 1, p. 1–9., 2017.

CHAPTER 2: RESULTS AND DISCUSSION OF IMIDAZO[1,2-a]PYRIDINE AND PYRAZOLO[1,5-a]PYRIDINE.

2.1 Synthesis of 3,6-substituted imidazo[1,2-a]pyridine derivatives

The main aim of this investigation was to synthesize 6-chloro imidazo[1,2-a]pyridine to be used as substrate for the synthesis of 3,6-substituted imidazo[1,2-a]pyridine derivatives. To achieve this, 6-chloro imidazo[1,2-a]pyridine used as substrate in this investigation was synthesized from commercially available 5-chloropyridin-2-amine and 2-chloroacetaldehyde as discussed below.

2.1.1 Synthesis of 6-chloro imidazo[1,2-a]pyridine (29)

Literature has reported numerous methods for the synthesis of imidazo [1,2-a]pyridine scaffold, such as multicomponent reaction [1] and cyclo-condensation reaction [2]. Juillet *et al*, reported the synthesis of imidazo [1,2-a]pyridine from the cyclo-condensation of commercially available substituted amino pyridine and chloroacetaldehyde [2]. Adopting the literature procedure, commercially available 5-chloropyridin-2-amine **27** and 2-chloroacetaldehyde **28** were refluxed in ethanol overnight to afford the 6-chloro imidazo[1,2-a]pyridine **29** in 75% yield. The prepared 6-chloro imidazo[1,2-a]pyridine **29** was confirmed using ^{1}H-NMR and ^{13}C-NMR. The ^{1}H-NMR spectrum revealed the presence of two doublets at the region 7.64 ppm and 7.56 ppm corresponding to H-2 and H-3, respectively. The ^{13}C-NMR spectrum, on the other hand, reveled the appearance of seven carbon peaks belonging to compound **29** (**Fig. 2.1**).

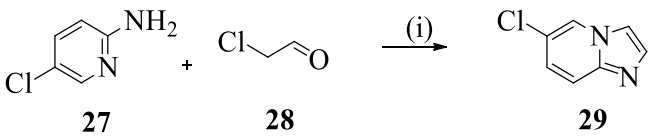

27 **28** **29**

Reagents and conditions: (i) EtOH, reflux, 17 h.

Scheme 1: Cyclo-condensation of 5-chloropyridin-2-amine and 2-chloroacetaldehyde

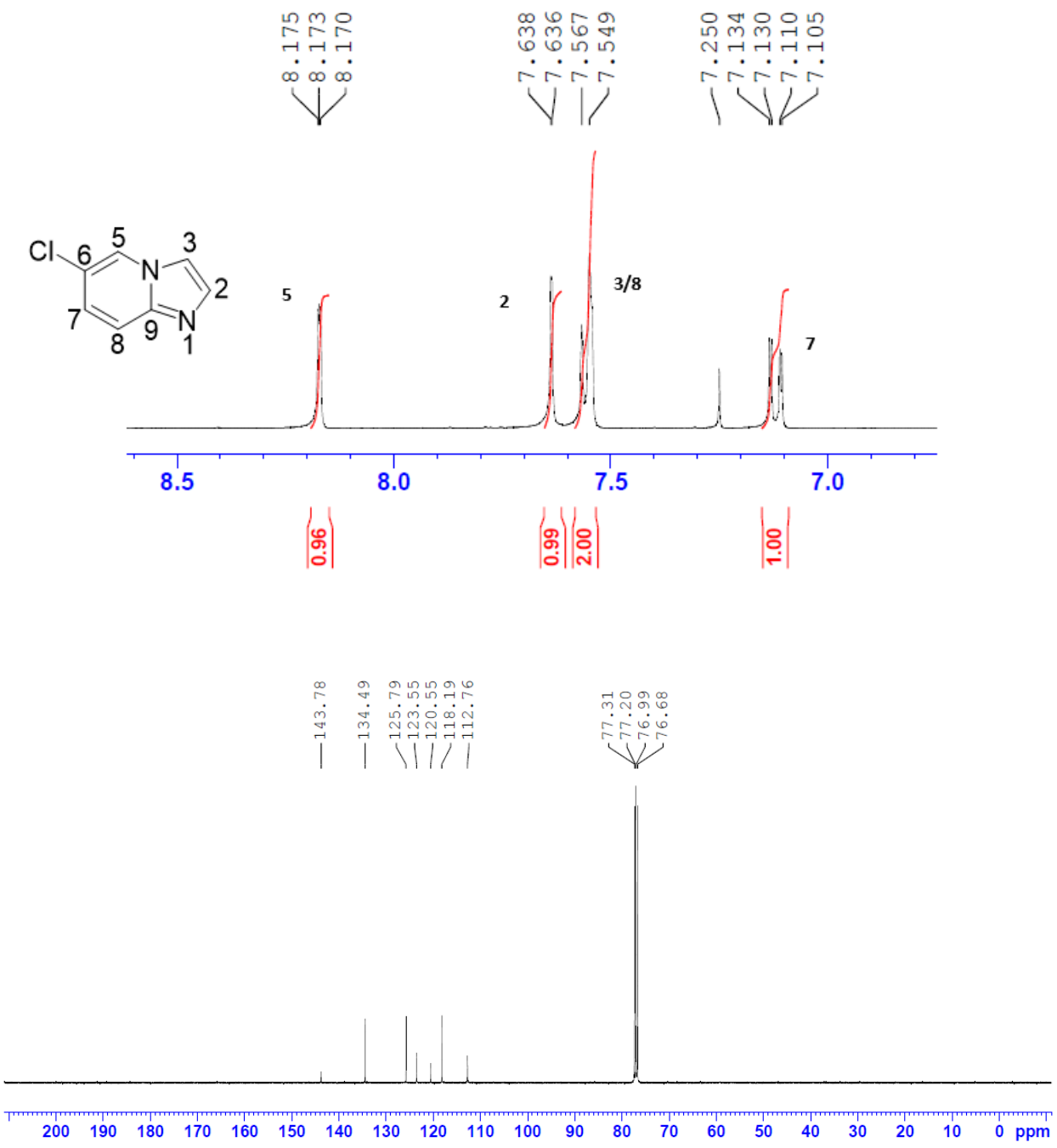

Figure 2.1**:** ^{1}H NMR and ^{13}C NMR spectra of 6-chloro imidazo[1,2-a]pyridine $CDCl_3$ at 400 and 100 MHz respectively.

With the interest of incorporating a sulfone moiety on the 3rd-position of the 6-chloro imidazo[1,2-a]pyridine, we decided to take advantage of the nucleophilic reactivity of the 3rd position based on the proposed resonance structures as described in the next section.

2.1.2. Synthesis of 6-chloro-3-iodo imidazo[1,2-a]pyridine (30)

Literature has reported the halogenation of 6-substituted imidazo[1,2-a]pyridine through regioselective electrophilic aromatic halogenation [2], [3]. Zhao and co-workers, reported the iodination of 6-nitroimidazo[1,2-a]pyridine with NIS [4]. Following the literature procedure, a solution of compound **29** in DMF was treated with NIS overnight at room temperature to afford 6-chloro-3-iodo imidazo[1,2-a]pyridine **30** upon purification by column chromatography. The successful incorporation of the iodine atom at position 3 of the imidazole framework was confirmed by the absence of the H-3 proton peak in the ^{1}H-NMR spectrum of compound **30** that was evident in the spectrum of **29** at the region 7.57 – 7.55 ppm. The ^{13}C-NMR spectrum also revealed the appearance of a distinct C-I peak at a region 61.48 ppm, both spectra (**Fig. 2.2**).

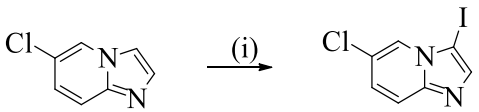

29 **30**

Reagents and conditions: (i) NIS, DMF, rt, over night.

Scheme 2**:** Selective mono-iodination of 6-chloro imidazo[1,2-a]pyridine

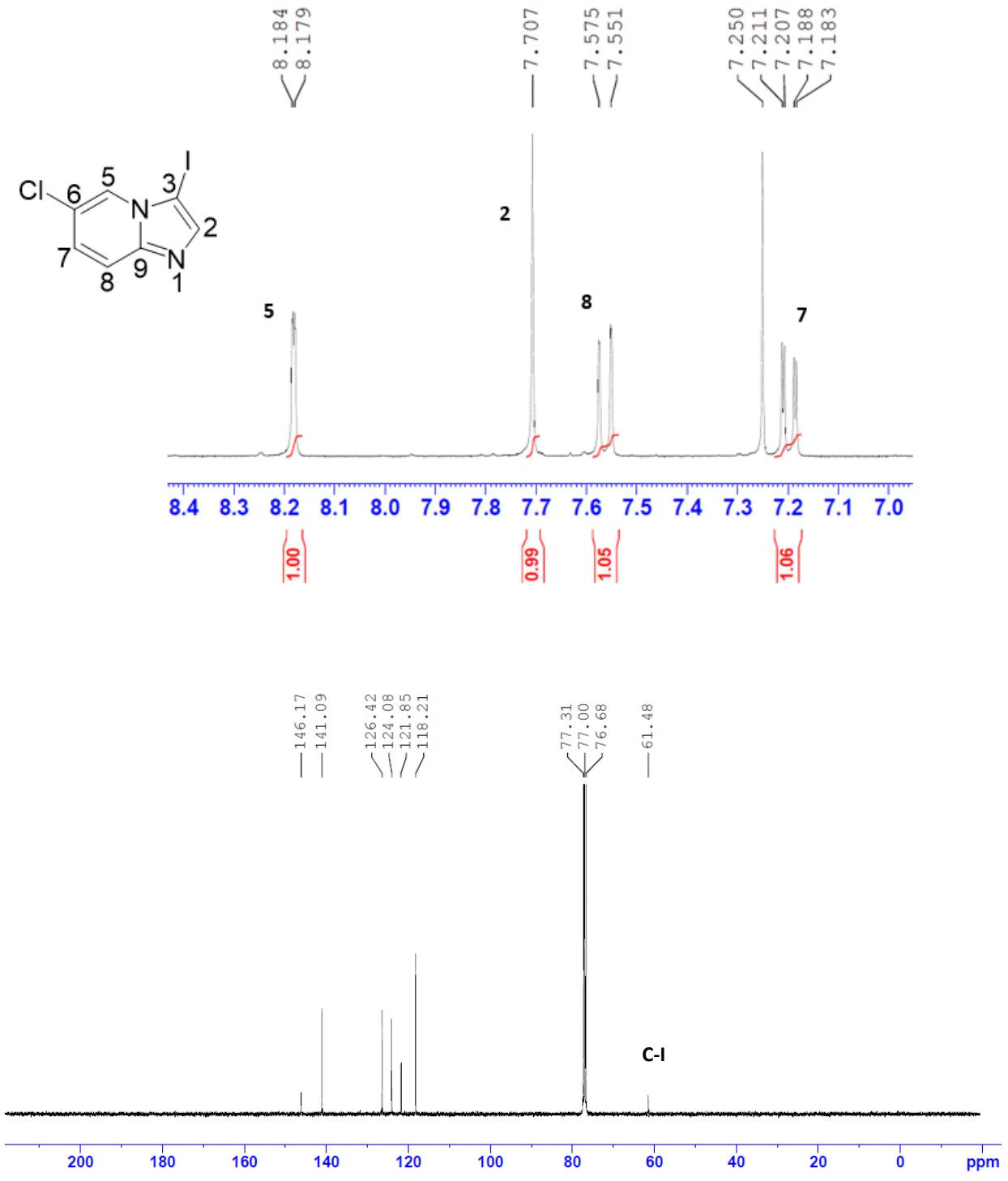

Figure 2.2**:** ^{1}H NMR and ^{13}C NMR spectra of 6-chloro-3-iodo imidazo[1,2-a]pyridine $CDCl_3$ at 400 and 100 MHz respectively.

The precipitated di-halogenated intermediate upon addition of NIS proceeded via the known NIS-mediated electrophilic aromatic iodination. The π-electrons between **C-2** and **C-3** of the imidazo ring system act as a nucleophile attacking the electrophilic iodine in the NIS to displace the good leaving succinimide anion [3]. Eventually, the anticipated 6-chloro-3-iodo imidazo[1,2-a]pyridine in adequate yield of 76% was isolated. The numerous number of resonance structures of the positively charged heteroarenium intermediate **2.1a** favours the regioselectivity of iodination at C-3 relative to C-2 (**2.1e**) of the 6-chloro imidazo[1,2-a]pyridine (**Scheme 2.1**).

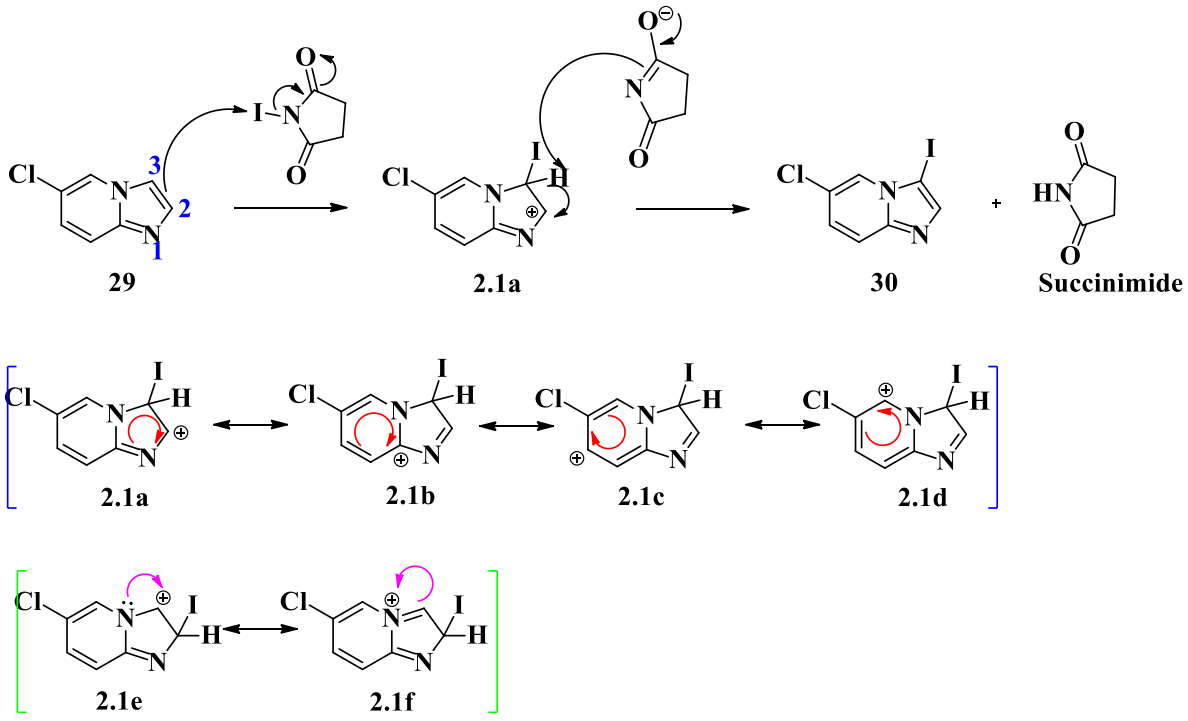

scheme 2.1: Postulated mechanistic steps for selective electrophilic aromatic iodination.

2.1.3. Synthesis of 3-aryl-6-chloro- imidazo[1,2-a]pyridine (31a-b)

The presence of the sulfone group in organic compounds have been reported to enhance their biological activities. This is due to the interaction of the sulfone group with various amino acids residues, such as the Lys 570 of the crystal structure of the *Pv*PKG [5]. The

iodine atom in 6-chloro-3-iodo imidazo[1,2-a]pyridine **30** makes it suitable to undergo transition metal catalyzed cross coupling reactions. We opted for Suzuki-Miyaura over other cross coupling reactions due to availability and environmentally friendly nature of the boronic acid/ or ester [6] .The selective bond formation on the C-I bond is due to the relative C-halogen bond strengths (I < Br < Cl < F), which makes it possible for selective substitution on the iodine atom in the presence of the chlorine atom [7]. Palladium(*II*)bis(triphenylphosphine) dichloride ($(PdCl_2(PPh_3)_2$) catalyzed Suzuki cross coupling reaction of compound **30** in the presence of K_2CO_3 using (4-(methylsulfonyl)phenyl) and (6-(methylsulfonyl)pyridin-3-yl) boronic acids as coupling partners in 1,4-dioxane/H_2O (3:1, v/v) at 90 °C under nitrogen atmosphere for 3 hours afforded the desired 6-chloro-3-(4-(methylsulfonyl)phenyl)imidazo[1,2-a]pyridine **31a** and 6-chloro-3-(6-(methylsulfonyl)pyridin-3-yl)imidazo[1,2-a]pyridine **31b** in decent yields of 81% and 83%, respectively, upon column chromatography purification. The ^{1}H NMR spectra of the prepared compounds revealed the presence of additional peaks in the aromatic region. Their methyl protons resonate as a singlet in the aliphatic region around 3.12 ppm. The ^{13}C-NMR spectra, on the other hand, revealed the presence of additional peaks in the aromatic region as well as lacking the distinct C-I peak present in the spectrum of compound **29** at 61.48 ppm. The representative spectrum of compound **31a** is shown below in **Fig 2.3**.

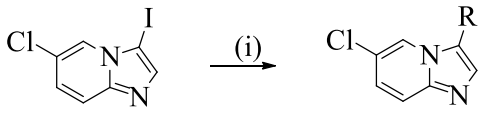

30 **31 (a,b)**

Reagents and conditions: (i) $PdCl_2(PPh_3)_2$, K_2CO_3, 4-SO_2Me-phenyl-B$(OH)_2$ (**31a**) and 6-SO_2Me-pyridin-3-yl-B$(OH)_2$ (**31b**), 1,4-dioxane/H_2O (3:1, v/v), 90 °C, 3 h.

Scheme 3**:** Suzuki-Miyaura cross coupling of 6-chloro-3-iodo imidazo[1,2-a]pyridine

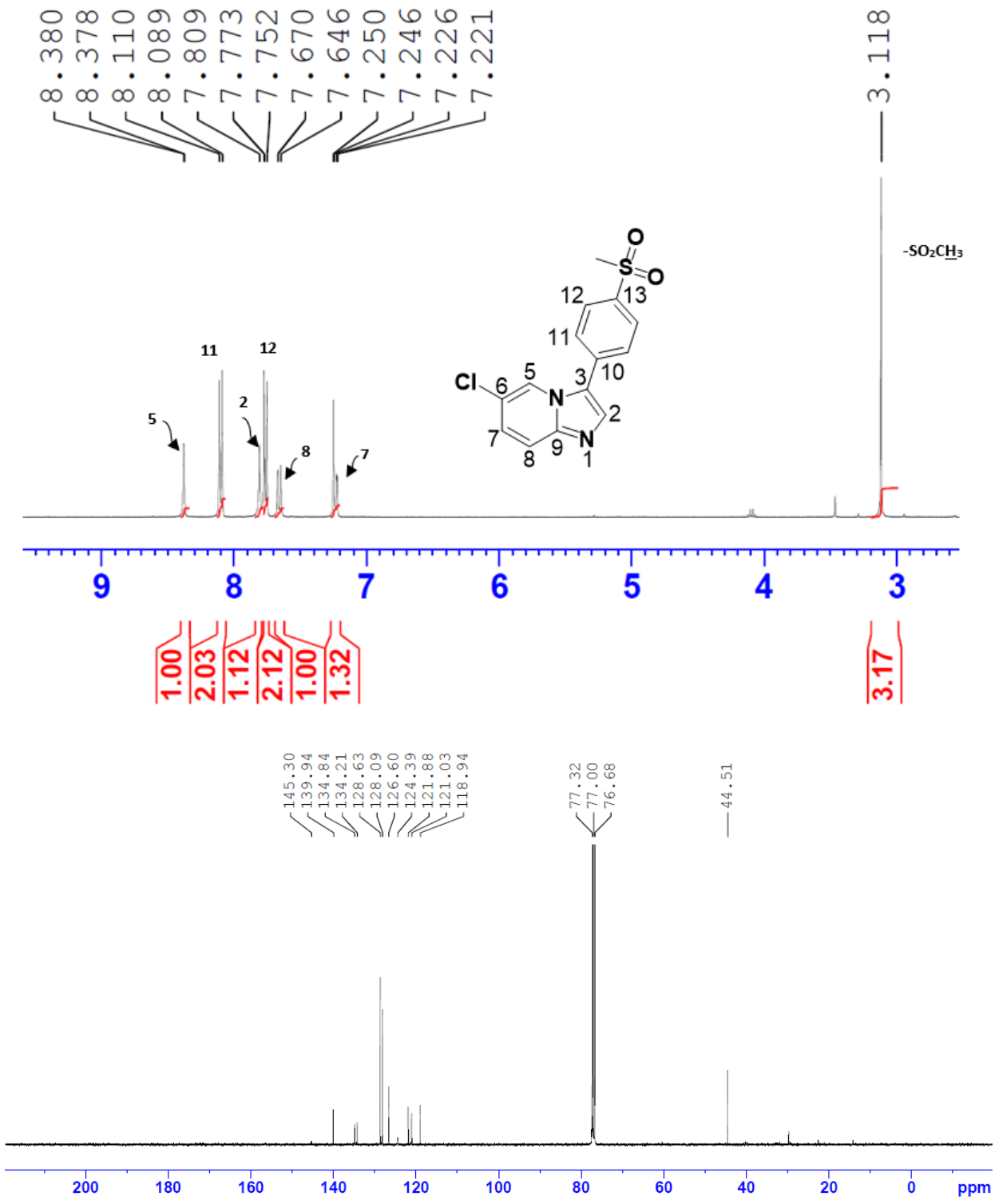

Figure 2.3: 1H NMR and 13C NMR spectra of 6-chloro-3-iodo imidazo[1,2-a]pyridine at 400 and 100 MHz respectively.

The main aim of this investigation was to synthesize the 3,6-substituted imidazo[1,2-a]pyridine derivatives. To achieve this, the prepared sulfonyl intermediate **31 (a, b)** were treated with various boronic acids and or esters to produce the target compounds as described in the next section below.

2.1.4. Synthesis of 3,6-aryl-sustituted imidazo[1,2-a]pyridine (32a-ac)

Le Manach and co-workers reported the structure activity relationship (SAR) around the central core and substituents combined with sulfone/sulfoxide. The strategy resulted in compound **20** (**Figure 1.6**) which displayed good *in vivo* efficacy, physicochemical properties in both *P.falciparum* SCID and *P.berhei* mouse models, and good oral pharmacokinetics [8]. The last step towards the accomplishment of target compounds involved derivatization of the crucial sulfone intermediates **31(a**, **b**), through Suzuki cross coupling with some alteration of the proposed conditions. The new proposed conditions are based on the bond formation on the C-Cl bond due to the relative C-halogen bond strengths (I < Br < Cl < F), which makes it less reactive for substitution on the chlorides [9]. Koubachi and co-workers reported efficient microwave assisted Suzuki cross coupling reaction of 6-halogenoimidazo[1,2-a]pyridines [10]. In this investigation we decided to adopt the literature with alterations based on the influence of ligands in palladium catalyzed reactions. Microwave assisted Palladium(0) tetrakis(triphenylphosphine) ($Pd(PPh_3)_4$) catalyzed Suzuki reaction of compounds **31a** and **31b** in the presence of K_2CO_3 and tricyclohexylphosphine (PCy_3) as ligand using various boronic acids or esters as coupling partners in 1,4-dioxane/H_2O (3:1, v/v) at 150 °C under nitrogen gas afforded the desired 3,6-aryl-sustituted imidazo[1,2-a]pyridine derivatives in moderate yields (32 - 55 %) after 3 hours. All the prepared compounds isolated in this reaction step were characterized using a combination of both ^{1}H-NMR and ^{13}C-NMR complemented with HPLC-MS. As expected, the ^{1}H NMR spectra of the prepared compounds revealed the presence of additional peaks in the aromatic and aliphatic region. The ^{13}C-NMR spectra, on the other hand, revealed the presence of additional peaks in the aromatic region and aliphatic region with respect to the attached moiety. The HPLC-MS, additionally confirming the increase in mass of the isolated compounds. The representative spectrum of compound **32a** is shown below in **Fig. 2.4**.

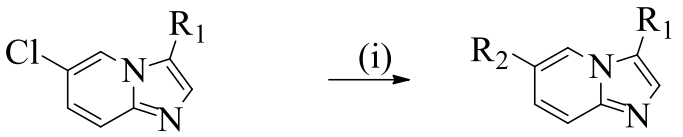

31 (a, b) **32a-ag**

Reagents and conditions: (i) $Pd(PPh_3)_4$, PCy_3, K_2CO_3, appropriate boronic acid, 1,4-dioxane/H_2O (3:1, v/v), 150 °C, 3 h, M.W.

Scheme 4**:** Suzuki-Miyaura cross coupling of 6-chloro-3-iodo imidazo[1,2-a]pyridine.

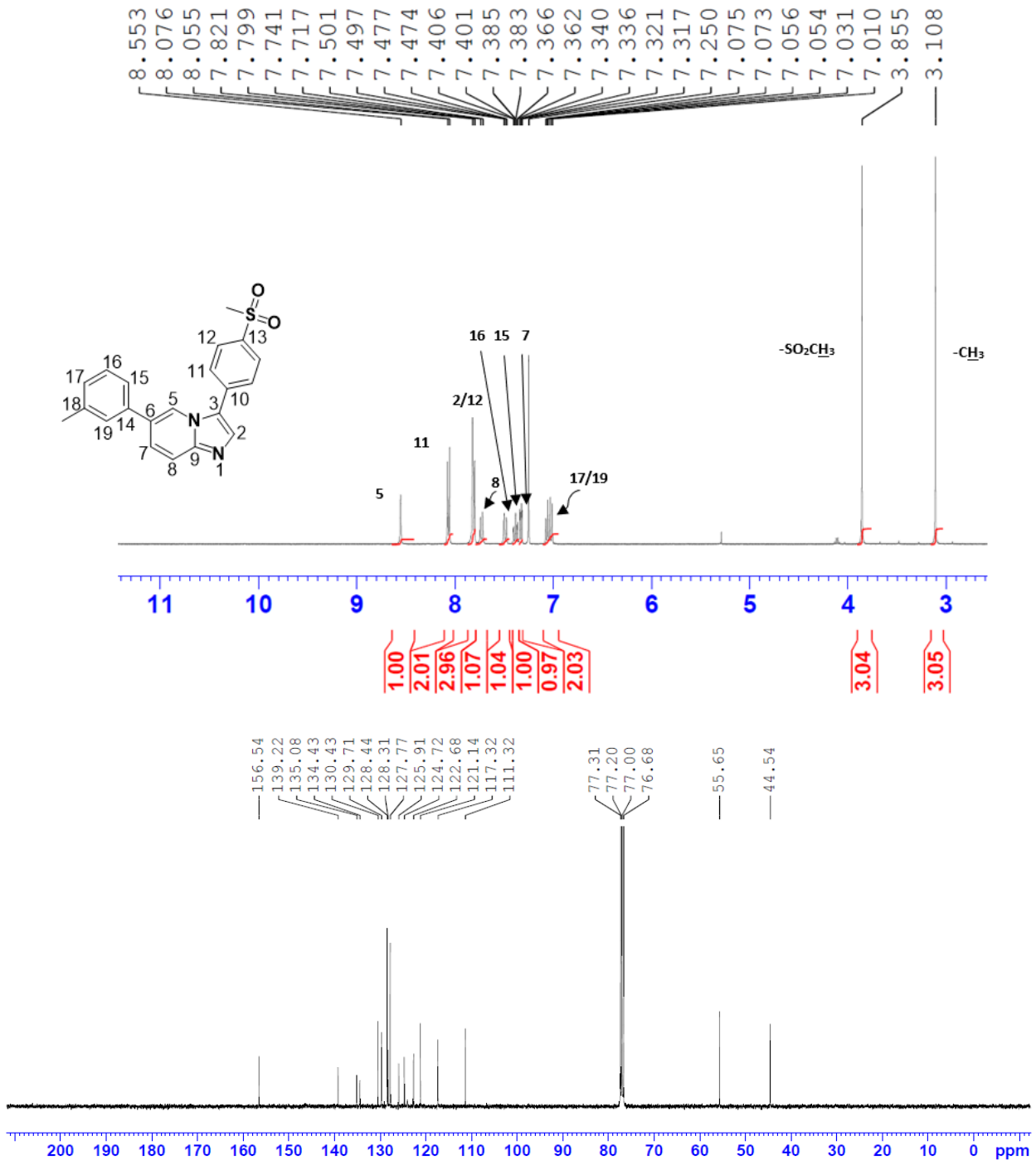

Figure 2.4: ^{1}H NMR and ^{13}C NMR spectra of 3-(4-(methylsulfonyl)phenyl)-6-(m-tolyl)imidazo[1,2-a]pyridine $CDCl_3$ at 400 and 100 MHz respectively.

Table 1: substitution pattern, percentage yield and melting point of **32** (**a- ac**)

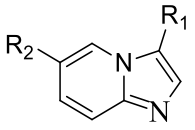

Compound	**R_1**	**R_2**	**%Yield**	**Melting point (**°C)
32a	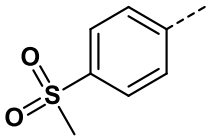	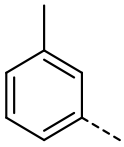	53	208 – 210
32b	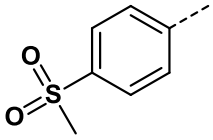	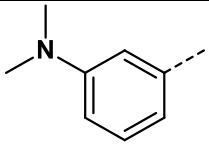	38	207 – 209
32c	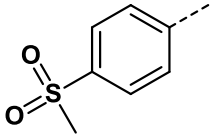	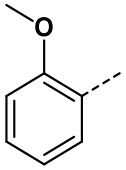	45	209 – 211
32d	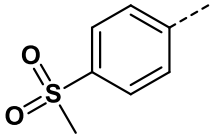	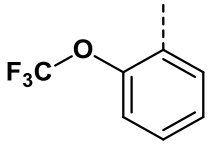	50	170 – 174
32e	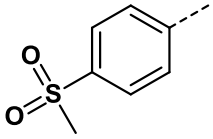	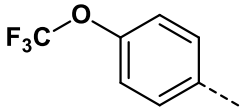	35	187 – 190
32f	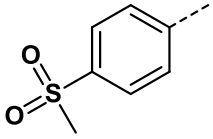	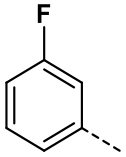	42	162 – 165
32g	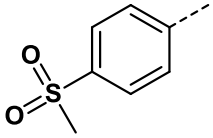	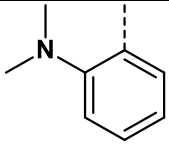	40	116 – 120

32h	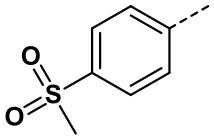	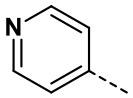	55	275 – 277
32i	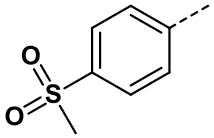	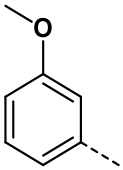	36	114 –118
32j	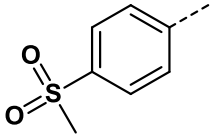	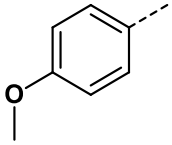	30	113 – 116
32k	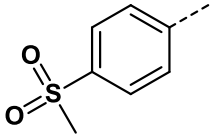	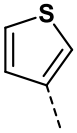	41	176 – 179
32l	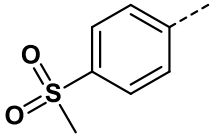	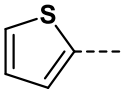	44	177 – 179
32m	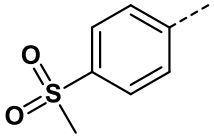	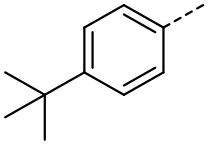	54	173 – 177
32n	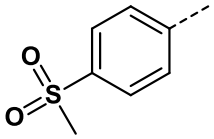	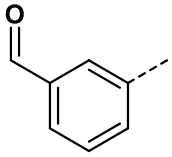	46	233 – 237
32p	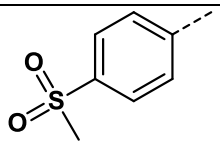	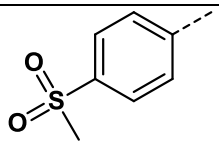	29	181 – 184
32q	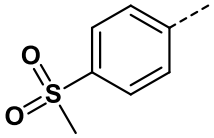	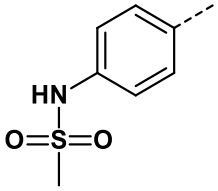	25	248 – 252
32r	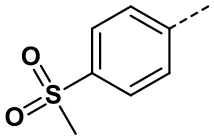	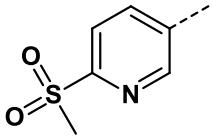	27	152 – 155

32aa	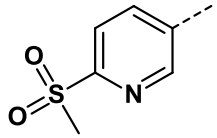	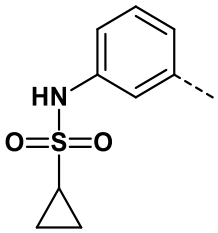	28	155 – 159
32ab	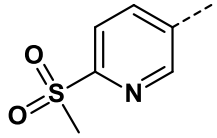	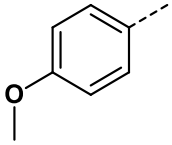	56	210 – 213
32ac	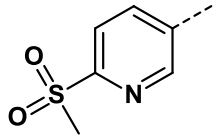	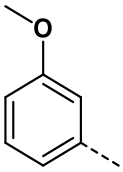	51	198 – 201

Some of the potential drugs containing the imidazo[1,2-a]pyridine scaffold has shown *Pf*PKG and *Pf*PI4k inhibition and similarly to the pyrazolo[1,5-a]pyridine scaffold. Although some data for 3,6-sustituted pyrazolo[1,5-a]pyridine scaffold has been reported [11]. In this investigation we intend to look into fixing the position-3 with a particular moiety and vary position-5 as described in the next section.

2.2. Synthesis of 3,5-substituted pyrazolo[1,5-a]pyridine derivatives

The main aim of this investigation is to synthesize 5-amino-3-arylpyrazolo[1,5-a]pyridine to be used as substrate for the synthesis of 3,5-substituted pyrazolo[1,5-a]pyridine derivatives. To achieve this, 5-bromo pyrazolo[1,5-a]pyridine obtained from the selective mono-halogenation of commercially available 5-aminopyrazolo[1,5-a] pyridine was used as a precursor.

2.2.1. Synthesis of 5-bromo pyrazolo[1,5-a]pyridine

Literature has reported the halogenation of primary amines through Sandmeyer reaction, which involves the activation of NH_2 into diazonium salt for radical-nucleophilic aromatic substitution [12]. The first approach was to subject commercially available 5-aminopyrazolo[1,5-a] pyridine (**33**) to Sandmeyer reaction for the preparation of 5-bromo pyrazolo[1,5-a] pyridine. The anticipated 5-bromo pyrazolo[1,5-a]pyridine was not isolated, however, 3,5-dibromo pyrazolo[1,5-a] pyridine (**34**) was isolated, confirmed by ^{1}H-NMR shown in **Figure 2.5**. Organic compounds containing the thiophene moiety have been reported to possess good antimalarial activity against the *P.falciparum* 3D7 strain and inhibited parasite growth [13]. As a result, the di-halogenated compound **34** was subject to transition metal catalyzed Suzuki Miyaura cross coupling reaction using thiophene boronic acids as coupling partners to afford the desired 3,5-substituted pyrazolo[1,5-a] pyridine (**35a, 35b**) in 80 and 83 % yield after 3 hours, respectively. Both the ^{1}H NMR and ^{13}C-NMR spectra of the prepared compounds (**35a, 35b**) revealed additional peaks in the aromatic region. The representative spectrum of compound **35a** is shown below in **Fig. 2.6**.

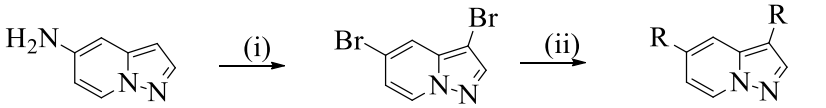

Reagents and conditions: (i) $NaNO_2$, H_2O, HBr, 15 min then $CuBr_2$, HBr, 50 °C, 15 min (ii) $PdCl_2(PPh_3)_2$, K_2CO_3, appropriate boronic acid, 1,4-dioxane/H_2O (3:1, v/v), 90 °C, 3 h.

Scheme 5**:** Suzuki-Miyaura cross coupling of 3,5-dibromo pyrazolo[1,5-a]pyridine.

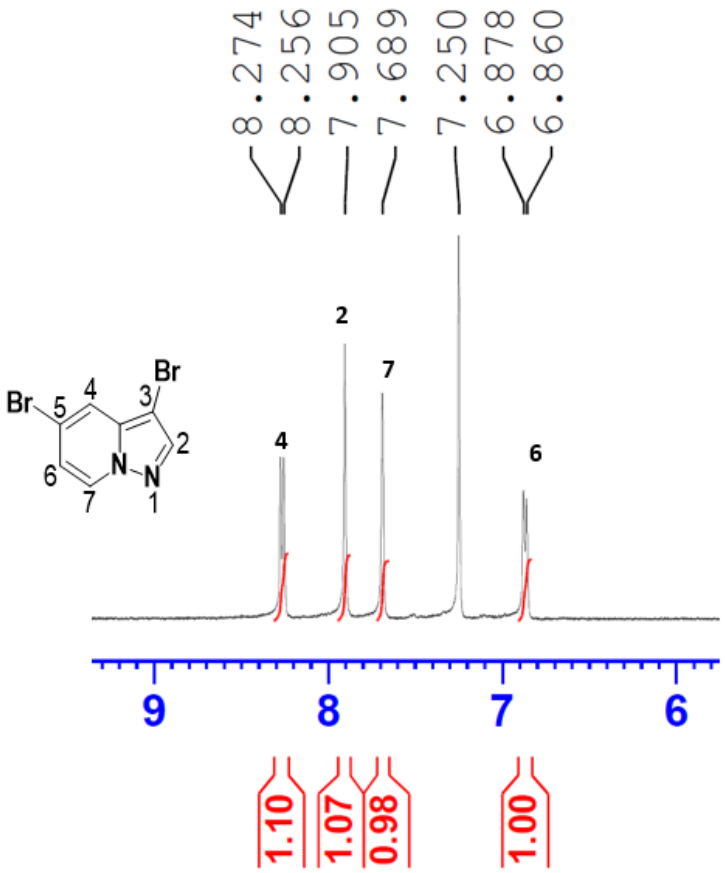

Figure 2.5: 1H NMR spectrum in CDCl3 at 400 MHz of 3,5-dibromo pyrazolo[1,5-a]pyridine (32) in CDCl3.

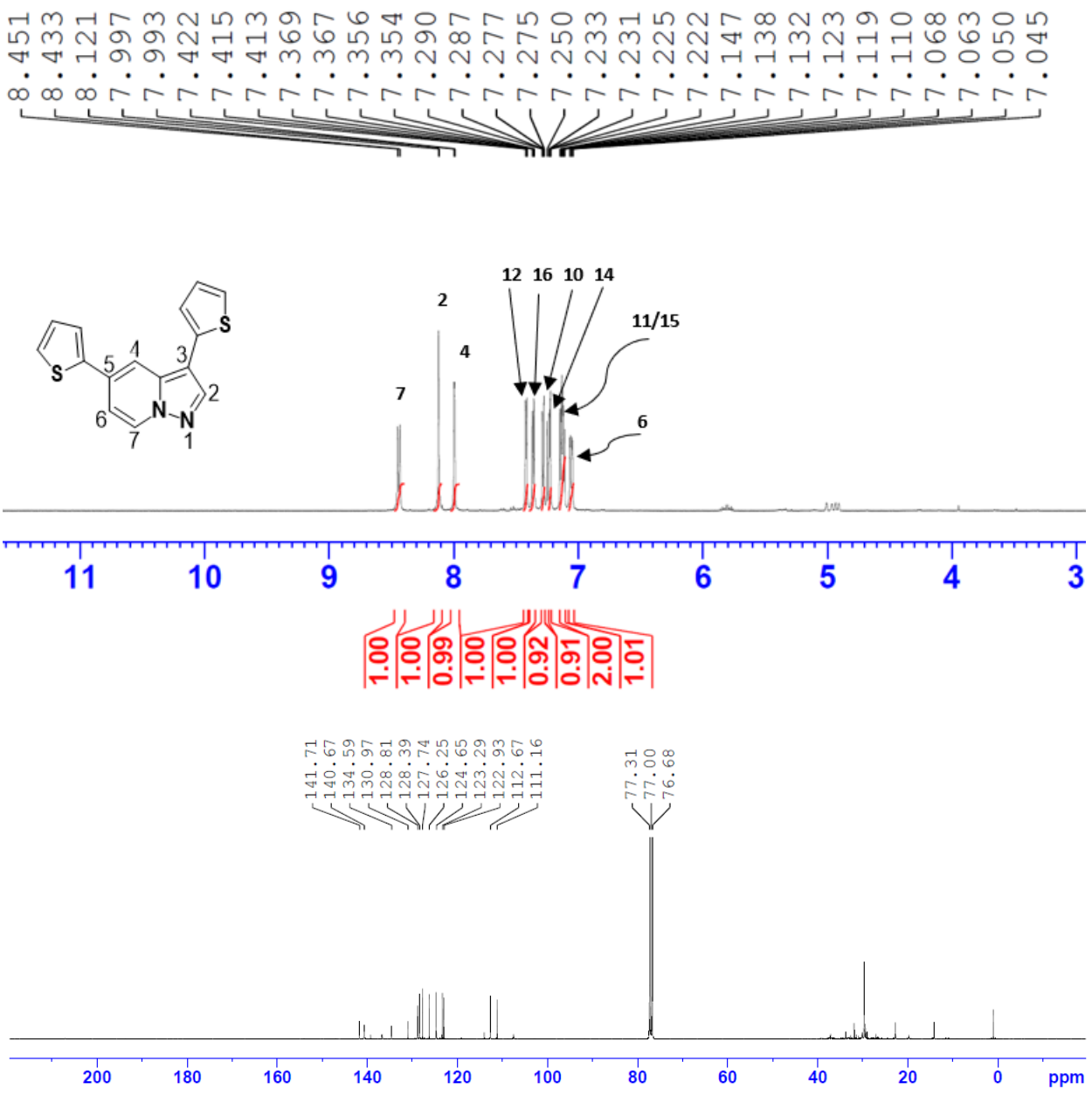

Figure 2.6: 1H NMR and 13C NMR spectra of 3,5-di(thiophen-2-yl)pyrazolo[1,5-a]pyridine (35a) in CDCl3 at 400 and 100 MHz respectively.

To navigate the challenge associated with the dibromination, we decided to halogenate the 3rd position with an aim of fixing a sulfone moiety on position-3 as described in the next section.

2.2.2. Synthesis of 5-amino-3-iodopyrazolo[1,5-a]pyridine (36)

Numerous reagents such as *N*-iodosuccinimide (NIS) [14], *N*-bromosuccinimide (NBS) [15] and molecular iodine (I_2) [16], have been reported for the halogenation of pyrazolo[1,5-a] pyridine and related pyrazolo[1,5-a] pyrimidine scaffold using various solvents such as methanol, acetonitrile and chloroform. Ning Xi and co-workers reported the synthesis of 5-bromo-3-iodopyrazolo[1,5-a] pyridine from 5-bromopyrazolo[1,5-a] pyridine [14]. Adopting literature procedure, commercially available 5-aminopyrazolo[1,5-a] pyridine (**33**) was treated with *N*-iodosuccinimide (NIS) in methanol at - 10 °C to afford the desired 5-amino-3-iodopyrazolo[1,5-a]pyridine (**36**) in 97% yield after 30 minutes. The prepared 5-amino-3-iodopyrazolo[1,5-a]pyridine (**36**) was characterized using a combination of ^{1}H-NMR and ^{13}C-NMR . The ^{1}H-NMR spectra lacked the H-3 proton peak that was evident in the spectrum of the substrate. The ^{13}C-NMR spectrum, on the other hand, revealed a peak at a region 42.70 ppm which is distinct to the C-I peak (**Fig. 2.7**).

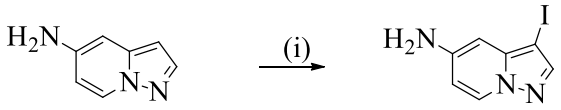

33 **36**

Reagents and conditions: (i) NIS, MeOH, - 10 °C, 30 minutes.

Scheme 6**:** Selective mono-iodination of 5-aminopyrazolo[1,5-a] pyridine

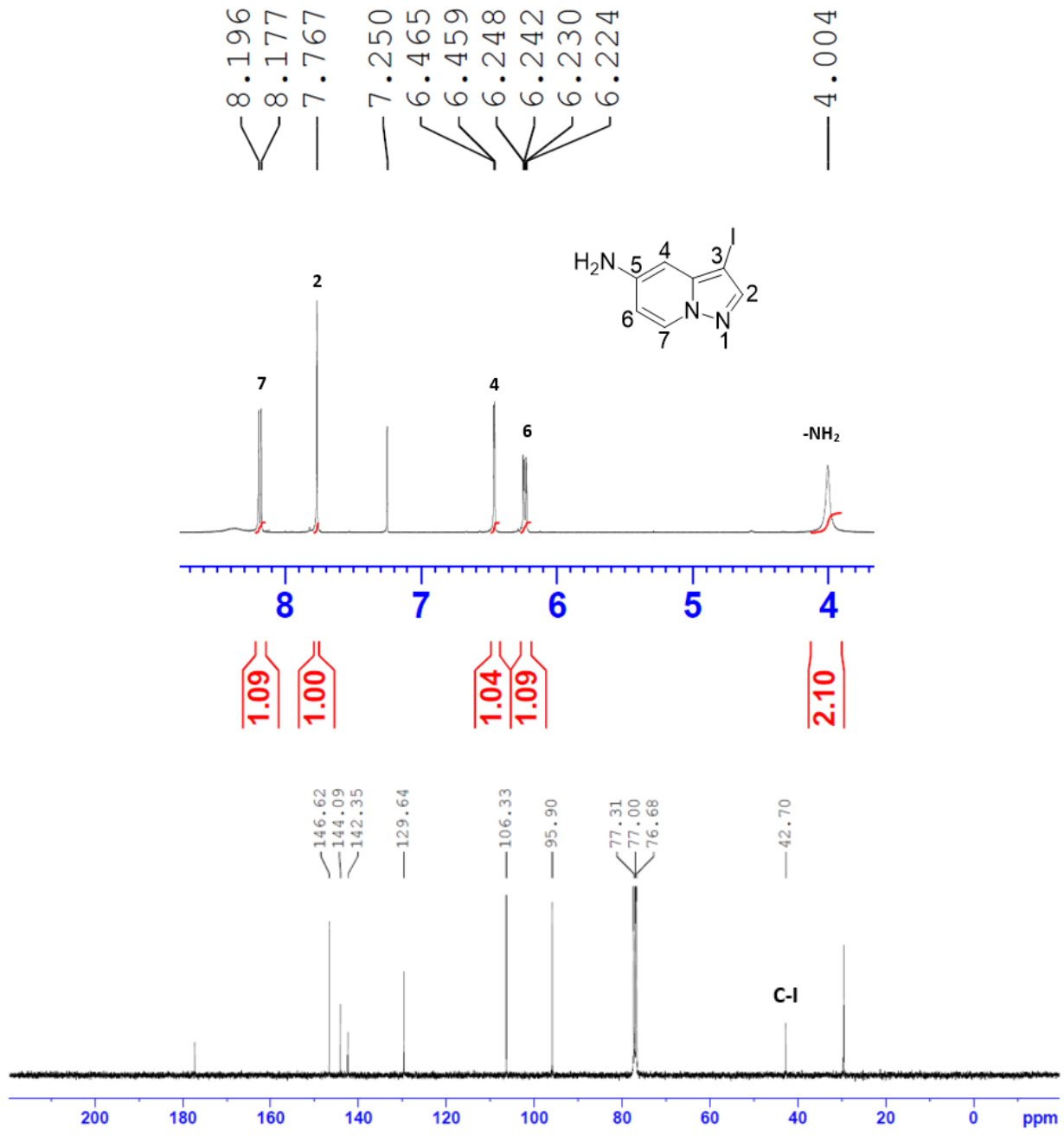

Figure 2.7: 1H NMR and 13C NMR spectra of 5-amino-3-iodopyrazolo[1,5-a]pyridine in CDCl3 at 400 and 100 MHz, respectively.

The successful mono-halogenated intermediate, after addition of NIS proceeded similarly as described in section **2.1.2** via the known NIS-mediated electrophilic aromatic iodination. The π-electrons between **C-3** and **C-3a** of the pyrazolo ring system act as a

nucleophile attacking the electrophilic iodine atom in NIS to displace the good leaving group which is succinimide anion [3]. Eventually, deprotonation of the heteroarenium ion by the succinimide anion to form the anticipated 5-amino-3-iodopyrazolo[1,5-a]pyridine in adequate yield (98%) and succinimide as a by-product. Before completion and monitoring of the reaction, two spots on the TLC of closer R_f values were observed, signifying isomeric mixtures, however the desired intermediate was formed in large quantity as the fast rate and regioselectivity of this reaction can be confirmed by the numerous number of resonance structures of the positively charged heteroarenium intermediate **6.1a**, hence, favouring iodination at **C-3** relative to **C-4** (**6.1f**) of the 5-amino pyrazolo[1,5-a]pyridine (**Scheme 6.1**).

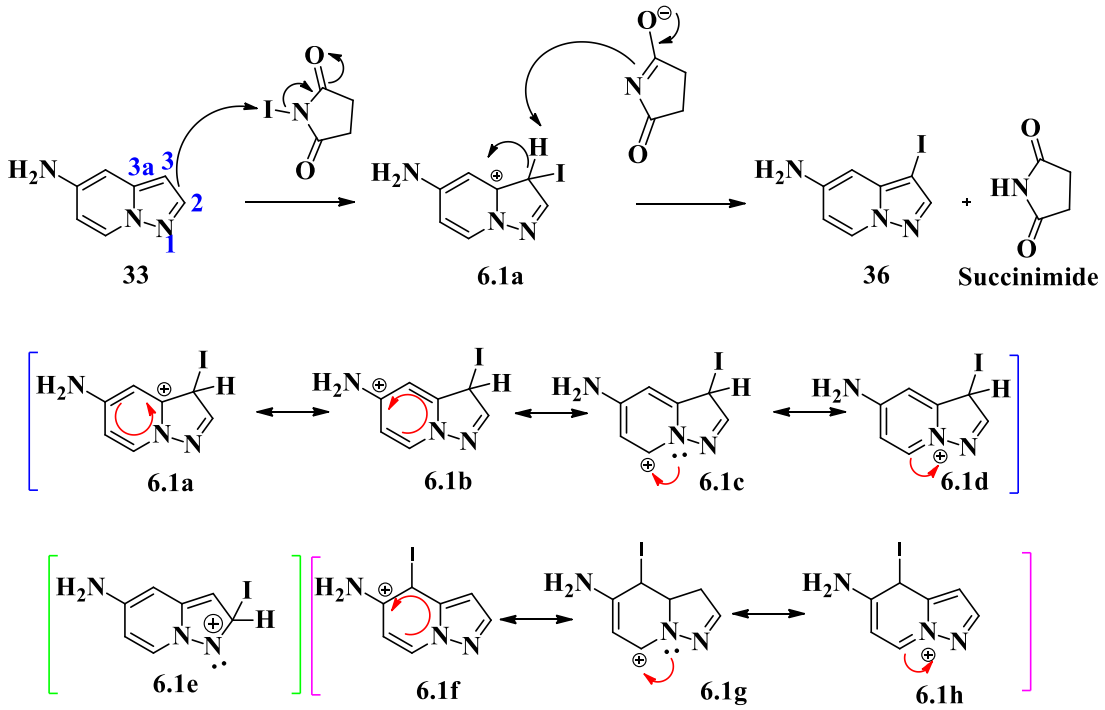

scheme 6.1**:** Proposed mechanistic steps for the selective electrophilic aromatic iodination of pyrazolo [1,5-a]pyridine.

Similarly, as described for the imidazo[1,2-a]pyridine scaffold in section **2.1.3**, With the iodine atom successfully incorporated, the resulting 5-amino-3-iodopyrazolo[1,2-a]pyridine (**36**) was subjected to Suzuki-Miyaura cross coupling conditions using (4-(methylsulfonyl)phenyl) and (6-(methylsulfonyl)pyridin-3-yl) boronic acids as coupling partners to afford the corresponding 3-(4-(methylsulfonyl)phenyl)pyrazolo[1,5-a]pyridin-5-amine (37a) and 3-(6-(methylsulfonyl)pyridin-3-yl)pyrazolo[1,5-a]pyridin-5-amine (**40b**) in 80 % and 65% yield, respectively. The ^{1}H NMR spectra of the prepared compounds revealed the presence of additional peaks in the aromatic region. Their methyl protons resonate as a singlet in the aliphatic region around 3.08 ppm. The ^{13}C-NMR spectra, on the other hand, revealed the presence of additional peaks in the aromatic region as well as lacking the distinct C-I peak at 42.7 ppm. The representative spectrum of compound **37a** is shown below in **Fig. 2.7**.

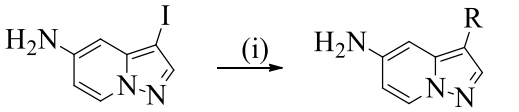

36 **37 (a, b)**

Reagents and conditions: (i) $PdCl_2(PPh_3)_2$, K_2CO_3, 4-SO_2Me-phenyl-B$(OH)_2$ (**37a**) and 6-SO_2Me-pyridin-3-yl-B$(OH)_2$ (**37b**), 1,4-dioxane/H_2O (3:1, v/v), 90 °C, 3 h.

Scheme 7**:** Suzuki-Miyaura cross coupling of 5-amino-3-iodopyrazolo[1,5-a]pyridine.

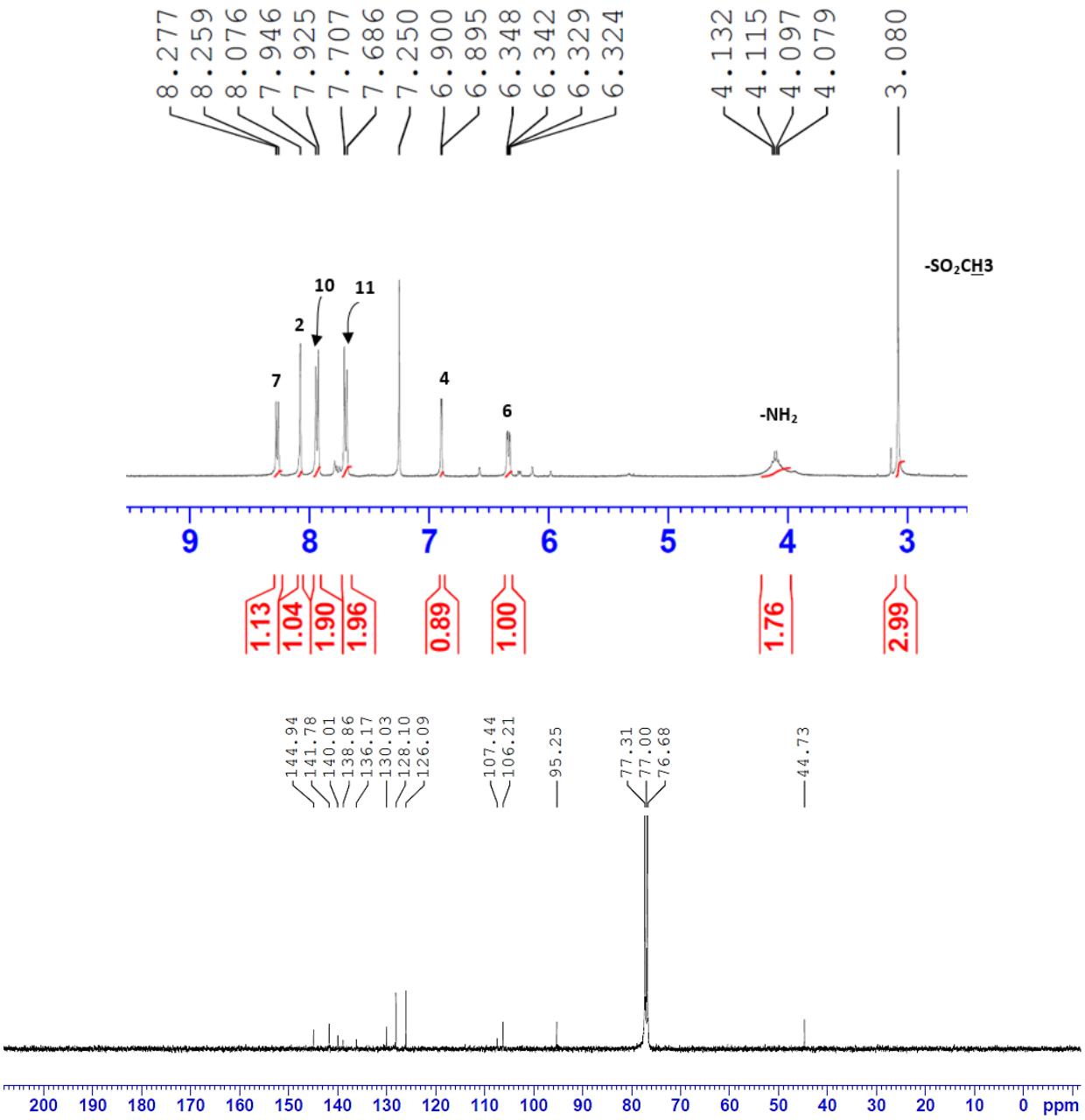

Figure 2.8: 1H NMR and 13C NMR spectra of 3-(4-(methylsulfonyl)phenyl)pyrazolo[1,5-a]pyridin-5-amine in CDCl3 at 400 and 100 MHz respectively.

To finally achieve the main aim of this investigation which is to synthesize the 3,5-substituted pyrazolo[1,5-a]pyridine derivatives, the amino (NH_2) group of the 5-amino-3-arylpyrazolo[1,5-a]pyridine (**37a** and **37b**) were converted into a bromine (Br) atom for

further transformation via metal catalyzed cross coupling reaction as described in the next section.

2.2.3. Synthesis of 5-bromo-3-(4-(methylsulfonyl)phenyl)pyrazolo[1,5-a]pyridine (39)

Based on the literature from section **2.2.1** for the halogenation of primary amines through Sandmeyer reaction. A solution of compound **37a** in concentrated hydrobromic acid (HBr) at room temperature was treated with a dropwise aqueous solution of $NaNO_2$ over 5 minutes, for the formation of aryl diazonium salt. The reaction was stirred for 10 minutes followed by the addition of a solution of copper (ii) bromide ($CuBr_2$) in HBr and the reaction mixture heated to 50 °C for 15 minutes until gas evolution ceased. At completion, the reaction mixture was poured into ice containing 3 – 5 drops of NaOH(aq.) (6 M). To our dismay, we isolated dibrominated compound **38** instead of the expected compound **39** shown in scheme (**9**). The dihalogenated compound (**38**) was, confirmed by ^{1}H-NMR which lacked H-4 proton around the region 6.90 ppm ortho to -NH_2 of compound **37a**, on the hand, the protons around 7.05 (H-6) and 8.34 (H-7) ppm revealed same splitting J-constant (*J* =*7*.6 Hz). Further characterization with high resolution mass spectrometry (HRMS) revealed the molecular ion peaks of m/z values of 428.8919, 430.8889, 432.8863 corresponding to $[C_{14}H_{10}Br_2N_2O_2S]^+$ with an intensity ratio of 1:2:1, confirming the addition of two bromine atoms (**Fig. 2.9**).

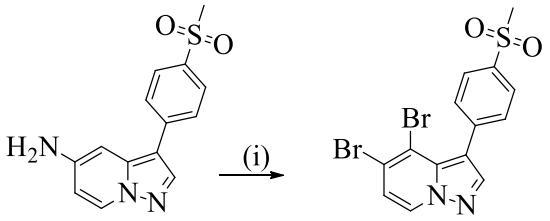

37a **38**

Reagents and conditions: (i) $NaNO_2$, H_2O, HBr, 15 min then $CuBr_2$, HBr, 50 °C, 15 min.

Scheme 8: Radical-nucleophilic aromatic substitution reaction of 3-(4-(methylsulfonyl)phenyl)pyrazolo[1,5-a]pyridin-5-amine.

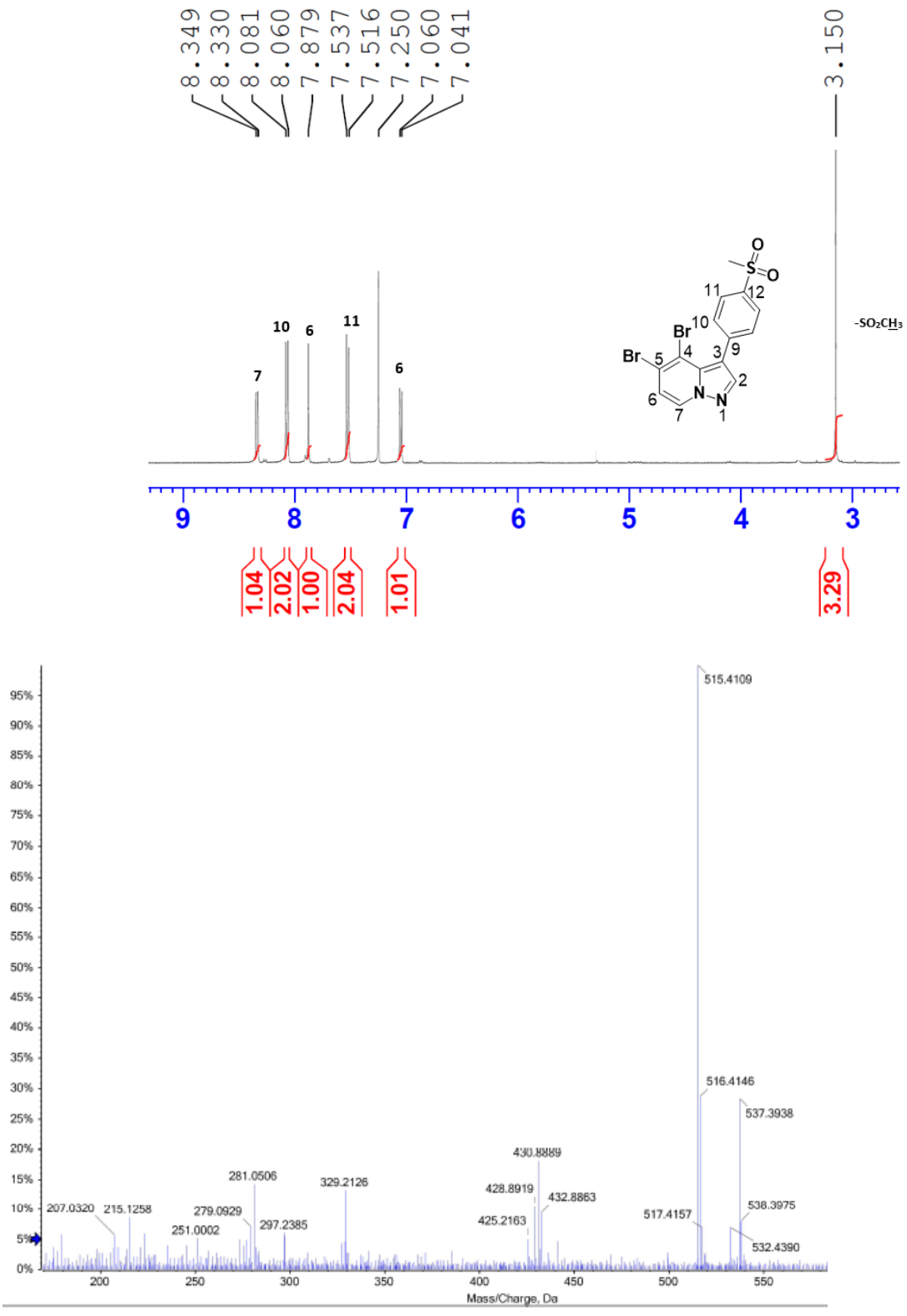

Figure 2.9**:** ^{1}H-NMR in $CDCl_3$ at 400 MHz spectrum and Mass Spectrometry of 4,5-bromo-3-(4-(methylsulfonyl)phenyl)pyrazolo[1,5-a]pyridine.

In trying to monobrominate 3-(4-(methylsulfonyl)phenyl)pyrazolo[1,5-a]pyridin-5-amine, we decided to investigate the effect of lowering the reaction rate by performing the Sandmeyer reaction at a lower temperature. 3-(4-(methylsulfonyl)phenyl)pyrazolo[1,5-a]pyridin-5-amine was subjected to Sandmeyer reaction at 0 °C for 15 minutes. The precipitate was filtered and purified by column chromatography to afford the desired 5-bromo-3-(4-(methylsulfonyl)phenyl)pyrazolo[1,5-a]pyridine **39a** in 52 % yield. The ^{1}H-NMR spectra lacked the NH_2 proton peak that was evident in the spectrum of its precursor **37a** around 4.11 ppm integrating for 2H protons (**Fig. 2.10**).

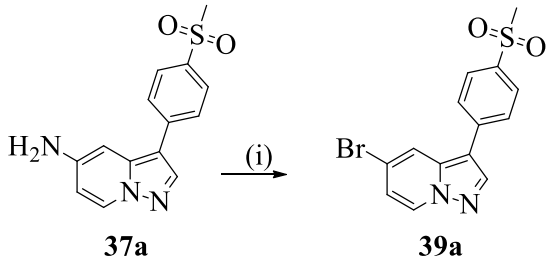

37a **39a**

Reagents and conditions: (i) $NaNO_2$, H_2O, HBr, 15 min then $CuBr_2$, HBr, 0 °C, 15 min.

Scheme 9**:** Radical-nucleophilic aromatic substitution reaction of 3-(4-(methylsulfonyl)phenyl)pyrazolo[1,5-a]pyridin-5-amine.

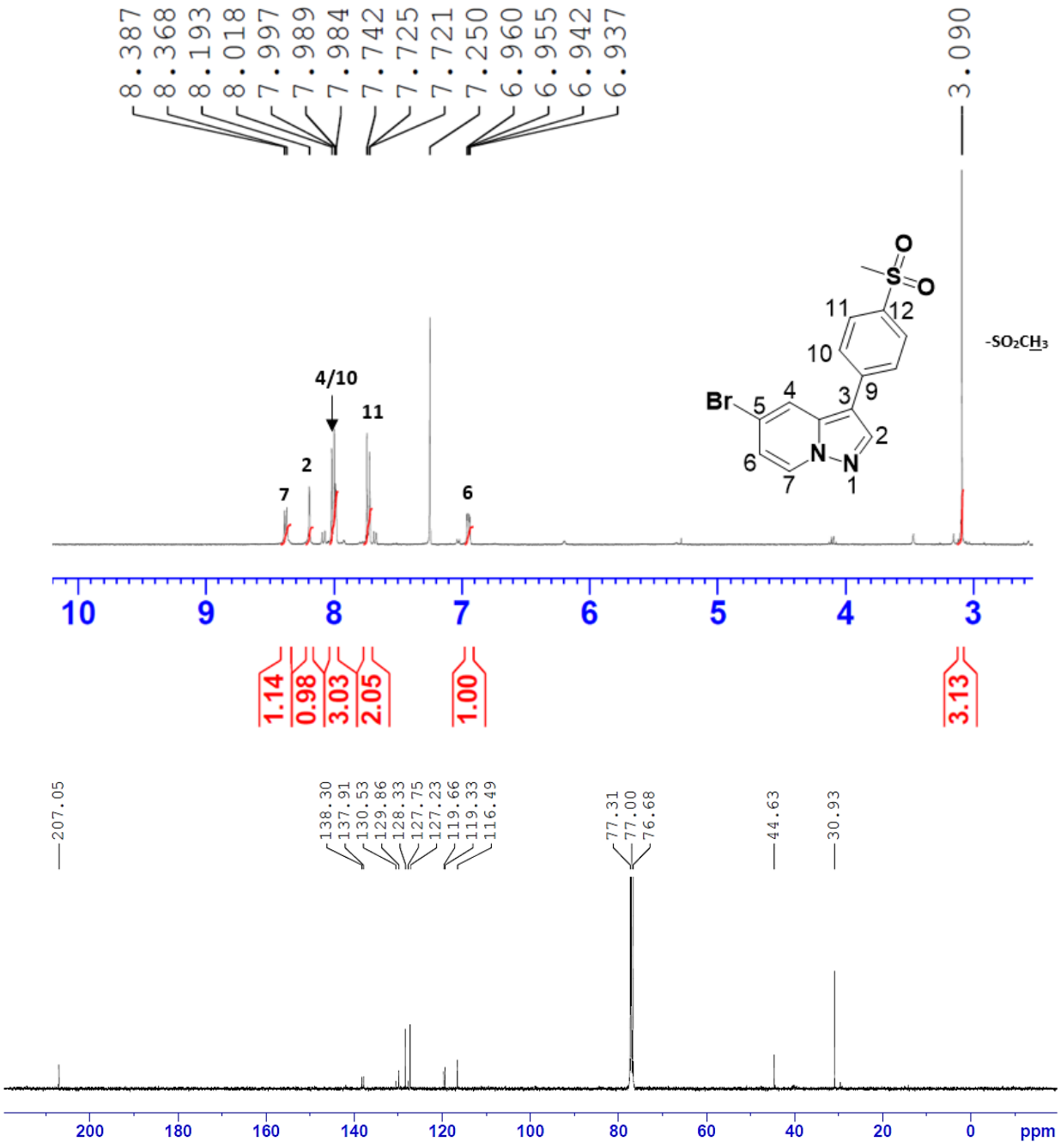

Figure 2.10: ^{1}H NMR and ^{13}C NMR spectra of 5-bromo-3-(4-(methylsulfonyl)phenyl)pyrazolo[1,5-a]pyridine in $CDCl_3$ at 400 and 100 MHz respectively.

Compounds **39a** and **39b** were in turn subjected to Suzuki-Miyaura cross coupling with various boronic acid as described in the next section.

2.2.4. Synthesis of 3-(4-(methylsulfonyl)phenyl)-5-(thiophen-3-yl)pyrazolo[1,5-a]pyridine (40a)

The strategy reported by Le Manach and co-workers that resulted in compound **20** (**Figure 1.6**) described in section **2.1.4**, regarding structure activity relationship (SAR) around the central core and substituents combined with sulfone/sulfoxide. With literature precedent, 5-bromo-3-(4-(methylsulfonyl)phenyl)pyrazolo[1,5-a]pyridine **39a** was subjected to the above Suzuki-Miyaura cross coupling conditions using thiophen-3-ylboronic acids to afford the desired 3-(4-(methylsulfonyl)phenyl)-5-(thiophen-3-yl)pyrazolo[1,5-a]pyridine (**40a**) in 53% yield after 3 hours. The isolated compound **40a** was characterized using ^{1}H-NMR and ^{13}C-NMR. The ^{1}H-NMR spectra confirmed the successful Suzuki-Miyaura cross coupling with appearance of additional protons around the aromatic region. The ^{13}C-NMR spectrum, on the other hand, revealed an increase in carbon peaks (**Fig. 2.11**).

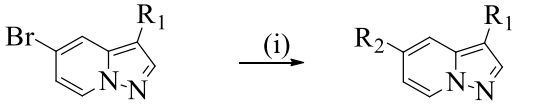

39(a, b) **40 (a, b)**

Reagents and conditions: (i) $PdCl_2(PPh_3)_2$, K_2CO_3, appropriate boronic acid, 1,4-dioxane/H_2O (3:1, v/v), 90 °C, 3 h.

Scheme 10**:** Suzuki-Miyaura cross coupling of 5-bromo-3-(4-(methylsulfonyl)phenyl)pyrazolo[1,5-a]pyridine.

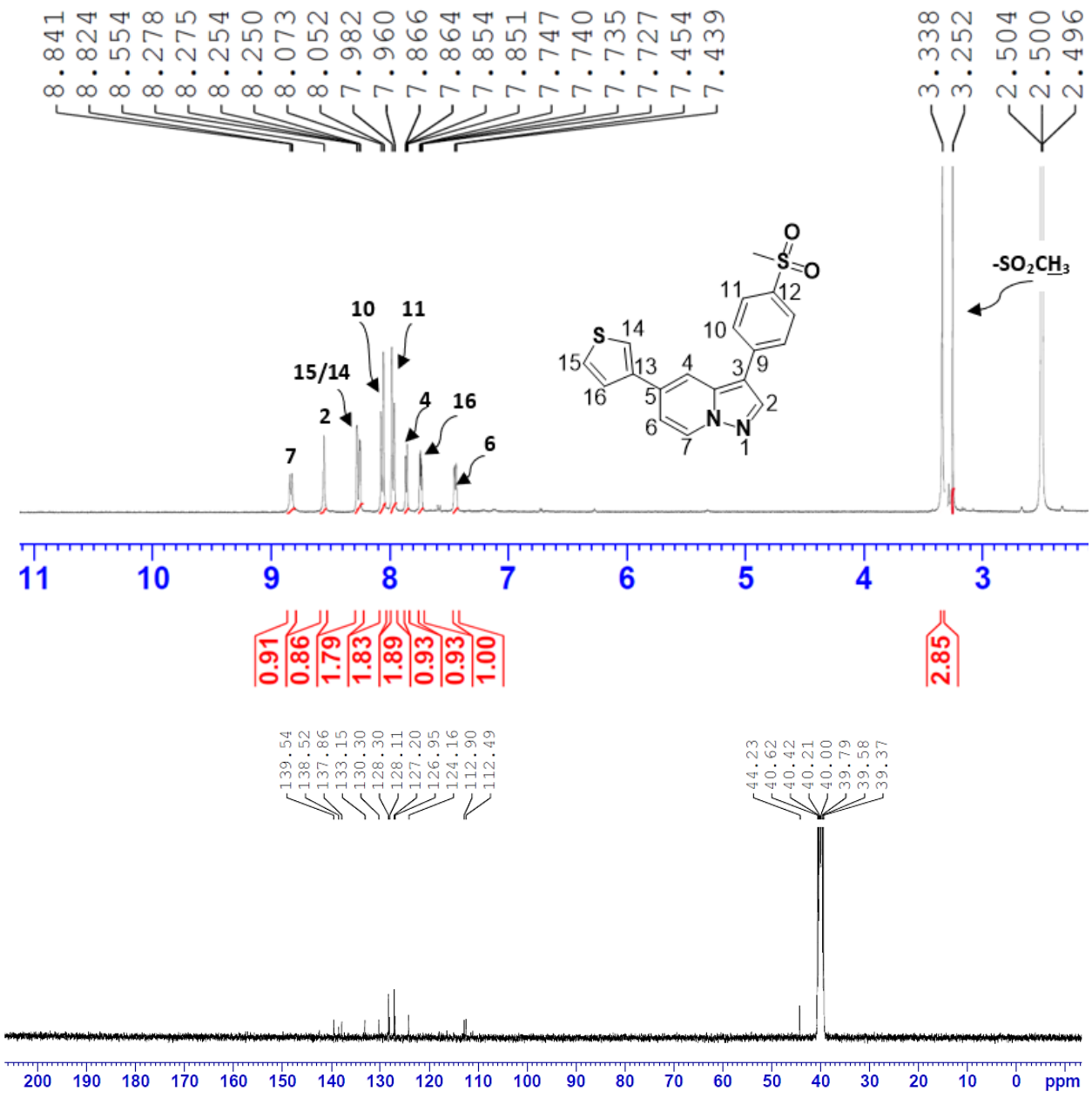

Figure 2.11: 1H NMR and 13C NMR spectra of 5-bromo-3-(4-(methylsulfonyl)phenyl)pyrazolo[1,5-a]pyridine in CDCl3 at 400 and 100 MHz respectively.

Table 2: substitution pattern, percentage yield and melting point of **35** (**a, b**) and **40** (**a**, **b**).

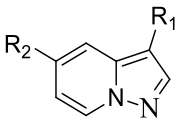

Compound	**R_1**	**R_2**	**%Yield**	**Melting point (**°C)
35a	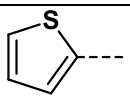	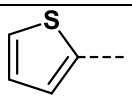	80	136 – 142
35b	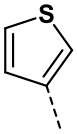	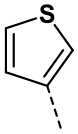	83	138 – 143
40a	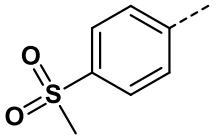	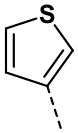	53	194 –198
40b	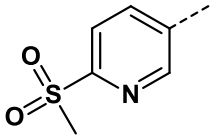	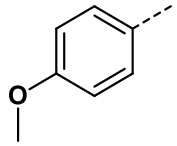	60	212 – 215

The molecular framework of the synthesized compounds resembles that of biologically important pyrazolo[1,5-a]pyridine and imidazo[1,2-a]pyridine scaffolds reported in literature [8]. The SAR strategy adopted led us to evaluate the pyrazolo[1,5-a]pyridine and imidazo[1,2-a]pyridine derivatives as potential kinase inhibitors (***Pf*PKG** and ***Pv*PI4K**) of *plasmodium falciparum* parasite.

2.3. Biological evaluation of the pyrazolo[1,5-a]pyridine and imidazo[1,2-a]pyridine derivatives

In this section, the biological and biochemical activities of the synthesized pyrazolo[1,5-a]pyridine and imidazo[1,2-a]pyridine derivatives will be discussed. First, the anti-plasmodium activity, *Plasmodium* PKG and PI4K inhibitory activity will be discussed.

Furthermore, cytotoxicity, selective index and solubility of the selected compounds will be discussed.

2.3.1. Anti-plasmodium, Cytotoxicity, In vitro PfPKG and PvPI4k inhibition, and in silico docking studies of the selected pyrazolo[1,5-a]pyridine and imidazo[1,2-a]pyridine derivatives

The *in vitro* asexual blood-stage anti-plasmodium activities of synthesized imidazopyridines and pyrazolopyridine were evaluated against the chloroquine (CQ) sensitive strain of *P. falciparum* (*Pf*NF54) using the previously described parasite LDH assay [17]. Positive controls such as chloroquine and artesunate were included in the assay. Compounds exhibiting potency of IC_{50} value less than 1 µM against the sensitive strain (*Pf*NF54) were progressed for testing against the multidrug-resistant strain (K1) using the same protocol. In parallel, evaluation of kinetic turbidimetric solubility was undertaken for all synthesized imidazopyridines. A summary of the anti-plasmodium activity (IC_{50} values) and kinetic solubility (based on the modified HPLC DMSO "dry-down" method) is provided in **Table 2.** To investigate the cytotoxicity of the imidazopyridine and pyrazolopyridine derivatives, the cytotoxicity of compounds exhibiting high anti-plasmodium potency (*Pf*NF54 < 1 µM) were evaluated based on the well-established colorimetric 3-(4,5-dimethylthiazol-2-yl)-2,5-diphenyltetrazolium bromide (MTT) assay in CHO cells [18], [19]. This work was conducted at H3D within the Division of Clinical Pharmacology, Department of Medicine, UCT. The IC_{50} values were determined, and selectivity indices (**SI**) were derived as summarized in **Table 2**.

To validate these compounds as PI4K inhibitors, *in vitro* PI4K inhibition was assessed using purified *Pv*PI4K recombinant protein in an ADP detection assay using the ADP-Glo Kinase assay (Promega) [20]. Evaluation against *Pf*PI4K would have been more desirable*, Pv*PI4K is the only recombinantly expressed and purified *Plasmodium* PI4K available. Notwithstanding, the catalytic domains of *Pf*PI4K and *Pv*PI4K are well conserved and share over 97% sequence similarity. Consequently, *Pv*PI4K serves as an adequate surrogate for *Pf*PI4K which is more challenging to express recombinantly. In support of this, inhibition assays using a heavily truncated *Pf*PI4K construct demonstrated comparable IC_{50} values for a number of ATP competitive inhibitors previously tested

against *Pv*PI4K [21]. The potential of this class of compounds to act as dual *Plasmodium* inhibitors was evaluated by testing selected compounds against full-length recombinant *Pf*PKG (PF3D7_1436600) expressed and purified according to methods previously described [22], [23] . The assay was performed in the presence of kinase-activator cGMP and peptide substrate (GRTGRRNSINH2). ADP formation was detected using the ADP Glo Kinase assay.

Table 3: anti-plasmodium, Cytotoxicity, In vitro PfPKG and PvPI4k inhibition activity (IC_{50} values) of target pyrazolo[1,5-a]pyridine and imidazo[1,2-a]pyridine.

Code	**[a]*Pf*NF54 (IC_{50}, µM)**	**[a]*Pf*K1 (IC_{50}, µM)**	**[b]RI**	**[c]Solubility (µM, pH 6.5)**	**[d]Cytotoxicity (IC_{50}, µM)**	**[e]SI**	***Pv*PI4k (IC_{50}, µM)**	***PfPKG* (IC_{50}, µM)**
32ab 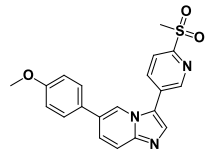	0.2360	>6	>25	190	>50	>212	0.554	6.910
32ac 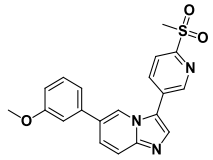	>6	–	–	–	–	–	–	–
40b 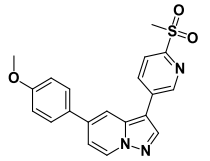	0.3709	0.6447	2	<5	46.45	132	0.032	2.210
Controls [5]								
Chloroquine	0.010							
Artesunate	0.008							

"-" = Not determined, [a]asexual blood stage IC_{50} values are means of n ≥ 2 determinations; Artesunate [IC_{50} = 4 nM (*Pf*NF54), 3 nM (*Pf*K1)] and chloroquine [IC_{50} = 10 nM (*Pf*NF54), 194 nM (*Pf*K1)] were used as reference drugs; [b]RI = resistance index i.e., *Pf*K1 IC50/*Pf*NF54 IC_{50}; [c]HPLC solubility in µM (pH 6.5); determined via HPLC-based DMSO "dry-down" method, [d]CHO = Chinese hamster ovarian cell line; [e]SI = selectivity index i.e. CHO IC_{50}/*Pf*NF54 IC_{50}.

The tested compounds showed potent activity against the chloroquine sensitive strain of the parasite (*Pf*NF54 IC_{50} <1 µM). Furthermore, low cross-resistance (**RI** < 2) against the multidrug resistant (K1) strain was determined. Compound **32ab** displayed high potency against the *Pf*NF54 strain (IC_{50} = 0.2360 µM) but displayed poor activity against the multidrug resistant strain (*Pf*K1 IC_{50} > 6 µM) resulting into high cross resistance (**RI** > 25). Substitution of 4-methoxyphenyl moiety with 3-methoxyphenyl (compound **32ac**) led to a loss of activity against the sensitive strain (*Pf*NF54 IC_{50} > 6 µM) (**Table 2**) compared to compound **32ab**. However, compound **32ac** was not progressed for multidrug resistant testing due to its poor activity against the chloroquine resistant strain (*Pf*NF54)

On the other hand, compound **40b** displayed good potency against the *Pf*NF54 strain (IC_{50} = 0.3709 µM) and good activity against the multidrug resistant strain (*Pf*K1 IC_{50} = 0.6447 µM) compared to compound **32ab**. Moreover, Compound **40b** displayed a low cross resistance of two (**RI** =2) compared to compound **32ab** (**RI** >25).

With that in mind, solubility test was undertaken for both compound **32ab** and **40b** based on the H3D-adapted HPLC method (**Table 2**). Compound **32ab** displayed high solubility (> 100 µM) while compound **40b** displayed poor solubility (< 5 µM), however, the solubility of compound **32ac** was not tested due to its poor activity against the *Pf*NF54 strain (IC_{50} > 6 µM).

The compounds tested against the CHO cell line demonstrated a low cytotoxicity profile (CHO IC_{50} > 50 µM). Compound **32ab** displayed high anti-plasmodium potency (*Pf*NF54 IC_{50} = 0.2360 µM) and low CHO cytotoxicity with a selective index of more than 100, resulting in the most favourable safety profile (CHO IC_{50} > 50 µM; SI > 179). On the hand compound **40b** displayed high anti-plasmodium potency (*Pf*NF54 IC_{50} = 0.3709 µM) and

moderate CHO cytotoxicity of IC_{50} = 46.45 µM with a selective index of more than 100, however, this compound **40b** does not meet the favourable safety profile (CHO IC_{50} > 50 µM; SI > 100) due to CHO cytotoxicity of less than 50 µM.

Generally, the enzymatic data compliments well with the observed anti-plasmodium activity with the moderately potent compound against *Pf*NF54, **40b** (IC_{50} = 0.3709 µM), also exhibiting significant activity against the kinase *Pv*PI4K (IC_{50} = 0.032 µM). Subjecting this compound to molecular docking (MD) in the *Pf*PI4K homology model predicted a H-bond interaction between N1 of the scaffold and the Val 598 residue of the model (**Figure 2.12**). Furthermore, a H-bond interaction between the pyridinyl sulfone moiety and the glutamine residue (GLN 606; **Figure 2.12**) was observed. However, the interaction between Lys 549 and **40b** was not observed compared to the ligand PIK93, let alone π–π interaction.

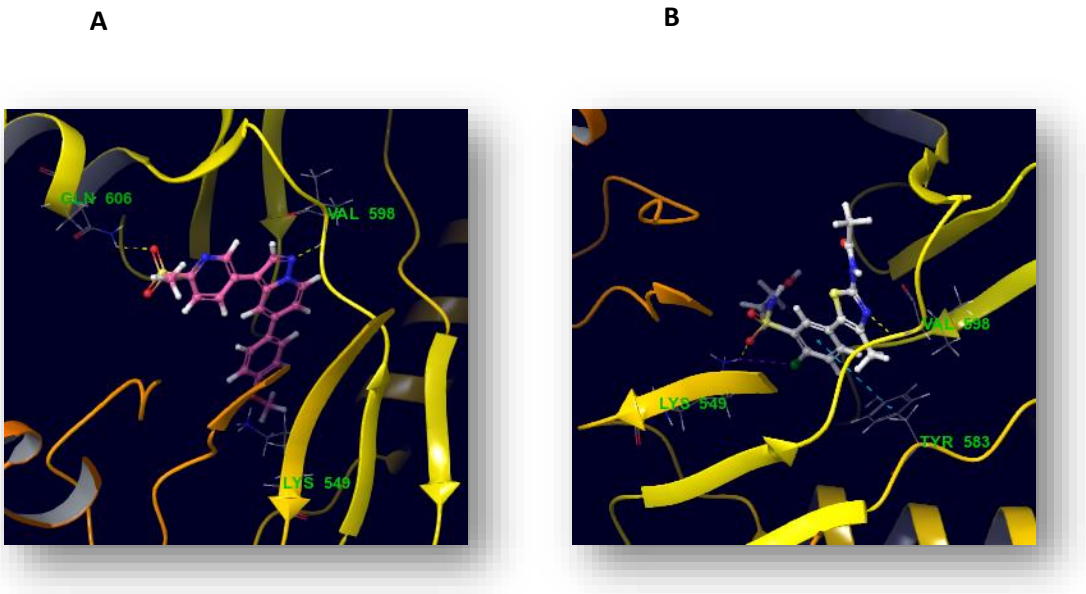

Figure 2.12: (**A**) Docking representation of compound **40b** in the PfPI4K homology model and (**B**) The ATP-binding site of PfPI4K homology model (PDB ID: **4D0L**) with the co-crystallized ligand PIK93. The interacting residues are labelled and shown respectively.

Compound **32af** (*Pv*PI4K IC50 = 0.554 µM) was moderately potent although the observed interaction in the pocket binding site with Lys 549 was not observed but only similar interactions of compound **40b** (**Figure 2.13**). On the other hand, compound **32ac** with poor anti-plasmodium activity, in the docking site predicted a H-bond interaction between the methoxy oxygen atom and the Val 598 residue while the five membered ring of the core made a π–π interaction with Lys 549.

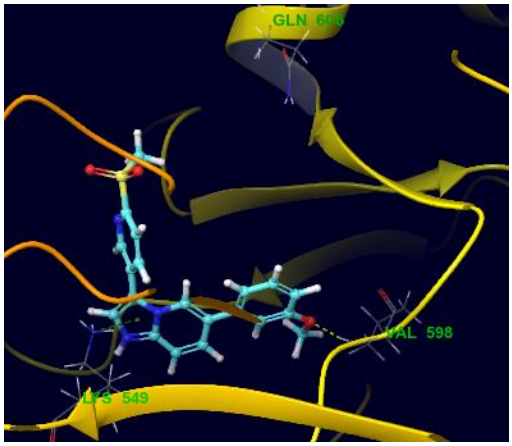

Figure 2.13**:** Docking representation of compound **32ac** in the PfPI4K homology model (PDB ID: **4D0L**). The interacting residues are labelled and shown.

To further investigate the potency of the compounds against the *Pf*PKG kinase, the *in vitro Pf*PKG inhibitory activities of both compounds (**32ab** and **40b**) were investigated using the method described above. The inhibitory concentration (IC_{50}) values of the compounds are listed in **Table 2**. The IC_{50} determined indicated that the investigated compounds showed inhibitory concentrations > 2 µM, with compound **40b** exhibiting an inhibitory concentration of 2.210 µM against the *Pf*PKG kinase while compound **32ab** exhibiting a higher IC_{50} value of 6.910 µM. Docking compound **40b** in the ATP-binding site of the *Pv*PKG crystal structure (**PDB code: 5EZR; Figure 2.14**) predicted a pair of H-bond interaction between the sulfone moiety and the Asp 675 and Phe 676 residues. In addition, the pyridinyl sulfone Nitrogen atom interacts with Lys 563 explaining the moderate inhibitory activity.

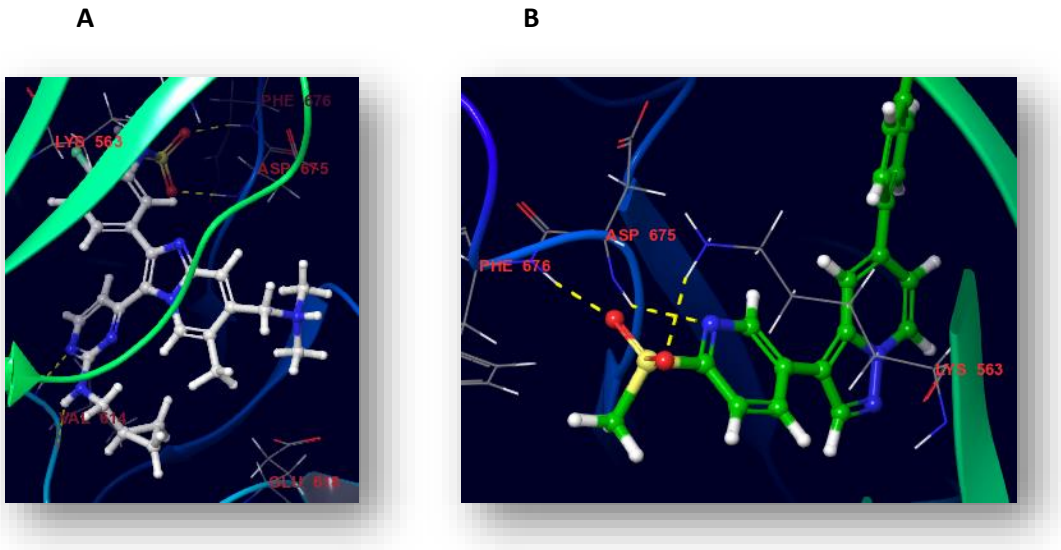

Figure 2.14**:** (**A**) The ATP-binding site of PvPKG crystal structure (PDB ID: **5EZR**) with the co-crystallized ligand 4ZS. (**B**) Docking representation of compound **40b** in the PvPKG ATP-binding site and the interacting residues are labelled and shown respectively.

On the other hand, compound **32ab** docked in the active site of *Pv*PKG crystal structure has predicted a pair of H-bond from the Asp 675 and Val 614 residues (shown in **Figure 2.15**). A complete loss of interaction was observed between compound **32ab** (*Pf*PKG IC_{50} = 6.910 µM) and the Lys 563 and Phe 676 residues, explaining the loss in *Pf*PKG inhibitory activity.

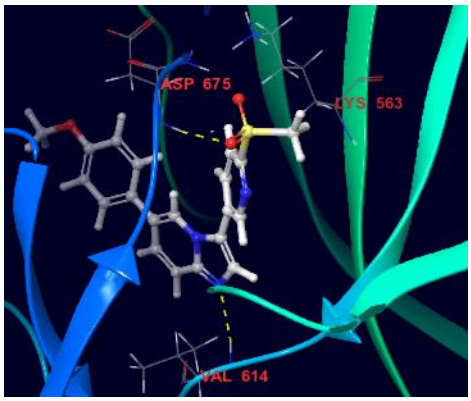

Figure 2.15**:** Docking representation of compound **32ab** in the PvPKG ATP-binding site (PDB ID: **5ERZ**). The interacting residues are labelled and shown.

Overall, this data for the investigated compounds shows that cytotoxicity is not a challenge for imidazopyridine core but a challenge for pyrazolopyridine. However, it will be important to evaluate the cytotoxicity of this cores in other cell lines. Although these compounds show moderate anti-plasmodium potency and a significant decline in *in vitro* *Pf*PKG activity compared to that of *Pv*PI4K. This suggests that the choice of moieties incorporated on the cores may not be suitable as shown by compound **32ac** (poor antiplasmodium activity) but require further investigation. On the other hand, *in silico* predictions associated with the fixed-core docking methodology used in this study, which assumes a rigid protein-ligand interaction and may not accurately predict binding of the core scaffold in the ATP-binding site. Although time consuming computations such as induced fit docking (IFD) and quantum molecular dynamic (QMD) methodology may be more accurate for such predictions. Furthermore, lack of π-π stacking interaction with Try 583 residue, as observed in *Pf*PI4K, provided an explanation for the loss in affinity observed in the *Pf*PKG biochemical assay for particularly compound **32ab**.

References

[1] Marandi, G; Saghatforoush, L.; Mendoza-Meroño, R.; García-Granda, S., "Catalyst-free synthesis of 3-(alkylamino)-2-arylimidazo[1,2-a]pyridine-8-carboxylic acids via a three-component condensation," *Tetrahedron Lett,* vol. 55, pp. 3052 - 3054, 2014.

[2] Juillet, C.; Ermolenko, L.; Boyarskaya, D.; Baratte, B.; Josselin, B.; Nedev, H.; Bach, S.; Iorga, B. I.; Bignon, J.; Ruchaud, S.; Al-Mourabit, A., "From Synthetic Simplified Marine Metabolite Analogues to New Selective Allosteric Inhibitor of Aurora B Kinase," *J. Med. Chem,* vol. 64, pp. 1197 - 1219, 2021.

[3] Carreno, M.; Ruano, J.; Sanz, G.; Toledo, M.; Urbano, A., "Mild and regiospecific nuclear iodination of methoxybenzenes and napthalenes with N-iodosuccinimide in acetonitrile.," *Tetrahedron Lett. ,* vol. 37, no. 23, pp. 4081 - 4084, 1996.

[4] Zhao, C; Li, F; Yang, S; Liu, L; Huang, Z; Chai, H., "Chemoselective iodination of 6-substituted imidazo[1,2-a]pyridine," *Chemi Heterocycl Compd,* vol. 54, no. 5, p. 568–571, 2018.

[5] Gachuhi, S. N (2022), *Design, Synthesis, and Structure-Activity Relationship Studies of Dual Plasmodium falciparum Phosphatidylinositol 4-kinase and cGMP-dependent Protein Kinase Inhibitors.,* PhD, University of Cape Town.

[6] Lima, C. F. R. A. C.; Rodrigues, A. S. M. C.; Silva, V. L. M.; Silva, A. M. S.; Santos, L. M. N. B. F. , "Role of the Base and Control of Selectivity in the Suzuki–Miyaura Cross-Coupling Reaction," *ChemCatChem,* vol. 6, pp. 1291-1302, 2014.

[7] MALULEKA, M.M (2019), "SYNTHESIS, BIOLOGICAL EVALUATION AND MOLECULAR DOCKING STUDIES OF NOVEL INDOLE- AND BENZOFURAN-CHALCONE AND BENZOFURAN-QUINAZOLINE HYBRIDS AS ANTICANCER AGENTS.," *PhD, UNIVERSITY OF SOUTH AFRICA.*

[8] Le Manach, C.; Paquet, T.; Brunschwig, C.; Njoroge, M.; Han, Z.; Cabrera, D. G.; Bashyam, S.; Dhinakaran, R.; Taylor, D.; Reader, J.; Botha, M.; Churchyard, A.;

Lauterbach, S.; Coetzer, T. L.; Birkholtz, L. M.; Meister, S.; Winzeler, E. A., "A Novel Pyrazolopyridine with in Vivo Activity in Plasmodium berghei- and Plasmodium falciparum-Infected Mouse Models from Structure−Activity Relationship Studies around the Core of Recently Identified Antimalarial Imidazopyridazines.," *J. Med. Chem.,* vol. 58, pp. 8713 - 8722, 2015.

[9] Almond-Thynne, J; Blakemore, D. C; Pryde, D. C; Spivey, A. C., "Site-selective Suzuki-Miyaura coupling of heteroaryl halides - understanding the trends of pharmaceutically important classes," *Chem.Sci,* vol. 8, pp. 40 - 62, 2017.

[10] Koubachi, J.; Kazzouli, S. E.; Berteina-Raboin, S.; Mouaddib, A.; Guillaumet, G., "EFFICIENT MICROWAVE-ASSISTED SUZUKI-MIYAURA CROSS COUPLING REACTION OF 6-HALOGENOIMIDAZO[1,2-a]PYRIDINES," *J.mar.Chim.Heterocycl.,* vol. 7, no. 1, pp. 1-9, 2008.

[11] Chapman, T.; Osborne, S.; Wallace, C.; Birchall, K.; Bouloc, N.; Jones, H.; Ansell, K.; Taylor, D.; Clough, B.; Green, J.; Holder, A., "Optimization of an imidazopyridazineseries of inhibitors of Plasmodium falciparum calcium-dependent protein kinase 1 (PfCDPK1)," *Med. Chem. ,* vol. 8, no. 4, pp. 636 - 648., 2014.

[12] Kendall, J. D.; O'Connor, P. D.; Marshall, A. J. ; Frédérick, Raphaël; Marshall, E. S.; Lill, C. L. ; Lee, W-J.; Kolekar, S.; Chao, M.; Malik, A.; Yu, S.; Chaussade, C.;Buchanan, C.; Rewcastle, G. W.; Baguley, B. C.; Flanagan, J. U.; Jamieson, S. M.F. ;, "Discovery of pyrazolo[1,5-a]pyridines as p110a-selective PI3 kinase inhibitors," *Biorg. Med. Chem,* vol. 20, pp. 69-85, 2012.

[13] Pérez-Silanes, S.; Berrade, L.; García–Sánchez, R.N.; Mendoza, A.; Galiano, S.; Pérez-Solórzano, B.M.; Nogal-Ruiz, J.J.; Martínez-Fernández, A.R.; Aldana, I.; Monge, A. , "New 1-Aryl-3-Substituted Propanol Derivatives as Antimalarial Agents.," *Molecules. ,* vol. 14, p. 4120 – 4135, 2009.

[14] N. Xi, Newbury-Park, (US) and CA., "HETEROAROMATIC COMPOUNDS AS PI3 KINASE MODULATORS AND METHODS OF USE". United states Patent US 2014/0234254 Al, 21 August 2014.

[15] Martins, M. A. P.; Scapin, E.; Frizzo, C. P.; Rosa, F. A.; Bonacorso, H. G.; Zanatta, N. , "2-Methyl-7-Substituted Pyrazolo[1,5-a]pyrimidines: Highly Regioselective Synthesis and Bromination.," *J. Braz. Chem. Soc. ,* vol. 20, no. 2, pp. 205 - 213, 2009.

[16] M. G. Stanton, N. Noucti, D. J. Sloman, B. Munoz and J. Lim, "PYRAZOLO[1,5-A]PYRIMIDINE DERIVATIVES". United state Patent WO 2009/014620 A1, 29 January 2009.

[17] Makler, M.; Hinrichs, D. , " Measurement of the lactate dehydrogenase activity of Plasmodium falciparum as an assessment of parasitemia.," *Am. J. Trop. Med. Hyg.,* vol. 48, no. 2, pp. 205 - 210, 1993.

[18] Liu, Y.; Peterson, D.; Kimura, H.; and Schubert, D. , "Mechanism of cellular 3-(4,5-Dimethylthiazol-2-yl)-2,5-diphenyltetrazolium bromide (MTT) reduction.," *J.Neurochem,* vol. 69 , no. 2, pp. 581 - 593, 1997.

[19] Verlinden, B.; Niemand, J.; Snyman, J.; Sharma, S.; Beattie, R.; Woster, P.; Birkholtz, L. , " Discovery of novel alkylated (bis)urea and (bis)thiourea polyamine analogues with potent antimalarial activities.," *J. Med. Chem. ,* vol. 54, no. 19, pp. 6624 - 6633, 2011.

[20] Cheuka, P.; Centani, L.; Arendse, L.; Fienberg, S.; Wambua, L.; Renga, S.; Dziwornu, G.; Kumar, M.; Lawrence, N.; Taylor, D.; Wittlin, S.; Coertzen, D.; Reader, J.; van der Watt, M.; Birkholtz, L.; Chibale, K., "New amidated 3,6-diphenylated imidazopyridazines with potent anti-plasmodium activity are dual inhibitors of Plasmodium phosphatidylinositol-4-kinase and cGMP-dependent protein kinase," *ACS Infect. Dis. ,* vol. 7 , no. 1, pp. 34 - 46. , 2021.

[21] Sternberg, A.; Roepe, P. , "Heterologous expression, purification, and functional analysis of the Plasmodium falciparum phosphatidylinositol 4-kinase IIIβ.," *Biochemistry.,* vol. 59, no. 27, pp. 2494 - 2506, 2020; .

[22] Baker, D.; Stewart, L.; Large, J.; Bowyer, P.; Ansell, K.; Jiménez-Díaz, M.; El Bakkouri, M.; Birchall, K.; Dechering, K.; Bouloc, N.; Coombs, P.; Whalley, D.; Harding, D.; Smiljanic-Hurley, E.; Wheldon, M.; Walker, E.; Dessens, J.; Lafuente, M.; Sanz, L., "A potent series targeting the malarial cGMP-dependent protein kinase clears infection and blocks transmission.," *Nat. Commun. ,* vol. 8, no. 1, pp. 1 - 9, 2017.

[23] Vanaerschot, M.; Murithi, J.; Pasaje, C.; Ghidelli-Disse, S.; Dwomoh, L.; Bird, M.; pottiswoode, N.; Mittal, N.; Arendse, L.; Owen, E.; Wicht, K.; Siciliano, G.; Bosche, M.; Yeo, T.; Kumar, T.; Mok, S.; Carpenter, E.; Giddins, M.; Sanz, O.; Ottilie, S.; A, "Inhibition of resistance-refractory P. falciparum Inhibition of resistance-refractory P. falciparum kinase PKG delivers prophylactic, blood stage, and transmission-blocking anti-plasmodial activity.," *Cell Chem. Bio. ,* pp. 1 - 11, 2020.

CHAPTER 3: SUMMARY, CONCLUSIONS AND RECOMMENDATIONS FOR FUTURE WORK

3.1. SUMMARY AND CONCLUSION

The aim of the study was to synthesize novel imidazo[1,2-a] pyridine and pyrazolo[1,5-a] pyridine derivatives that will be tested for their antimalarial activity through the inhibition of *Pv*PI4K and *Pf*PKG. The first objective was to synthesize a new library of imidazo[1,2-a] pyridine and pyrazolo[1,5-a] pyridine derivatives, with substituents at 3rd & 6th positions and 3rd & 5th position, respectively. The synthesis of compounds embodying the imidazo[1,2-a]pyridine and pyrazolo[1,5-a]pyridine cores were successfully conducted in this study in moderate to good yields and acceptable purity.

The second objective was to evaluate the activity of synthesized compounds against *Plasmodium falciparum*. In which the synthesized compounds were evaluated for asexual blood-stage antiplasmodium activities against the *Pf*NF52 strain. However, only compounds **32ab**, **32ac** and **40b** were tested, compound **32ab** (***Pf*NF54**; IC_{50} = 0.2360 μM**)** and **40b** (***Pf*NF54**; IC_{50} = 0.3709 μM**)** exhibited potent activity to be tested against the chloroquine resistant strain (*Pf*K1) in which compound **40b** (***Pf*K1**; IC_{50} = 0.6447 μM**)** was quite potent. After the evaluation of antiplasmodium activity, these compounds **32ab** and **40b** were tested for solubility and cytotoxicity. Compound **32ab** displayed high solubility (> 100 μM) while compound **40b** displayed poor solubility (< 5 μM). Moreover, compounds **32ab** and **40b** were tested against the CHO cell line and found to demonstrate cytotoxicity profile of (CHO IC_{50} > 50 μM) and (CHO IC_{50} < 50 μM), respectively. Compound **32ab** displayed high anti-plasmodium potency (***Pf*NF54**; IC_{50} = 0.2360 μM) and low CHO cytotoxicity with a selective index of more than 100, resulting in the most favourable safety profile (CHO IC_{50} > 50 μM; SI > 179).

The final objective was to investigate the inhibition of the prepared compounds against *Pv*PI4K and *Pf*PKG kinases. The enzymatic data revealed moderate and significant anti-plasmodium activity for compound **40b** with IC_{50} values of *Pf*NF54 (IC_{50} = 0.3709 μM) and

*Pv*PI4K (IC_{50} = 0.032 µM) compared to compound **32ab** (***Pv*PI4K**; IC_{50} = 0.554 µM) which was moderately potent.

The *in vitro Pf*PKG inhibitory activities of both compounds **32ab** and **40b** were investigated, the IC_{50} determined indicated that the investigated compounds displayed inhibitory concentrations > 2 µM, with compound **40b** displaying an inhibitory concentration of 2.210 µM against the *Pf*PKG kinase while compound **32ab** displayed a higher IC_{50} value of 6.910 µM against the *Pf*PKG.

Molecular docking studies of compounds **40b** and **32ab** into the ATP-binding site of the *Pv*PKG crystal structure (**PDB code: 5EZR; Figure 2.14**) revealed a pair of hydrogen bond interaction between the sulfone moiety of **40b** and the Asp 675 and Phe 676 residues. In addition, the interaction between the nitrogen atom of the pyridinyl sulfone group of **40b** with Lys 563 could be responsible for the moderate inhibitory activity for this compound. Compound **32ab**, on the other hand, predicted a pair of hydrogen bonding from the Asp 675 and Val 614 residues (shown in **Figure 2.15**). No interaction was observed between compound **32ab** and the Lys 563 and Phe 676 residues, explaining the loss in *Pf*PKG inhibitory activity.

Compounds **40b** and **32ab** were also docked into the *Pf*PI4K homology model (**PDB ID: 4D0L**). This predicted a hydrogen bond interaction between the N1 of the scaffold and the Val 598 residue of the model for compound **40b**. Furthermore, a hydrogen bond interaction between the pyridinyl sulfone moiety and the glutamine residue (GLN 606; **Figure 2.12**) was also observed. Similar interactions were observed for compound **32ab**.

In conclusion, this project led to the successful synthesis of imidazo[1,2-a]pyridine and pyrazolo[1,5-a]pyridine derivatives. Their associated potency has been linked to *Pv*PI4K inhibition with the strategies proving poor potency against *Pf*PKG kinase.

3.2. RECOMMENDATION FOR FUTURE WORK

In this study, the anti-plasmodium potency and inhibitory properties against the kinases (*Pv*PI4K & *Pf*PKG) of the imidazo[1,2-a]pyridine and pyrazolo[1,5-a]pyridine derivatives were demonstrated. It is recommended that the compounds which were not investigated for anti-plasmodium potency and inhibitory properties against the kinases (*Pv*PI4K & *Pf*PKG) to be subjected to *in vitro* studies as well to establish safety profile before subjecting the compounds to *in vivo* proof-of-concept studies in a relevant mouse model to establish its efficacy and PK properties. It is also important to investigate the potential multi-stage (gametocytocidal and liver-stage) activities of these compounds to determine their transmission blockade to support efforts towards malaria eradication.

CHAPTER 4: EXPERIMENTAL

4.1. GENERAL INFORMATION.

All commercially available reagents and solvents were purchased from either Sigma Aldrich (South Africa) and Merck (South Africa), or Enamine building blocks (USA) and were used without further purification. All reactions involving moisture-sensitive reagents were carried out in an oven-dried glassware under a nitrogen (N_2) atmosphere. Reactions that needed hot or cold temperatures were carried out at the appropriate temperatures in an oil bath, an ice bath, test tube heat block, and monowave 200 microwave synthesis reactor. All the measurements were carried out at room temperature with fluctuations ranging from 20 °C to 27 °C. Glassware was thoroughly washed with distilled water, followed by rinsing with acetone and oven dried at 80 °C the day before use. The intermediate and target molecules were synthesized in glass flasks and subjected to appropriate purification techniques such as column chromatography and re-crystallization. Thin layer chromatography (TLC) on aluminium-baked Merck silica 60 F254 was visualized under ultra-violent light with wavelength of 254 nm to monitor the reaction progress while purification was conducted using the flash column chromatography (Combi-Flash NextGen 300+). Analytical thin layer chromatography (TLC), performed on Merck silica gel 60 F254 pre-coated aluminum plates, was used to monitor the profile of reaction mixtures, fractions eluting from the columns, and compound purity. Chromatographic components were visualized under UV light at 254 nm while mobile phase analytical-reagent (AR) grade solvents for TLC and column/flash chromatography were used as purchased. Lasec Cole-Pamer Stuart SMP30 was used to record the melting point. Biological assays were performed at the Holistic Drug Discovery and Development (H3D) Centre at the university of Cape Town, South Africa

4.2. ANALYSIS AND CHARACTERIZATION TECHNIQUES

The ^{1}H NMR and ^{13}C NMR spectra were obtained from Nuclear Magnetic Resonance (NMR) (Bruker Ascend 400 MHz Topspin 3.2). The NMR spectra were referenced internally using solvent signals. For ^{1}H NMR, the signals were 7.25 ppm for $CDCl_3$, 2.50

ppm for DMSO-d_6, 3.31 ppm & 4.78 ppm MeOD and for ^{13}C NMR, the signals were 77.0 ppm for $CDCl_3$, 39.9 ppm for DMSO-d_6 , 49.15 ppm MeOD respectively at room temperature. The ^{1}H NMR spectra were presented as follows (I) chemical shift (δ) in ppm, (II) multiplicity (s = singlet, d = doublet, dd = doublet of doublets, t = triplet, q = quartet, m = multiplet), (III) coupling constant (*J*) in Hz. The structural properties of the compounds were recorded and confirmed by using LC-MS XS00R QTOF High-Resolution Mass Spectrometry (HRMS).

4.3. Synthesis and characterization of imidazo[1,2-a]pyridines

4.3.1. Synthesis of 6-Chloroimidazo[1,2-a]pyridine, 29 [1].

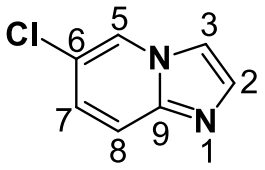

A mixture of 2-amino-5-chloro pyridine (10.0 g, 77.8 mmol) and 2-chloroacetaldehyde (1.2 eq.) in ethanol (20 mL) was refluxed overnight. After completion of the reaction, the solvent was vacuumed off and purified by reverse phase column chromatography (0 – 70%, water/MeOH) to afford the product, as a yellow solid (9.80 g, 83 %); R_f (100% EtOAc) 0.3; ^{1}H-NMR ($CDCl_3$, 400 MHz): δ 8.17 (d, *J* = 1.2 Hz, 1H; H-5), 7.64 (d, *J* = 0.8 Hz, 1H, H-2), 7.57 – 7.55 (d, 2H, H-3/8), 7.12 (dd, *J* = 9.6 and 1.6 Hz, 1H, H-7); ^{13}C-NMR ($CDCl_3$, 100 MHz): δ 143.8, 134.5, 125.8, 123.6, 120.6, 118.2, and 112.8. HRMS-ESI : (m/z) $[M+H]^+$ = 153.0194, calculated = 152.0141.

4.3.2. Synthesis of 6-Chloro-3-iodoimidazo[1,2-a]pyridine, 30

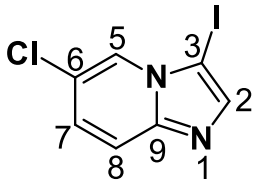

To a stirred solution of 6-chloroimidazo[1,2-a] pyridine (1.0 g, 6.55 mmol) in acetonitrile (20 mL) was added N-iodosuccinimide (1.6 g, 7.21 mmol, 1.1 eq.). The reaction mixture was then stirred at 25°C for 24 hours. At completion of the reaction, monitored by a thin layer chromatography, the resulting precipitate was filtered, washed with ACN (30 mL), and allowed to dry affording the product, as a white solid (1.30 g, 71%); R_f (100% EtOAc) 0.7; ^{1}H-NMR ($CDCl_3$, 400 MHz): δ 8.17 (d, *J* = 1.2 Hz, 1H; H-5), 7.70 (s, 1H, H-2), 7.55 (d, *J* = 9.2 Hz, 1H, H-8), 7.19 (dd, *J* = 9.6 and 2.0 Hz, 1H, H-7); ^{13}C-NMR ($CDCl_3$, 100 MHz): δ 146.2, 141.1, 126.4, 124.1, 121.9, 118.2, 61.5. HRMS-ESI : (m/z) $[M+H]^+$ = 278.9181, calculated = 277.9108.

4.4. General procedure 1: Synthesis of intermediates 31a and 31b [2].

In a sealed tube, a solution of 6-chloro-3-iodo imidazo[1,2-a] pyridine (1.0 g, 3.59 mmol), K_2CO_3 (0.745 g, 5.39 mmol, 1.5 eq.), $Pd(PPh_3)_2Cl_2$ (0.126 g, 0.180 mmol, 0.05 eq.) and an appropriate boronic acid (1.1 eq.) in 10 mL dioxane/ water mixture (3:1) was purged with N_2 for 5 min. The mixture was heated to 90 ºC while stirring for 3 h. At completion, the reaction mixture was cooled to 20 ºC, concentrated under *vacuo* and purified by flash column chromatography (0 – 5 %, DCM/MeOH) to afford the expected product.

4.4.1. 6-chloro-3-(4-(methylsulfonyl)phenyl)imidazo[1,2-a]pyridine, 31a

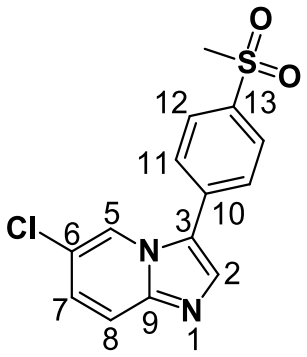

Using general procedure 1 and a reaction mixture containing **30** (1.0 g, 3.59 mmol) and (4-(methylsulfonyl)phenyl)boronic acid (0.790 g, 3.95 mmol, 1.1 eq.), the product was obtained as white solid. (0.810 g, 73%); R_f (100% EtOAc) 0.48; ^{1}H-NMR ($CDCl_3$, 400 MHz): δ 8.38 (d, *J* = 0.8 Hz, 1H; H-5), 8.10 (d, *J* = 8.4 Hz, 2H, H-11), 7.80 (s, 1H, H-2), 7.76 (d, *J* = 8.4 Hz, 2H, H-12), 7.66 (d, *J* = 9.6 Hz, 1H, H-8), 7.24 (dd, *J* = 10 and 1.6 Hz, 1H, H-7), 3.12 (s, 3H, -$SO_2C\underline{H}_3$); ^{13}C-NMR ($CDCl_3$, 100 MHz): δ 145.3, 139.9, 134.8, 134.2, 128.6 (2C), 128.1 (2C), 126.6, 124.4, 121.9, 121.0, 118.9, 44.5. HRMS-ESI : (m/z) $[M+H]^+$ = 307.0294, calculated = 306.0230.

4.4.2. 6-chloro-3-(6-(methylsulfonyl)pyridin-3-yl)imidazo[1,2-a]pyridine, 31b

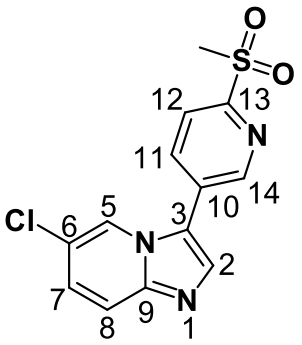

Using general procedure 1 and a reaction mixture containing **30** (1.0 g, 3.59 mmol) and (6-(methylsulfonyl)pyridin-3-yl)boronic acid (0.794 g, 3.95 mmol, 1.1 eq.), the product was obtained as white solid. (0.78 g, 72%); R_f (100% EtOAc) 0.46; ^{1}H-NMR ($CDCl_3$, 400 MHz):

δ 8.94 (s, 1H, H-14), 8.35 (s, 1H, H-5), 8.25 (d, *J* = 7.84 Hz, 1H, H-11), 8.14 (d, *J* = 5.88 Hz, 1H, H-12), 7.87 (s, 1H, H-2), 7.69 (d, *J* = 9.28 Hz, 1H, H-8), 7.29 (d, *J* = 7.96 Hz, 1H, H-7), 3.30 (s, 3H, -$SO_2C\underline{H}_3$); ^{13}C-NMR (MeOD-d_4, 100 MHz): δ 158.2, 150.1 (2C), 138.2, 135.8, 130.3, 129.3, 123.8, 123.6 (2C), 122.9, 119.0, 40.6. HRMS-ESI : (m/z) $[M+H]^+$ = 308.0255, calculated = 307.0182.

4.5. General procedure 2: Synthesis of target compounds, 32 a-ac [3].

A solution of **31a** (50 mg), K_2CO_3 (1.5 eq.) and $Pd(PPh_3)_4$ (0.1 eq.), PCy_3 (0.1 eq.) and the appropriate boronic acid (1.1 eq.) in 10 ml dioxane/ water mixture (3:1) was purged with N_2 for 5 min. The reaction mixture was microwave irradiated at 150 ºC while stirring for 3 h. The mixture was cooled to 20 ºC, concentrated under *vacuo* and purified by flash column chromatography (100% EtOAc) to afford the expected product.

4.5.1. 3-(4-(methylsulfonyl)phenyl)-6-(m-tolyl)imidazo[1,2-a]pyridine, 32a

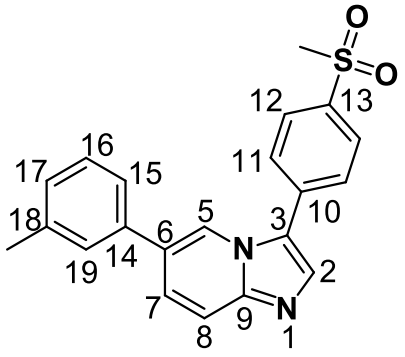

Using general procedure 2 and a reaction mixture containing **31a** (50 mg, 0.163 mmol) and m-tolylboronic acid (0.0243 g, 0.179 mmol, 1.1 eq.), the product was obtained as white solid. (30 mg, 51%); mp. 208 – 210 ºC; R_f (100% EtOAc) 0.5; ^{1}H-NMR ($CDCl_3$, 400 MHz): δ 8.55 (s, 1H; H-5), 8.07 (d, *J* = 8.4 Hz, 2H, H-11), 7.82 (s, 1H, H-2), 7.81 (d, *J* = 8.8 Hz, 2H, H-12), 7.73 (d, *J* = 9.6 Hz, 1H, H-8), 7.49 (dd, *J* = 9.6 and 1.6 Hz, 1H, H-16),

7.38 (m, *J* = 9.2 and 7.2 Hz, 1H, H-15), 7.33 (dd, *J* = 7.6 and 1.6 Hz, 1H, H-7), 7.07 – 7.01 (m, 1H, H-17, 19), 3.86 (s, 3H, -$SO_2C\underline{H}_3$), 3.11 (s, 3H, -$C\underline{H}_3$); ^{13}C-NMR ($CDCl_3$, 100 MHz): δ 156.5, 139.2, 135.1, 134.3, 130.4, 129.7, 128.5 (3C), 128.4, 127, 8 (2C), 125.9, 124.8, 122.7, 121.2 (2C), 117.3, 111.3, 55.7, 44.6. HRMS-ESI : (m/z) $[M+H]^+$ = 363.1162, calculated = 362.1089.

4.5.2. N,N-dimethyl-3-(3-(4-(methylsulfonyl)phenyl)imidazo[1,2-a]pyridin-6-yl)aniline, 32b

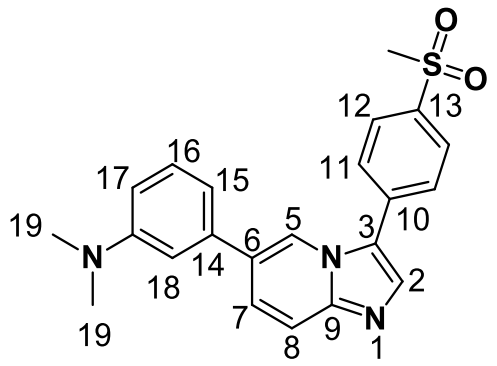

Using general procedure 2 and a reaction mixture containing **31a** (50 mg, 0.163 mmol) and (3-(dimethylamino)phenyl)boronic acid (0.0295 g, 0.179 mmol, 1.1 eq.), the product was obtained as white solid. (46 mg, 72%); mp. 207 – 209 ºC; R_f (100% EtOAc) 0.47; ^{1}H-NMR ($CDCl_3$, 400 MHz): δ 8.96 (s, 1H; H-5), 8.56 (d, *J* = 6.68 Hz, 2H, H-11), 7.80 (s, 1H, H-15, 17), 8.27 (d, *J* = 6.8 Hz, 2H, H-12), 8.09 (s, 1H, H-8), 7.78 (m, *J* = 7.64 Hz, 1H, H-16), 7.71 (s, 1H, H-2), 7.30 – 7.23 (m, 2H, H-7, 18), 3.58 (s, 3H, -$SO_2C\underline{H}_3$), 3.58 (s, 6H, -$C\underline{H}_3$); ^{13}C-NMR ($CDCl_3$, 100 MHz): δ 151.0, 139.4, 138.1, 135.0, 134.6, 129.8 (2C), 129.1 (2C), 128.5 (2C), 127.9, 126.5, 120.4, 118.1, 115.3, 112.2 (2C), 110.9, 44.5, 40.6 (2C). HRMS-ESI : (m/z) $[M+H]^+$ = 392.1427, calculated = 391.1354.

4.5.3. 6-(2-methoxyphenyl)-3-(4-(methylsulfonyl)phenyl)imidazo[1,2-a]pyridine, 32c

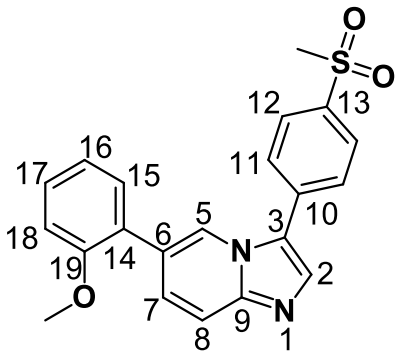

Using general procedure 2 and a reaction mixture containing **31a** (50 mg, 0.163 mmol) and 2-methoxyphenylboronic acid (0.0272 g, 0.179 mmol, 1.1 eq.), the product was obtained as white solid. (32 mg, 52%); mp. 209 – 211 ºC; R_f (100% EtOAc) 0.54; ^{1}H-NMR ($CDCl_3$, 400 MHz): δ 8.55 (s, 1H; H-5), 8.06 (d, *J* = 8.4 Hz, 2H, H-11), 7.82 – 7.80 (d, 1H, H-2, 12), 7.72 (d, *J* = 9.6 Hz, 1H, H-8), 7.48 (dd, *J* = 9.2 and 1.2 Hz, 1H, H-7), 7.38 (m, *J* = 7.6 and 1.6 Hz, 1H, H-15), 7.33 (dd, , *J* = 7.6 and 1.6 Hz, 1H, H-17), 7.07 (m, 2H, H-16, 18), 3.85 (s, 3H, -OC$\underline{H}_3$), 3.11 (s, 3H, -$SO_2C\underline{H}_3$); ^{13}C-NMR ($CDCl_3$, 100 MHz): δ 156.5, 139.2, 135.1, 134.4, 130.4, 129.7, 128.4 (2C), 128.3, 127.8 (2C), 125.9, 124.7, 122.7, 121.1 (2C), 117.3, 111.3 (2C), 55.7, 44.5. HRMS-ESI : (m/z) $[M+H]^+$ = 379.1077, calculated = 378.1038.

4.5.4. 3-(4-(methylsulfonyl)phenyl)-6-(2-(trifluoromethoxy)phenyl)imidazo[1,2-a]pyridine, 32d

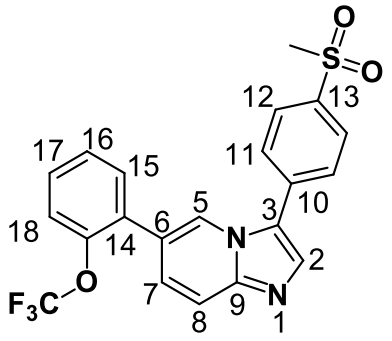

Using general procedure 2 and a reaction mixture containing **31a** (50 mg, 0.163 mmol) and (2-(trifluoromethoxy)phenyl)boronic acid (0.0369 g, 0.179 mmol, 1.1 eq.), the product was obtained as white solid. (35 mg, 50%); mp. 170 – 174 ºC; R_f (100% EtOAc) 0.56; ^{1}H-NMR ($CDCl_3$, 400 MHz): δ 8.33 (s, 1H; H-5), 8.04 (d, *J* = 8.36 and 10.36 Hz, 2H, H-11), 7.77 – 7.70 (m, 4H, H-2, 12, 15), 7.61 (d, *J* = 9.20 Hz, 1H, H-8), 7.41 – 7.34 (m, 3H, H-16, 17, 18), 7.19 (m, 1H, H-7), 3.07 (s, 3H, -$SO_2C\underline{H}_3$); ^{13}C-NMR ($CDCl_3$, 100 MHz): δ 139.9, 134.8, 134.2, 132.1, 132.0, 131.9, 131.9, 131.3, 129.8, 128.6 (2C), 128.6, 128.4, 128.1 (2C), 127.5, 127.3, 126.6, 121.9, 121.5, 121.1, 118.9, 118.1, 44.5. HRMS-ESI : (m/z) $[M+H]^+$ = 433.0828, calculated = 432.0755.

4.5.5. 3-(4-(methylsulfonyl)phenyl)-6-(4-(trifluoromethoxy)phenyl)imidazo[1,2-a]pyridine, 32e

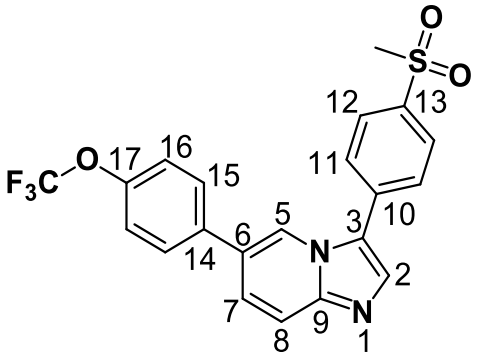

Using general procedure 2 and a reaction mixture containing **31a** (50 mg, 0.163 mmol) and (4-(trifluoromethoxy)phenyl)boronic acid (0.0369 g, 0.179 mmol, 1.1 eq.), the product

was obtained as white solid. (33 mg, 47%); mp. 187–190 ºC; R_f (100% EtOAc) 0.53; ^{1}H-NMR ($CDCl_3$, 400 MHz): δ 8.47 (s, 1H; H-5), 8.10 (d, *J* = 8.4 Hz, 2H, H-11), 7.84 - 7.78 (m, 4H, H-12, 2, 8), 7.55 (d, *J* = 8.8 Hz 1H; H-15), 7.48 (dd, *J* = 9.2 and 1.2 Hz, 1H, H-7), 7.32 (d, *J* = 8.4 Hz, 2H, H-16), 3.12 (s, 3H, -$SO_2C\underline{H}_3$); ^{13}C-NMR ($CDCl_3$, 100 MHz): δ 149.2, 146.2, 139.7, 135.8, 134.8, 134.7, 128.6 (2C), 128.5 (2C), 128.1 (2C), 126.8, 125.7, 124.4, 121.7 (2C), 120.5, 118.7, 44.5. HRMS-ESI : (m/z) $[M+H]^+$ = 433.0804, calculated = 432.0755.

4.5.6. 6-(3-fluorophenyl)-3-(4-(methylsulfonyl)phenyl)imidazo[1,2-a]pyridine, 32f

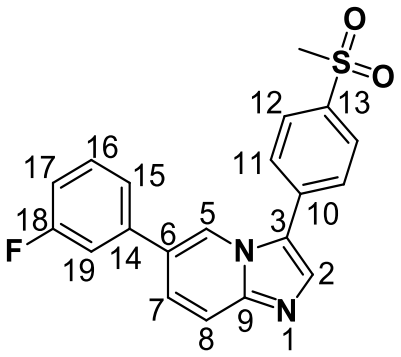

Using general procedure 2 and a reaction mixture containing **31a** (50 mg, 0.163 mmol) and 3-fluorophenylboronic acid (0.0250 g, 0.179 mmol, 1.1 eq.), the product was obtained as white solid. (48 mg, 80%); mp. 162–165 ºC; R_f (100% EtOAc) 0.48; ^{1}H-NMR ($CDCl_3$, 400 MHz): δ 8.50 (s, 1H; H-5), 8.10 (d, *J* = 8.4 Hz 1H, H-11), 7.84 – 7.77 (m, 4H, H-2, 8, 12), 7.50 (dd, *J* = 9.2 and 1.2 Hz, 1H, H-7), 7.44 (m, *J* = 8.0 and 6.0 Hz, 1H, H-19), 7.31 (d, *J* = 7.6 Hz, 1H, H-15), 7.22 (d, *J* = 3.6 Hz, 1H, H-16), 7.09 (m, *J* = 8.4 and 2.4 Hz, 1H, H-17), 3.13 (s, 3H, -$SO_2C\underline{H}_3$); ^{13}C-NMR ($CDCl_3$, 100 MHz): δ 164.4, 161.9, 139.7, 139.2 (d, $J_{C\text{-}F}$ = 7.75 Hz), 134.7 (d, $J_{C\text{-}F}$ = 8.91 Hz), 132.1, 131.9, 130.8 (d, $J_{C\text{-}F}$ = 8.55 Hz), 128.6 (2C), 128.1 (2C), 126.9 (d, $J_{C\text{-}F}$ = 2.12 Hz), 125.7, 122.7 (d, $J_{C\text{-}F}$ = 2.77 Hz), 120.6, 118.6, 115.1 (d, $J_{C\text{-}F}$ = 20.98 Hz), 114.0 (d, $J_{C\text{-}F}$ = 22.17 Hz), 44.5. HRMS-ESI : (m/z) $[M+H]^+$ = 367.0911, calculated = 366.0838.

4.5.7. N,N-dimethyl-2-(3-(4-(methylsulfonyl)phenyl)imidazo[1,2-a]pyridin-6-yl)aniline, 32g

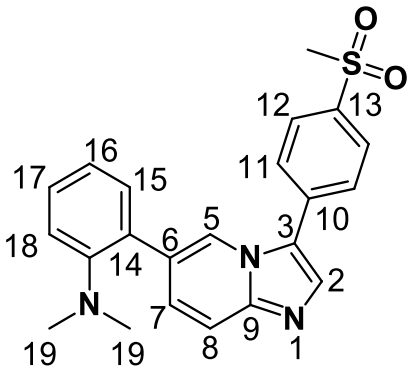

Using general procedure 2 and a reaction mixture containing **31a** (50 mg, 0.163 mmol) and (2-(dimethylamino)phenyl)boronic acid (0.0295 g, 0.179 mmol, 1.1 eq.), the product was obtained as white solid. (48 mg, 75%); mp. 116–120 ºC; R_f (100% EtOAc) 0.55; ^{1}H-NMR ($CDCl_3$, 400 MHz): δ 8.59 (s, 1H; H-5), 8.07 (d, *J* = 8.28 Hz, 2H, H-11), 7.84 – 7.78 (m, 4H, H-2, 12, 15), 7.73 (d, *J* = 8.96 Hz, 1H, H-8), 7.33 (m, *J* = 7.64 and 1.24 Hz, 1H, H-17), 7.22 (dd, *J* = 6.36 and 1.08 Hz, 1H, H-7), 7.10 (d, *J* = 8.04 Hz, 1H, H-16), 7.05 (m, *J* = 7.36 Hz 1H, H-18), 3.10 (s, 3H, -$SO_2C\underline{H}_3$), 2.59 (s, 6H, -$C\underline{H}_3$); ^{13}C-NMR ($CDCl_3$, 100 MHz): δ 151.60, 139.78, 134.14, 131.97, 131.10, 129.50, 129.40, 129.28, 128.87, 128.54 (3C), 128.06 (2C), 124.26, 122.51, 121.61, 118.71, 116.93, 44.49, 43.59 (2C). HRMS-ESI : (m/z) $[M+H]^+$ = 392.1247, calculated = 391.1354.

4.5.8. 3-(4-(methylsulfonyl)phenyl)-6-(pyridin-4-yl)imidazo[1,2-a]pyridine, 32h

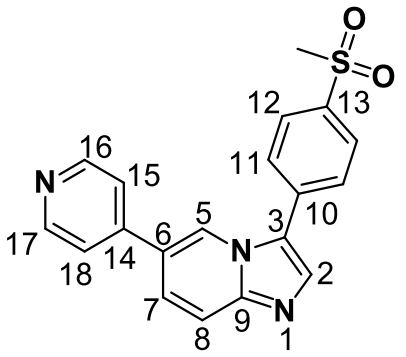

Using general procedure 2 and a reaction mixture containing **31a** (50 mg, 0.163 mmol) and pyridin-4-ylboronic acid (0.0220 g, 0.179 mmol, 1.1 eq.), the product was obtained as white solid. (40 mg, 70%); mp. 275 – 277 ºC; R_f (100% EtOAc) 0.46; ^{1}H-NMR ($CDCl_3$, 400 MHz): δ 8.71 (s, 2H; H-16), 8.59 (s, 1H, H-5), 8.12 (d, *J* = 8.4 Hz, 2H, H-11), 7.86 (d, *J* = 6.0 Hz, 1H, H-8), 7.83 (s, 1H, H-2), 7.81 (d, *J* = 8.4 Hz, 2H, H-12), 7.54 (d, *J* = 9.2 Hz, 1H, H-7), 7.46 (d, *J* = 7.6 Hz, 2H, H-15), 3.13 (s, 3H, -$SO_2C\underline{H}_3$); ^{13}C-NMR ($CDCl_3$, 100 MHz): δ 150.7 (2C), 144.5, 140.0, 135.1, 134.5, 128.7 (3C), 128.2 (2C), 125.2, 124.7 (2C), 121.4, 121.1, 119.1 (2C), 44.5. HRMS-ESI : (m/z) $[M+H]^+$ = 350.0958, calculated = 349.0885.

4.5.9. 6-(3-methoxyphenyl)-3-(4-(methylsulfonyl)phenyl)imidazo[1,2-a]pyridine, 32i

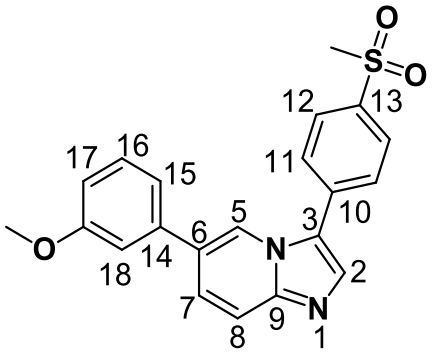

Using general procedure 2 and a reaction mixture containing **31a** (50 mg, 0.163 mmol) and (3-methoxyphenyl)boronic acid (0.0272 g, 0.179 mmol, 1.1 eq.), the product was obtained as white solid. (45 mg, 73%); mp. 114 –118 ºC; R_f (100% EtOAc) 0.57; ^{1}H-NMR

($CDCl_3$, 400 MHz): δ 8.49 (s, 1H; H-5), 8.08 (d, *J* = 8.4 Hz, 2H, H-11), 7.79 (d, *J* = 8.4 Hz, 2H, H-12), 7.67 – 7.62 (m, 2H, H-8, 15), 7.53 – 7.50 (m, 2H, H-2, 18), 7.37 (m, *J* = 7.96 Hz, 1H, H-16), 7.10 (d, *J* = 7.68 Hz, 2H, H-17), 6.93 (dd, *J* = 8.20 and 2.2 Hz, 1H, H-7), 3.84 (s, 3H, -OC<u>H</u>$_3$), 3.11 (s, 3H, -SO_2C<u>H</u>$_3$); ^{13}C-NMR ($CDCl_3$, 100 MHz): δ 160.0, 139.5, 138.4, 134.7, 132.0 (2C), 131.9, 130., 128.5, 128.5, 128.4, 128.0 (2C), 126.2, 120.4, 119.4, 118.2, 113.2, 112.9, 55.3, 44.5. HRMS-ESI : (m/z) $[M+H]^+$ = 379.1085, calculated =378.1038.

4.5.10. 6-(4-methoxyphenyl)-3-(4-(methylsulfonyl)phenyl)imidazo[1,2-a]pyridine, 32j

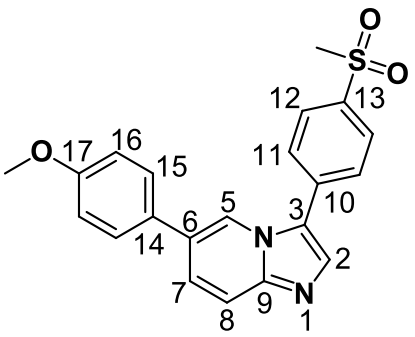

Using general procedure 2 and a reaction mixture containing **31a** (50 mg, 0.163 mmol) and (4-methoxyphenyl)boronic acid (0.0272 g, 0.179 mmol, 1.1 eq.), the product was obtained as white solid. (49 mg, 79%); mp. 113–116 ºC; R_f (100% EtOAc) 0.56; ^{1}H-NMR ($CDCl_3$, 400 MHz): δ 8.46 (s, 1H, H-5), 8.10 (d, *J* = 8.44 Hz, 2H, H-11), 7.82 (d, *J* = 8.48 Hz, 2H; H-12), 7.68 – 7.63 (m, 2H, H-15), 7.54 – 7.52 (m, 2H, H-2, 8), 7.48 – 7.45 (m, 2H, H-16), 7.01 (dd, *J* = 6.72 and 2.00 Hz, 1H, H-7,), 3.85 (s, 3H, -OC<u>H</u>$_3$); 3.13 (s, 3H, -SO_2C<u>H</u>$_3$); ^{13}C-NMR ($CDCl_3$, 100 MHz): δ 159.7, 139.4, 134.5, 132.1 (2C), 132.0 (2C), 131.9, 131.9, 128.6, 128.5 (2C), 128.4 (2C), 128.1, 127.9, 126.2, 118.3, 114.6, 55.4, 44.5. HRMS-ESI : (m/z) $[M+H]^+$ = 379.1080, calculated =378.1038.

4.5.11. 3-(4-(methylsulfonyl)phenyl)-6-(thiophen-3-yl)imidazo[1,2-a]pyridine, 32k

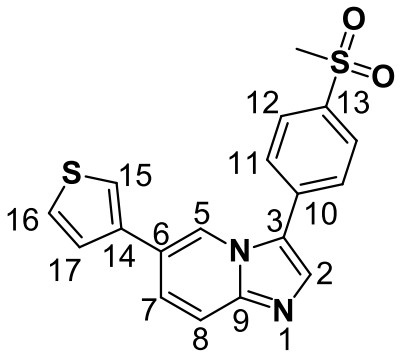

Using general procedure 2 and a reaction mixture containing **31a** (50 mg, 0.163 mmol) and thiophen-3-ylboronic acid (0.0229 g, 0.179 mmol, 1.1 eq.), the product was obtained as white solid. (45 mg, 78%); mp. 176 – 179 ºC; R_f (100% EtOAc) 0.44; ^{1}H-NMR ($CDCl_3$, 400 MHz): δ 8.52 (d, *J* = 0.4 Hz, 1H; H-5), 8.09 (d, *J* = 8.8 Hz, 2H, H-11), 7.81 – 7.79 (m, 3H, H-2, 12), 7.73 (d, *J* = 9.2 Hz, 1H, H-8), 7.52 (dd, *J* = 9.2 and 1.6 Hz, 1H, H-7), 7.45 – 7.43 (m, 2H, H-15, 16), 7.30 (dd, *J* = 4.4 and 2.0 Hz, 1H, H-7), 3.12 (s, 3H, -$SO_2C\underline{H}_3$); ^{13}C-NMR ($CDCl_3$, 100 MHz): δ 146.2, 139.5, 137.8, 134.9, 134.6, 128.6 (2C), 128.0 (2C), 127.3, 125.7, 125.6, 124.2, 123.0, 121.3, 119.6, 118.5, 44.5. HRMS-ESI : (m/z) $[M+H]^+$ = 355.0550, calculated = 354.0497.

4.5.12. 3-(4-(methylsulfonyl)phenyl)-6-(thiophen-2-yl)imidazo[1,2-a]pyridine, 32l

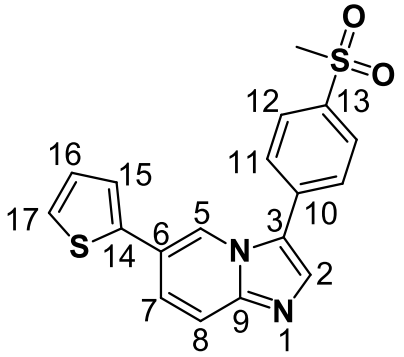

Using general procedure 2 and a reaction mixture containing **31a** (50 mg, 0.163 mmol) and thiophen-2-ylboronic acid (0.0229 g, 0.179 mmol, 1.1 eq.), the product was obtained as white solid. (46 mg, 80%); mp. 177 – 179 ºC; R_f (100% EtOAc) 0.54; ^{1}H-NMR ($CDCl_3$,

400 MHz): δ 8.55 (s, 1H; H-5), 8.11(d, *J* = 8.4 Hz, 2H, H-11), 7.81 (d, *J* = 8.4 Hz, 2H, H-12), 7.82 (s, 1H; H-2) 7.74 (d, *J* = 9.6 Hz, 1H, H-8), 7.53 (dd, *J* = 9.6 and 2.0 Hz, 1H, H-7), 7.33 (dd, *J* = 5.2 and 1.2 Hz, 1H, H-17), 7.27 (dd, *J* = 3.6 and 1.2 Hz, 1H, H-15), 7.11 (q, *J* = 5.2 and 3.6 Hz, 1H, H-16), 3.13 (s, 3H, -$SO_2C\underline{H}_3$); ^{13}C-NMR ($CDCl_3$, 100 MHz): δ 139.7, 139.5, 134.7, 128.6 (3C), 128.3, 128.0 (2C), 125.7 (2C), 125.4, 124.4 (2C), 122.0, 119.2, 118.6, 44.5. HRMS-ESI : (m/z) $[M+H]^+$ = 355.0553, calculated = 354.0497.

4.5.13. 6-(4-(tert-butyl)phenyl)-3-(4-(methylsulfonyl)phenyl)imidazo[1,2-a]pyridine, 32m

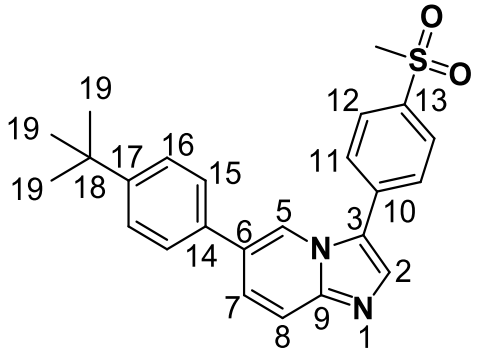

Using general procedure 2 and a reaction mixture containing **31a** (50 mg, 0.163 mmol) and 4-(tert-butyl)phenylboronic acid (0.0319 g, 0.179 mmol, 1.1 eq.), the product was obtained as white solid. (35 mg, 53%); mp. 173 – 177 ºC; R_f (100% EtOAc) 0.59;^{1}H-NMR ($CDCl_3$, 400 MHz): δ 8.50 (s, 1H, H-5), 8.09 (d, *J* = 9.6 Hz, 2H, H-11), 7.82 – 7.77 (m, 4H; H-2, 12, 8), 7.55 - 746 (m, 5H, H-7, 15, 16), 3.12 (s, 3H, -$SO_2C\underline{H}_3$), 1.35 (s, 9H, -$C\underline{H}_3$); ^{13}C-NMR ($CDCl_3$, 100 MHz): δ 151.5, 139.5, 134.9, 134.5, 134.1, 132.1, 132.0, 128.6 (2C), 128.4, 128.0 (2C), 126.7 (2C), 126.3, 126.2 (2C), 120.1, 118.3, 44.6, 34.6, 31.3 (3C). HRMS-ESI : (m/z) $[M+H]^+$ = 405.1631, calculated = 404.1558.

4.5.14. 3-(3-(4-(methylsulfonyl)phenyl)imidazo[1,2-a]pyridin-6-yl)benzaldehyde, 32n

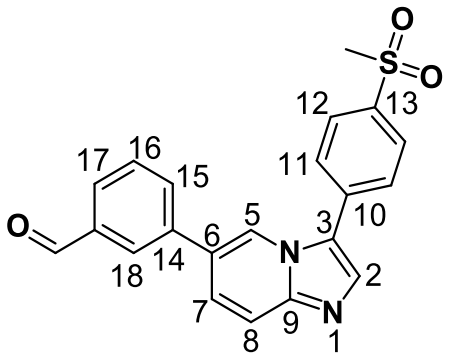

Using general procedure 2 and a reaction mixture containing **31a** (50 mg, 0.163 mmol) and (3-formylphenyl)boronic acid (0.0268 g, 0.179 mmol, 1.1 eq.), the product was obtained as white solid. (39 mg, 64%); mp. 233 – 237 ºC; R_f (100% EtOAc) 0.43; ^{1}H-NMR ($CDCl_3$, 400 MHz): δ 10.08 (s, 1H, C<u>H</u>O), 8.54 (s, 1H; H-5), 8.14 (d, *J* = 7.96 Hz, 2H, H-11), 8.08 (d, *J* = 9.04 Hz, 1H, H-17), 8.04 (s, 1H, H-18), 7.94 (d, *J* = 7.44 Hz, 2H, H-8, 15), 7.84 – 7.80 (m, 3H, H-2, 12), 7.75 (d, *J* = 8.84 Hz, 1H, H-7), 7.69 (m, *J* = 7.68 Hz, 1H, H-16), 3.13 (s, 3H, -SO_2C<u>H_3</u>); ^{13}C-NMR ($CDCl_3$, 100 MHz): δ 191.7, 140.9, 137.2, 137.2, 132.9 (2C), 130.6, 130.2 (2C), 128.9 (4C), 128.6, 128.4, 127.3 (2C), 121.0, 117.5, 44.4. HRMS-ESI : (m/z) $[M+H]^+$ = 377.0954, calculated = 376.0882.

4.5.15. 3,6-bis(4-(methylsulfonyl)phenyl)imidazo[1,2-a]pyridine, 32o

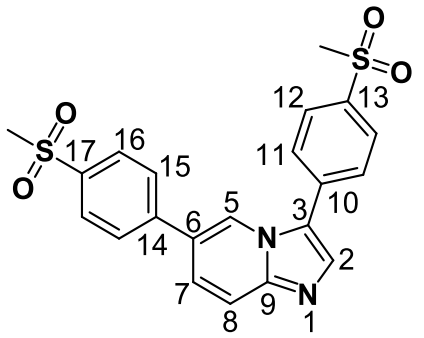

Using general procedure 2 and a reaction mixture containing **31a** (50 mg, 0.163 mmol) and (4-(methylsulfonyl)phenyl)boronic acid (0.0358 g, 0.179 mmol, 1.1 eq.), the product was obtained as white solid. (46 mg, 66%); mp. 181 – 184 ºC; R_f (100% EtOAc) 0.34; ^{1}H-NMR ($CDCl_3$, 400 MHz): δ 8.56 (s, 1H; H-5), 8.14 (d, *J* = 8.04 Hz, 2H, H-11), 8.05 (d, *J* = 8.00 Hz, 2H, H-15), 8.00 (d, *J* = 9.2 Hz, 1H, H-8), 7.91 (s, 1H, H-2), 7.83 (d, *J* = 8.04 Hz, 2H, H-12), 7.75 (d, *J* = 8.08 Hz, 2H, H-16), 7.66 (d, *J* = 9.20 Hz, 1H, H-7), 3.13 (s, 3H, -$SO_2C\underline{H}_3$), 3.09 (s, 3H, -$SO_2C\underline{H}_3$); ^{13}C-NMR ($CDCl_3$, 100 MHz): δ 146.3, 142.6, 140.1, 139.9, 135.1, 134.5, 128.7 (2C), 128.4 (2C), 128.2 (2C), 127.9 (2C), 126.2, 125.2, 124.6, 121.2, 119.1, 44.6, 44.5. HRMS-ESI : (m/z) $[M+H]^+$ = 427.0741, calculated = 426.0708.

4.5.16. N-(4-(3-(4-(methylsulfonyl)phenyl)imidazo[1,2-a]pyridin-6-yl)phenyl)methanesulfonamide, 32p

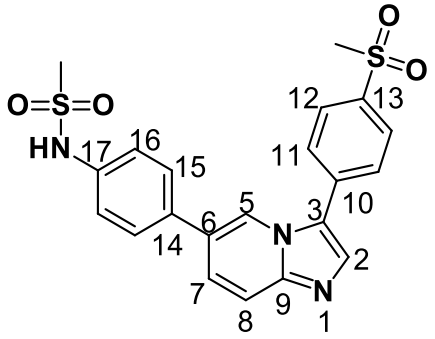

Using general procedure 2 and a reaction mixture containing **31a** (50 mg, 0.163 mmol) and (4-(methylsulfonamido)phenyl)boronic acid (0.0385 g, 0.179 mmol, 1.1 eq.), the product was obtained as white solid. (41 mg, 57%); mp. 248 – 252 ºC; R_f (100% EtOAc) 0.35; ^{1}H-NMR (DMSO-d_6, 400 MHz): δ 9.92 (s, 1H; -NH), 8.74 (s, 1H; H-5), 8.06 (s, 4H, H-11, 12), 7.98 (s, 1H, H-2), 7.81 – 7.67 (m, 4H, H-15, 16), 7.32 (d, J = 8.32 Hz, 2H, H-7, 8), 3.29 (s, 3H, -$SO_2C\underline{H}_3$), 3.03 (s, 3H, -$NHSO_2C\underline{H}_3$); ^{13}C-NMR (DMSO-d_6, 100 MHz): δ 139.8, 138.7, 135.3, 134.4, 132.5, 129.3, 128.5 (2C), 128.5 (2C), 128.2 (2C), 126.5, 126.0, 124.8, 121.3, 120.5 (2C), 118.2, 44.0, 41.0. HRMS-ESI : (m/z) $[M+H]^+$ = 442.0889, calculated = 441.0817.

4.5.17. 3-(4-(methylsulfonyl)phenyl)-6-(6-(methylsulfonyl)pyridin-3-yl)imidazo[1,2-a]pyridine, 32q

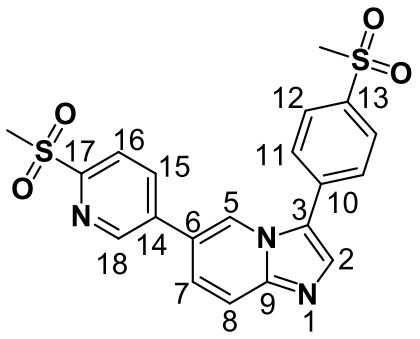

Using general procedure 2 and a reaction mixture containing **31a** (50 mg, 0.163 mmol) and (6-(methylsulfonyl)pyridin-3-yl)boronic acid (0.0360 g, 0.179 mmol, 1.1 eq.), the product was obtained as white solid (44.2 mg, 63%); mp. 152 – 155 ºC; R_f (100% EtOAc) 0.33; ^{1}H-NMR ($CDCl_3$, 400 MHz): δ 8.91 (s, 1H; H-18), 8.57 (s, 1H, H-5), 8.20 – 8.11 (m, 4H, H-11, 15, 16), 7.89 – 7.80 (m, 4H, H-2, 8, 12), 7.51 (d, J = 8.96 Hz, 1H, H-7), 3.27 (s, 3H, -pyridinyl-$SO_2C\underline{H}_3$), 3.13 (s, 3H, -$SO_2C\underline{H}_3$); ^{13}C-NMR ($CDCl_3$, 100 MHz): δ 157.4, 148.2, 146.2, 140.2, 136.9, 136.4, 135.3, 134.2, 128.7 (2C), 128.3 (2C), 124.8, 124.6, 123.1, 121.6, 121.4, 119.6, 44.5, 40.1. HRMS-ESI : (m/z) $[M+H]^+$ = 428.0733, calculated = 427.0660.

4.5.18. N-(3-(3-(6-(methylsulfonyl)pyridin-3-yl)imidazo[1,2-a]pyridin-6-yl)phenyl)cyclopropanesulfonamide, 32aa

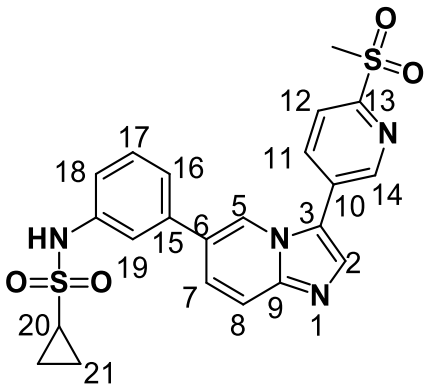

Using general procedure 2 and a reaction mixture containing **31b** (50 mg, 0.164 mmol) and (3-(cyclopropanesulfonamido)phenyl)boronic acid (0.0434 g, 0.180 mmol, 1.1 eq.), the product was obtained as white solid (45.2 mg, 57%); mp. 155 – 159 ºC; R_f (100% EtOAc) 0.35; ^{1}H-NMR (DMSO-d_6, 400 MHz): δ 9.93 (s, 1H; H-14), 9.01 (s, 1H; H-5), 8.65 (dd, *J* = 8.12 and 1.72 Hz, 1H, H-11), 8.38 (s, 1H, H-2), 8.28 (m, *J* = 8.20 Hz, H-8, 12), 8.08 – 8.01 (m, 2H, H-16, 18), 7.90 (d, *J* = 7.72 Hz, 1H, H-7), 7.73 (m, *J* = 7.84 Hz, 1H, H-17), 7.52 (s, 1H, H-19), 3.38 (s, 3H, -$SO_2C\underline{H}_3$), 2.14 (m, *J* = 9.76 and 3.20 Hz, 1H, H-20), 0.50 (m, *J* = 7.40 and 5.00 Hz, 2H, H-21), 0.44 – 0.40 (m, 2H, H-21); ^{13}C-NMR (DMSO-d_6, 100 MHz): δ 157.2, 149.6, 145.4, 143.9, 138.2, 137.2, 132.0, 131.3, 130.3, 129.6, 128.2, 127.5, 125.7, 124.7, 123.9, 122.7, 121.7, 116.4, 40.4, 24.7, 5.6. HRMS-ESI : (m/z) $[M+H]^+$ = 469.0999, calculated = 483.0926.

4.5.19. 6-(4-methoxyphenyl)-3-(6-(methylsulfonyl)pyridin-3-yl)imidazo[1,2-a]pyridine, 32ab

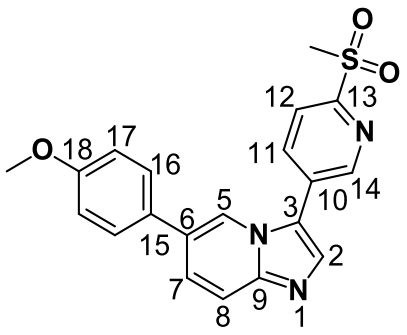

Using general procedure 2 and a reaction mixture containing **31b** (50 mg, 0.164 mmol) and and (4-(methylsulfonamido)phenyl)boronic acid (0.0274 g, 0.180 mmol, 1.1 eq.), the product was obtained as white solid. (36.1 mg, 58%); mp. 210 – 213 ºC; R_f (100% EtOAc) 0.42; ^{1}H-NMR ($CDCl_3$, 400 MHz): δ 8.94 (s, 1H; H-14), 8.34 (s, 1H; H-5), 8.26 (d, 1H, *J* = 7.76 Hz, H-11), 8.14 (d, 2H, *J* = 7.52 Hz, H-16), 8.01 (d, 1H, *J* = 7.64 Hz, H-11), 7.91 (s, 1H, H-2), 7.78 (d, 1H, *J* = 9.32 Hz, H-8), 7.32 (d, 1H, *J* = 9.28 Hz, H-7), 6.93 (d, *J* = 7.96 Hz, 2H, H-17), 3.83 (s, 3H, -OC<u>H</u>$_3$), 3.30 (s, 3H, -SO_2C<u>H</u>$_3$); ^{13}C-NMR ($CDCl_3$, 100 MHz): δ 161.0, 156.4, 147.5 (2C), 135.5 (2C), 134.4, 133.2, 127.6, 127.0, 122.0, 120. (2C), 119.9, 117.8 (2C), 112.5, 112.3, 54.1, 39.1. HRMS-ESI : (m/z) $[M+H]^+$ = 380.1063, calculated = 379.0991

4.5.20. 6-(3-methoxyphenyl)-3-(6-(methylsulfonyl)pyridin-3-yl)imidazo[1,2-a]pyridine, 32ac

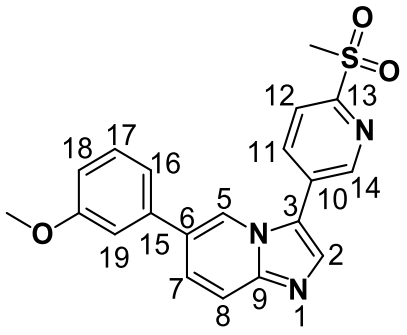

Using general procedure 2 and a reaction mixture containing **31b** (50 mg, 0.164 mmol) and and (4-(methylsulfonamido)phenyl)boronic acid (0.0274 g, 0.180 mmol, 1.1 eq.), the product was obtained as white solid. (39.4 mg, 64%); mp. 210 – 213 ºC; R_f (100% EtOAc) 0.48; ^{1}H-NMR ($CDCl_3$, 400 MHz): δ 7.82 (d, *J* = 7.36 Hz, 1H; H-14), 7.73 (d, *J* = 4.27 Hz, 1H; H-5), 7.67 – 7.62 (m, 2H, H-11, 12), 7.58 – 7.54 (m, 1H, H-8), 7.49 – 7.42 (m, 3H, H-16, 17, 19), 7.33 (s, 1H, H-2), 7.78 (dd, 1H, *J* = 7.80 and 2.32 Hz, H-7), 7.02 – 6.99 (m, 1H, H-18), 3.91 (s, 3H, -OC<u>H</u>$_3$), 3.82 (s, 3H, -SO_2C<u>H</u>$_3$); ^{13}C-NMR ($CDCl_3$, 100 MHz): δ 157.3, 148.5 (2C), 136.5, 136.5 (2C), 135.4, 127.7 (2C), 122.8, 121.7 (4C), 121.0, 118.95, 113.5 (2C), 113.3, 55.1, 40.1. HRMS-ESI : (m/z) $[M+H]^+$ = 380.1360, calculated = 379.0991.

4.6. Synthesis and characterization of pyrazolo[1,5-a]pyridines

4.6.1. 3,5-dibromopyrazolo[1,5-a]pyridine, 34 [4].

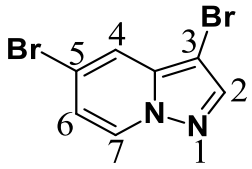

A solution of 5-aminopyrazolo[1,5-a]pyridine (0.5 g, 3.76 mmol) in concentrated HBr (6 mL) at room temperature was treated with a dropwise aqueous solution of $NaNO_2$ (0.389 g, 5.64 mmol, 1.5 eq.) over 5 minutes. The reaction was stirred for 10 minutes followed by the addition of a solution of $CuBr_2$ (1.08 g, 7.52 mmol, 2.0 eq.) in HBr (4 mL). The reaction mixture was heated to 50 °C for 15 minutes until gas evolution ceased. At completion, the reaction mixture was poured into ice containing 3 – 5 drops of NaOH(aq.) (6 M). The precipitate was filtered and purified by column chromatography (hexane/ethyl acetate, 2:1) to afford to afford compound **34** as a brown solid (183.5 mg, 94%); R_f (2:1, Hexane/EtOAc) 0.71; ^{1}H-NMR ($CDCl_3$, 400 MHz): δ 8.26 (d, *J* = 7.2 Hz, 1H; H-7), 7.90 (s, 1H, H-2), 7.69 (s, 1H, H-4), 6.87 (d, *J* = 7.16 Hz, 1H, H-6); ^{13}C-NMR ($CDCl_3$, 100

MHz): δ 142.7, 129.5, 118.9 (2C), 118.5, 116.3 (2C). HRMS-ESI : (m/z) $[M+H]^+$ = 274.8814, calculated = 273.8741.

4.6.2. 3,5-di(thiophen-2-yl)pyrazolo[1,5-a]pyridine, 35a

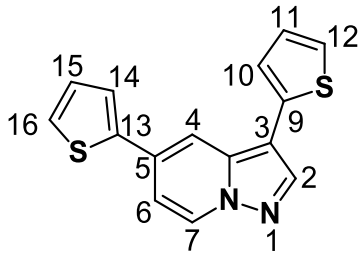

A solution of 3,5-dibromopyrazolo[1,5-a]pyridine (30 mg, 0.109 mmol), K_2CO_3 (30.13 mg, 0.218 mmol, 2.0 eq.) and $Pd(PPh_3)_2Cl_2$ (3.83 mg, 0.00545 mmol, 0.05 eq.) in 10 mL dioxane/ water mixture (3:1) was purged with N_2 for 5 min. To the mixture was added thiophen-2-ylboronic acid (27.90 mg, 0.218 mmol, 2.0 eq.) and the resulting mixture was heated to 90 ºC while stirring for 3 h. The mixture was cooled to 20 ºC, concentrated under *vacuo* and purified by flash column chromatography (2:1, hexane/ethyl acetate) to afford the expected product as a yellow solid (25.5 mg, 83%), mp. 136 –142 ºC; R_f (2:1, Hexane/EtOAc) 0.68; ^{1}H-NMR ($CDCl_3$, 400 MHz): δ 8.44 (d, *J* = 7.2 Hz, 1H; H-7), 8.12 (s, 1H, H-2), 7.99 (d, *J* = 1.6 Hz, 1H, H-4), 7.42 (m, 1H, H-12), 7.36 (m, 1H, H-16), 7.28 (m, 1H, H-10), 7.23 (m, 1H, H-14), 7.13 (m, 2H, H-11, 15), 7.42 (d, *J* = 7.2 and 2.0 Hz, 1H, H-6); ^{13}C-NMR ($CDCl_3$, 100 MHz): δ 141.7, 140.7, 134.6, 130.9, 128.8, 128.4 (2C), 127.7, 126.3, 124.7 (2C), 123.3, 122.9, 112.7, 111.2. HRMS-ESI : (m/z) $[M+H]^+$ = 283.0358, calculated = 282.0285.

4.6.3. 3,5-di(thiophen-3-yl)pyrazolo[1,5-a]pyridine, 35b

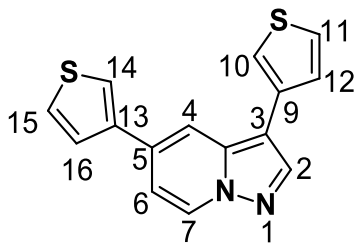

A solution of 3,5-dibromopyrazolo[1,5-a]pyridine (30 mg, 0.109 mmol), K_2CO_3 (30.13 mg, 0.218 mmol, 2.0 eq.) and $Pd(PPh_3)_2Cl_2$ (3.83 mg, 0.00545 mmol, 0.05 eq.) in 10 mL dioxane/ water mixture (3:1) was purged with N_2 for 5 min. To the mixture was added thiophen-3-ylboronic acid (27.90 mg, 0.218 mmol, 2.0 eq.) and the resulting mixture was heated to 90 ºC while stirring for 3 h. The mixture was cooled to 20 ºC, concentrated under *vacuo* and purified by flash column chromatography (2:1, hexane/ethyl acetate) to afford the expected product as yellow solid (24.5 mg, 80%), mp. 138 –143 ºC; R_f (2:1, Hexane/EtOAc) 0.65; ^{1}H-NMR ($CDCl_3$, 400 MHz): δ 8.48 (d, *J* = 7.2 Hz, 1H; H-7), 8.10 (s, 1H, H-2), 7.90 (d, *J* = 1.6 Hz, 1H, H-4), 7.42 (m, *J* = 2.4 Hz, 1H, H-12), 7.46 – 7.44 (m, 3H, H-11, 15, 16), 7.38 (d, *J* = 4.0 Hz, 2H, H-10, 14), 7.04 (dd, *J* = 7.2 and 2.0 Hz, 1H, H-6); ^{13}C-NMR ($CDCl_3$, 100 MHz): δ 140.3, 139.8, 133.0, 132.1, 128.7, 127.1, 126.8 (2C), 126.3, 125.8 (2C), 121.9, 119.0, 113.3, 111.7. HRMS-ESI : (m/z) $[M+H]^+$ = 282.2781 , calculated = 282.0285.

4.6.4. 5-amino-3-iodopyrazolo[1,5-a]pyridine, 36

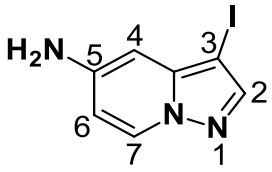

A solution of N-iodosuccinimide (186.0 mg, 0.83 mmol, 1.1 eq.) in methanol (5 mL) was added dropwise to a solution of 5-aminopyrazolo[1,5-a] pyridine (100.0 mg, 0.75 mmol) in methanol (10 mL) at -10°C over 30 minutes. Then the reaction mixture was quenched with $Na_2S_2O_3$ solution (5 mL) and extracted twice with CH_2Cl_2. The combined extracts were dried (Na_2SO_4) and the solvent removed under vacuo to afford compound **36** as a

brown solid (183.5 mg, 94%); R_f (2:1, Hexane/EtOAc) 0.61; ^{1}H-NMR ($CDCl_3$, 400 MHz): δ 8.19 (d, *J* = 7.6 Hz, 1H; H-7), 7.77 (s, 1H, H-2), 6.46 (d, *J* = 2.4 Hz, 1H, H-4), 6.24 (dd, *J* = 7.2 and 2.4 Hz, 1H, H-6)), 4.00 (s, 2H, NH_2); ^{13}C-NMR ($CDCl_3$, 100 MHz): δ 146.6, 144.1, 142.4, 129.6, 106.3, 95.9, 42.7. HRMS-ESI : (m/z) $[M+H]^+$ = 259.9663, calculated = 258.9606.

4.6.5. 3-(4-(methylsulfonyl)phenyl)pyrazolo[1,5-a]pyridin-5-amine, 37a

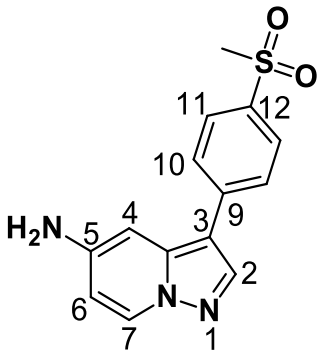

A solution of 5-amino-3-iodopyrazolo[1,5-a]pyridine (1.0 g, 3.88 mmol), K_2CO_3 (0.804 g, 5.82 mmol,1.5 eq.) and $Pd(PPh_3)_2Cl_2$ (0.136 g, 0.194 mmol, 0.05 eq.) in 10 mL dioxane/ water mixture (3:1) was purged with N_2 for 5 min. To the mixture was added (4-(methylsulfonyl)phenyl)boronic acid (0.854 g, 4.27 mmol, 1.1 eq.) and the resulting mixture was heated to 90 ºC while stirring for 3 h. The mixture was then cooled to 20 ºC, concentrated under *vacuo* and purified by flash column chromatography (hexane/ethyl acetate, 2:1) to afford the expected product as yellow solid (0.79 g, 72%), R_f (2:1, Hexane/EtOAc) 0.58; ^{1}H-NMR ($CDCl_3$, 400 MHz): δ 8.27 (d, *J* = 7.2 Hz, 1H; H-7), 8.08 (s, 1H, H-2), 7.94 (d, *J* = 8.4 Hz, 2H, H-10), 7.70 (d, *J* = 8.4 Hz, 2H, H-11), 6.90 (d, *J* = 2.0 Hz, 1H, H-4), 6.34 (dd, *J* = 7.6 and 2.4 Hz, 1H, H-6), 4.11 (q, *J* = 6.8 and 14 Hz, 2H, NH_2), 3.08 (s, 1H, -SO2C<u>H</u>3); ^{13}C-NMR ($CDCl_3$, 100 MHz): δ 144.9, 141.8, 140.0, 138.9,

136.2, 130.0, 128.1 (2C), 126.1 (2C), 107.4, 106.2, 95.3, 44.7. HRMS-ESI : (m/z) $[M+H]^+$ = 288.0801, calculated = 287.0728.

4.6.6. 4,5-dibromo-3-(4-(methylsulfonyl)phenyl)pyrazolo[1,5-a]pyridine, 38

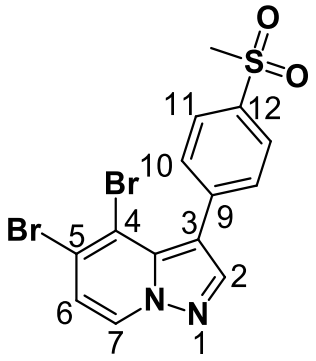

A solution of 3-(4-(methylsulfonyl)phenyl)pyrazolo[1,5-a]pyridin-5-amine (100. mg, 0.348 mmol) in concentrated HBr (6 mL) at room temperature was treated with a dropwise aqueous solution of $NaNO_2$ (36.02 mg, 0.522 mmol, 1.5 eq.) over 5 minutes. The reaction was stirred for 10 minutes followed by the addition of a solution of $CuBr_2$ (155.47 mg, 0.696 mmol, 2.0 eq.) in HBr (4 mL) and the reaction mixture heated to 50 °C for 15 minutes until gas evolution ceased. At completion, the reaction mixture was poured into ice containing 3 – 5 drops of NaOH(aq.) (6 M). The precipitate was filtered and purified by column chromatography (hexane/ethyl acetate, 2:1) to afford compound **38** as a brown solid (95.00 mg, 63%); R_f (2:1, Hexane/EtOAc) 0.83; ^{1}H-NMR ($CDCl_3$, 400 MHz): δ 8.34 (d, *J* = 7.6 Hz, 1H; H-7), 8.07 (d, *J* = 8.4 Hz, 2H, H-10), 7.88 (s, 1H, H-2), 7.53 (d, *J* = 8.4 Hz, 2H, H-11), 7.05 (d, *J* = 7.6 Hz, 1H, H-6), 3.15 (s, 1H, -$SO_2C\underline{H}_3$); ^{13}C-NMR ($CDCl_3$, 100 MHz): δ 144.5, 140.8, 140.5, 131.4 (3C), 130.1, 129.4, 127.2 (3C), 119.8, 116.7, 44.6. HRMS-ESI : (m/z) $[M+H]^+$ = 430.8889, calculated = 427.8830.

4.6.7. 5-bromo-3-(4-(methylsulfonyl)phenyl)pyrazolo[1,5-a]pyridine, 39a

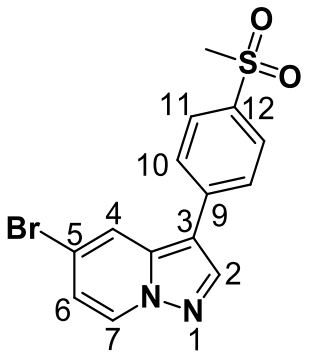

A solution of 3-(4-(methylsulfonyl)phenyl)pyrazolo[1,5-a]pyridin-5-amine (100. mg, 0.348 mmol) in concentrated HBr (6 mL) at 0 °C was treated with a dropwise aqueous solution of $NaNO_2$ (36.02 mg, 0.522 mmol, 1.5 eq.) over 5 minutes. The reaction was stirred for 10 minutes followed by the addition of a solution of $CuBr_2$ (155.47 mg, 0.696 mmol, 2.0 eq.) in HBr (4 mL) and the reaction mixture heated to 50 °C for 15 minutes until gas evolution ceased. At completion, the reaction mixture was poured into ice containing 3 – 5 drops of NaOH(aq.) (6 M). The precipitate was filtered and purified by column chromatography (hexane/ EtOAc, 2:1) to afford compound **39a** as a brown solid (86.00 mg, 70%); R_f (2:1, Hexane/EtOAc) 0.72; ^{1}H-NMR ($CDCl_3$, 400 MHz): δ 8.38 (d, *J* = 7.6 Hz, 1H; H-7), 8.19 (s, 1H, H-2), 8.01 (d, *J* = 8.4 Hz, 2H, H-10), 7.99 (d, *J* = 2.0 Hz, 1H, H-4), 7.73 (d, *J* = 8.4 Hz, 2H, H-11), 6.95 (dd, *J* = 7.2 and 2.0 Hz, 1H, H-6), 3.09 (s, 1H, -SO2C<u>H</u>3); ^{13}C-NMR ($CDCl_3$, 100 MHz): δ 138.3, 131.9, 130.5, 129.9, 128.3 (2C), 127.8, 127.2 (3C), 119.7, 119.3, 116.5, 44.6. HRMS-ESI : (m/z) $[M+H]^+$ = 352.9766, calculated = 349.9725.

4.6.8. 3-(4-(methylsulfonyl)phenyl)-5-(thiophen-3-yl)pyrazolo[1,5-a]pyridine, 40a

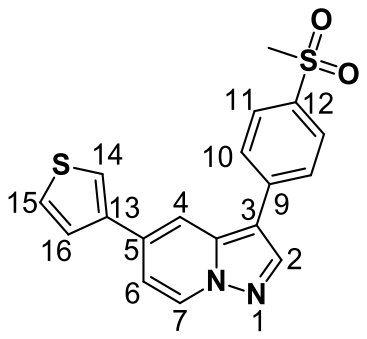

A solution of 5-bromo-3-(4-(methylsulfonyl)phenyl)pyrazolo[1,5-a]pyridine (30 mg, 0.0854 mmol), K_2CO_3 (17.69 mg, 0.128 mmol, 1.5 eq.) and $Pd(PPh_3)_2Cl_2$ (3.00 mg, 0.00427 mmol, 0.05 eq.) in 10 mL dioxane/ water mixture (3:1) was purged with N_2 for 5 min. To the mixture was added thiophen-3-ylboronic acid (16.38 mg, 0.128 mmol, 1.5 eq.) and the resulting mixture was heated to 90 ºC while stirring for 3 h. The mixture was then cooled to 20 ºC, concentrated under *vacuo* and purified by flash column chromatography (2:1, hexane/Ethylacetate) to afford compound **40a** as a yellow solid (15.97 mg, 53%), mp. 194–198 ºC; R_f (2:1, Hexane/EtOAc) 0.81; ^{1}H-NMR (DMSO-d_6, 400 MHz): δ 8.83 (d, *J* = 6.8 Hz, 1H; H-7), 8.55 (s, 1H, H-2), 8.28 – 8.25 (m, 2H, H-14, 15), 8.06 (d, *J* = 8.4 Hz, 2H, H-10), 7.97 (d, *J* = 8.8 Hz, 2H, H-11), 7.87 – 7.85 (m, 1H, H-4), 7.75 – 7.73 (m, 1H, H-16), 7.45 (d, *J* = 6.0 Hz, 1H, H-6), 3.25 (s, 1H, -SO2C<u>H</u>3); ^{13}C-NMR (DMSO-d_6, 100 MHz): δ 139.5, 138.5, 137.9, 133.2, 130.3, 128.3 (2C), 128.1, 127.2 (3C), 126.9 (2C), 124.2 (2C), 112.9, 112.5, 44.2. HRMS-ESI : (m/z) $[M+H]^+$ = 355.0569, calculated = 354.0497.

4.6.9. 5-(4-methoxyphenyl)-3-(6-(methylsulfonyl)pyridin-3-yl)pyrazolo[1,5-a]pyridine, 40b

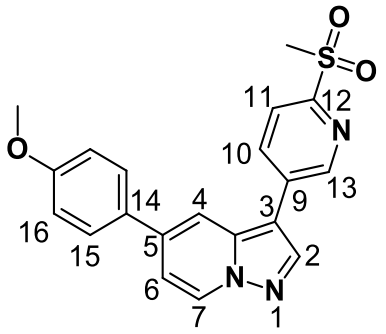

A solution of 5-bromo-3-(6-(methylsulfonyl)pyridin-3-yl)pyrazolo[1,5-a]pyridine, crude, (50 mg, 0.142 mmol), K_2CO_3 (29.44 mg, 0.213 mmol, 1.5 eq.) and $Pd(PPh_3)_2Cl_2$ (4.98 mg, 0.0071 mmol, 0.05 eq.) in 10 mL dioxane/ water mixture (3:1) was purged with N_2 for 5 min. To the mixture was added (4-methoxyphenyl)boronic acid (32.37 mg, 0.213 mmol, 1.5 eq.) and the resulting mixture was heated to 90 ºC while stirring for 3 h. The mixture was then cooled to 20 ºC, concentrated under *vacuo* and purified by flash column chromatography (2:1, hexane/Ethylacetate) to afford compound **40b** as a yellow solid (25.20 mg, 47%), mp. 212–215 ºC; R_f (2:1, Hexane/EtOAc) 0.67; ^{1}H-NMR ($CDCl_3$, 400 MHz): δ 9.02 (s, 1H; H-13), 8.56 (d, *J* = 7.2 Hz, 1H, H-7), 8.24 (s, 1H, H-2), 8.14 (s, 2H, H-10, 11), 7.90 (s, 1H, H-4), 7.60 (d, *J* = 8.4 Hz, 2H, H-15), 7.15 (d, *J* = 6.8 Hz, 1H, H-6), 7.02 (d, *J* = 8.4 Hz, 1H, H-16), 3.87 (s, 3H, -OC<u>H</u>$_3$), 3.26 (s, 3H, -SO$_2$C<u>H</u>$_3$); ^{13}C-NMR ($CDCl_3$, 100 MHz): δ 160.3, 154.5, 148.5, 147.6, 141.5, 139.2, 137.0, 134.7, 133.8, 132.1, 129.4, 128.6, 128.1 (2C), 121.7, 114.7 (2C), 112.9, 112.4, 55.5, 40.4. HRMS-ESI : (m/z) $[M+H]^+$ = 380.1013, calculated = 379.0991.

4.7. Molecular docking studies

4.7.1. Protein preparation

A high-resolution crystal structures of *Pf*PI4K homology model (4D0L) and *Pv*PKG protein (5EZR) were retrieved from Protein Data Bank (PDB) (https://www.rcsb.org) for molecular docking. The PDB crystal structures 4D0L and 5EZR were selected to dock the ATP-binding site. Each structure was prepared for docking according to the following protein preparation protocol using Maestro's protein preparation tool, Protein preparation workflow (Schrödinger Suite 13.8) with the following settings applied. Schrödinger Suite

13.8 was used to generate all images containing protein ribbons from crystal and docked structures [5].

Under Protein preparation workflow import and process tab, the Preprocess protocol was run on both **5EZR** and **4D0L** PDB files with the following boxes ticked; assign bond orders, add hydrogens, create zero order bonds to metals, fill in missing sidechains using prime the rest used as default. Furthermore, we optimized amino acids using neutral pH and the optimization H-bond assignments settings were used as default.

Under the minimize and delete waters tab, with the following box ticked; delete waters: distant from ligands (hets) beyond 5 Å. Lastly a restrained minimization was run with the heavy atom root-mean-square deviation (RMSD) set to converge on the default 0.30 Å using the OPLS4 force field.

4.7.2. Ligand Preparations

The next step was to prepare ligands in the workspace. The ligands were drawn using the 2D sketcher under the edit tab. The Maestro LigPrep protocol (Schrödinger Suite 13.8) was run on this ligand set rendering the 3D structures for each ligand in the most likely ionisation and tautomerisation state under biological conditions. To achieve this, the pH was set at 7.0 ± 2.0 allowing for multiple tautomers. This step created a few duplicate entries, but the acids were mostly deprotonated while the bases were mostly protonated.

4.8. Biological assays

4.8.1. *In vitro* asexual blood stage anti-plasmodium LDH assay

The chloroquine (CQ) sensitive *Pf*NF54 and multi-drug resistant *Pf*K1 strains were used in the assay. These assays were carried out at the Division of Clinical Pharmacology, Department of Medicine, UCT. Parasites were cultured and maintained according to the approach by Trager and Jensen with slight variations [6]. The anti-plasmodial activity was monitored using the parasite lactate dehydrogenase (pLDH) assay**.** Stock solutions of test compounds were prepared at 10 mM in 100% HPLC-grade DMSO (Sigma Aldrich). Subsequent dilutions of the stock solutions were prepared in medium to give the highest starting concentration of 6 µM. From these, serial dilutions in complete medium were

performed to achieve ten concentrations with the concentration range being between 0.2-100 µg/ml. Using these concentrations, dose response curves were generated to establish the concentration resulting in inhibition of parasite growth by 50%. Chloroquine and artesunate were employed as positive controls. The dilution approach adopted for the samples and controls was similar. Non-linear dose-response curves generated in GraphPad Prism v.6.01 software were used to evaluate the IC_{50} values.

4.8.2. *In vitro Pv*PI4K inhibition assay

Full-length *Pv*PI4K (PVX_098050) recombinant protein expressed in a baculovirus-insect cell expression system and purified as previously described was used in the assay [7]. The assay was undertaken at the H3D Biology Labs, Institute of Infectious Disease and Molecular Medicine, UCT. A 3-fold serial dilution of each inhibitor was carried out in DMSO (Sigma-Aldrich) and subsequently diluted into assay buffer (25 mM HEPES pH 7.4, 100 mM NaCl, 3 mM $MgCl_2$, 1 mM DTT, 0.025 mg/ml BSA, 0.2% (v/v) Triton-X-100) to 4 × the final required concentration. 5 µL of each inhibitor dilution was transferred into a white 384-shallow well plate (Nunc #264706). L-alpha-phosphatidylinositol (PI; Avanti Polar Lipid, cat. 840042P) dissolved in 3% n-Octylglucoside to a stock concentration of 20 mg/ml was used as the lipid substrate. The assay components were then manually dispensed 5 µL substrate buffer (ATP and PI), followed by 10 µL of *Pv*PI4K protein] and added to each well. The final 20 µL kinase reaction contained ~6 nM *Pv*PI4K protein (for 10% ATP conversion), 10 µM ATP, 0.1 mg/ml PI, 1% (v/v) DMSO and inhibitor in assay buffer. 10 µM MMV390048 was included in the assays as the positive control for the experiments. The reaction plates were then incubated at 22°C for 40 min then stopped by aliquoting 4 µL of the enzyme reaction and adding equal volume of ADP-Glo reagent prepared as per manufacturers protocol. This was then incubated for a further 30 min at the same temperature. Luciferase-coupled reaction was then effected by adding 8 µL Kinase Detection Reagent (KDR) and incubating at 22°C for 40 min. Luminescence proportional to the remaining ATP at the end of the reaction was measured using an EnSpire® Multimode Plate Reader (PerkinElmer) at λ = 680 nm). Ten-point dose-response curves were obtained from the 3-fold dilutions of the test compound, normalized and the IC_{50} values determined using GraphPad Prism® v6.02 (GraphPad Software Inc,

San Diego, CA, USA). The measurements were done in duplicates and the assay independently repeated.

4.8.3. *In vitro Pf*PKG inhibition assay

Full length *Pf*PKG (*Pf*3D7_1436600) expressed in *Escherichia coli* using methods previously described was used in the assay [8]. This assay was also undertaken at the H3D Biology Labs, Institute of Infectious Disease and Molecular Medicine, UCT. *Pf*PKG IC50 values were determined using an ADP-Glo Kinase kit from Promega® and conducted as per literature [9]. A-fold serial dilution of each inhibitor was carried out in DMSO (Sigma-Aldrich) and subsequently diluted into assay buffer (25 mM HEPES pH 7.4, 0.1 mg/mL BSA, 0.01 % (v/v) Triton-X 100, 20 mM $MgCl_2$, 2 mM DTT, 10 µM cGMP) to 4 × the final required concentration.11 5 µL of each inhibitor dilution was transferred into a white 384-shallow well plate (Nunc #264706). The remaining assay components were then manually dispensed [10 µL of *Pf*PKG protein, followed by 5 µL substrate buffer (ATP and peptide substrate GRTGRRNSI-NH2], and added to each well. The final 20 µL kinase reaction contained ˜0.6 nM *Pf*PKG protein, 10 µM ATP, 20 µM GRTGRRNSI-NH2, 1 % (v/v) DMSO and inhibitor in assay buffer. Control reactions using the peptide mix and 500 nM ML10 (LifeArc), a known *Pf*PKG inhibitor was included as positive control, and another using no protein to ensure that the inhibitor did not interfere with the ADP-Glo detection component of the assay and to account for background signal. Reactions were incubated at 22°C for 40 min. After the incubation, 4 µL of each kinase reaction mix was transferred into a white, 384-well plate in replicates, and the reaction terminated by adding 4 µL ADP-Glo reagent to quench any remaining ATP by incubating at 22°C for 30 min. Conversion of ADP generated in the kinase reaction to ATP for luciferase-coupled reaction was then effected by adding 8 µL Kinase Detection Reagent (KDR) and incubating at 22°C for 40 min. Luminescence measurements were then performed using an EnSpire® Multimode Plate Reader (PerkinElmer) at a λ = 680 nm and the IC50 values calculated using similar as those employed for *Pv*PI4K. Percentage PKG inhibition was evaluated for some compounds at a maximum concentration of 10 µM using the same protocol.

4.8.4. Cytotoxicity on the CHO cell line

In vitro cytotoxicity was conducted on the CHO cell lines using the 3-(4,5-dimethylthiazol-2-yl)-2,5-diphenyltetrazolium bromide (MTT) assay [10]. Test compounds were dissolved in 100% DMSO to yield a 20 mM stock solution while the reference standard, emetine, was dissolved in distilled water to a 2 mg/mL solution. From an initial test compound and control concentration of 100 µg/mL, serial 10-fold dilutions, in assay medium, were performed to achieve six concentrations with 0.001 µg/mL being the lowest concentration. The highest concentration of DMSO exposed to cells had no effects on cell viability. Plates were incubated for 48 h with 100 µL of drug and 100 µL of cell suspension in each well after which they were developed by the addition of 25 µL of sterile MTT (Thermo Fisher Scientific) to each well and a further incubation in the dark for 4 hours. Thereafter, the plates were centrifuged, the medium aspirated off and DMSO (100 µL) added to dissolve crystals and absorbance readings taken at 540 nM. Non-linear dose-response curve fitting analysis conducted using GraphPad Prism v.4.0 software (La Jolla, USA), was applied to generate IC50 values. The assay was conducted in triplicate and two independent assays (n = 2) were carried out for each compound.

4.9. Solubility evaluation

4.9.1. Solubility using HPLC-based DMSO “dry-down” method

This modified kinetic solubility determination method was employed to minimize solvent enhancement of solubility observed in the turbidimetric method [11]. Test compounds were dissolved in DMSO (Sigma-Aldrich) to yield 10 mM stock solutions. HPLC analysis was used with UV detection to construct calibration curves for each compound using low (11 µM), medium (100 µM), and high (220 µM) concentration standards. High and medium standards were prepared by placing 4.4 µL and 2 µL of the 10 mM stock solution into wells A and B of a 96-well microtiter plate and diluted by adding 195.6 µL and 198 µL DMSO, respectively. The low standard was prepared in well C by diluting 10 µL, obtained from well A, with 190 µL DMSO to obtain a 20-fold dilution of the 220 µM solution. Thereafter, each test sample (4 µL of 10 mM stock) was placed in triplicate in wells D, E,

and F and DMSO was removed by freeze-drying under Genevac®. This step reduces DMSOassociated solubility enhancement. PBS (200 µL, pH 7.4) was added to the wells now containing dry, solid material from test samples. The plates were covered and placed on a shaker at 37°C for 24 h. After this period, the plates were put under centrifugation (Digtor 21R®) at 3500 rpm for 15 min at a temperature of 23°C. The supernatants were then carefully transferred to an analytical 96-well microtiter plate for HPLC analysis fitted with UV detection. The concentrations of dissolved samples were determined by comparing the average peak areas of the samples (wells D, E, and F) against the previously constructed standard curve using samples in wells A, B, and C.

References

[1] Juillet, C.; Ermolenko, L.; Boyarskaya, D.; Baratte, B.; Josselin, B.; Nedev, H.; Bach, S.; Iorga, B. I.; Bignon, J.; Ruchaud, S.; Al-Mourabit, A., "From Synthetic Simplified Marine Metabolite Analogues to New Selective Allosteric Inhibitor of Aurora B Kinase," *J. Med. Chem,* vol. 64, pp. 1197 - 1219, 2021.

[2] Gachuhi, S. N (2022), *Design, Synthesis, and Structure-Activity Relationship Studies of Dual Plasmodium falciparum Phosphatidylinositol 4-kinase and cGMP-dependent Protein Kinase Inhibitors.,* PhD, University of Cape Town.

[3] Koubachi, J.; Kazzouli, S. E.; Berteina-Raboin, S.; Mouaddib, A.; Guillaumet, G., "EFFICIENT MICROWAVE-ASSISTED SUZUKI-MIYAURA CROSS COUPLING REACTION OF 6-HALOGENOIMIDAZO[1,2-a]PYRIDINES," *J.MAR.CHIM.HETEROCYCL.,* vol. 7, no. 1, pp. 1-9, 2008.

[4] Kendall, J. D.; O'Connor, P. D.; Marshall, A. J. ; Frédérick, Raphaël; Marshall, E. S.; Lill, C. L. ; Lee, W-J.; Kolekar, S.; Chao, M.; Malik, A.; Yu, S.; Chaussade, C.;Buchanan, C.; Rewcastle, G. W.; Baguley, B. C.; Flanagan, J. U.; Jamieson, S. M.F. ;, "Discovery of pyrazolo[1,5-a]pyridines as p110a-selective PI3 kinase inhibitors," *Biorg. Med. Chem,* vol. 20, pp. 69-85, 2012.

[5] Fienberg, S. (2017), "Development of N-domain selective angiotensin-I converting enzyme (ACE) inhibitors using computer aided drug discovery (CADD)," *PhD, University of Cape Town.*

[6] Jiménez-Díaz, M.; Mulet, T.; Viera, S.; Gomez, V.; Garuti, H.; Ibanez, J.; Alvarez-Doval, A.; Shultz, L.; Martinez, A.; Gargallo-Viola, D.; Angulo-Barturen, I., "Improved

murine model of malaria using Plasmodium falciparum competent strains and nonmyelodepleted NOD-scid IL2Rγnull mice engrafted with human erythrocytes.," *Antimicrob. Agents Chemother.,* vol. 53, no. 10, pp. 4533 - 4536. , 2009.

[7] McNamara, C.; Lee, M.; Lim, C.; Lim, S.; Roland, J.; Nagle, A.; Simon, O.; Yeung, B.; Chatterjee, A.; McCormack, S.; Manary, M.; Zeeman, A.; Dechering, K.; Kumar, T.; Henrich, P.; Gagaring, K.; Ibanez, M.; Kato, N.; Kuhen, K.; Fischli, C.; Rottmann, M.; P, "Targeting Plasmodium PI(4)K to eliminate malaria.," *Nature.,* vol. 504, no. 7479, pp. 248 - 253, 2013.

[8] Cheuka, P.; Centani, L.; Arendse, L.; Fienberg, S.; Wambua, L.; Renga, S.; Dziwornu, G.; Kumar, M.; Lawrence, N.; Taylor, D.; Wittlin, S.; Coertzen, D.; Reader, J.; van der Watt, M.; Birkholtz, L.; Chibale, K., "New amidated 3,6-diphenylated imidazopyridazines with potent anti-plasmodium activity are dual inhibitors of Plasmodium phosphatidylinositol-4-kinase and cGMP-dependent protein kinase.," *ACS Infect. Dis. ,* vol. 7, no. 1, pp. 34 - 46. , 2021.

[9] Vanaerschot, M.; Murithi, J.; Pasaje, C.; Ghidelli-Disse, S.; Dwomoh, L.; Bird, M.; Spottiswoode, N.; Mittal, N.; Arendse, L.; Owen, E.; Wicht, K.; Siciliano, G.; Bosche, M.; Yeo, T.; Kumar, T.; Mok, S.; Carpenter, E.; Giddins, M.; Sanz, O.; Ottilie, S., "Inhibition of resistance-refractory P . falciparum Inhibition of resistance-refractory P. falciparum kinase PKG delivers prophylactic, blood stage, and transmission-blocking anti-plasmodial activity.," *Cell Chem Biol,* pp. 1 - 11, 2020.

[10] Liu, Y.; Peterson, D.; Kimura, H.; Schubert, D. , "Mechanism of cellular 3-(4,5-Dimethylthiazol-2-yl)-2,5- Diphenyltetrazolium Bromide (MTT) reduction.," *J.Neurochem,* vol. 69, no. 2, pp. 581 - 593.] , 1997.

[11] A. Glomme and J. a. D. J. März, "Comparison of a miniaturized shake-flask solubility method with automated potentiometric acid/base titrations and calculated solubilities.," *J. Pharm. Sci.,* vol. 94, no. 1, pp. 1 - 16., 2005.